

**AES/RE/12-18**

**Processing of spinel-bearing compounds for  
zinc extraction**

**31/AUG/2012**

**J.P. Mardones**

Title of the Thesis : Processing of spinel-bearing compounds for zinc extraction

Author : Juan Pablo Mardones  
Engineer

Date : 31 August 2012

Programme director : Ir. Hans de Ruiter  
Associate Professor at CiTG, TU Delft

Thesis Supervisor : Dr. Yongxiang Yang  
Associate Professor at 3mE, TU Delft

TA Report number : AES/RE/12-18

Postal Address : Resource Engineering section  
Department of Applied Earth Sciences  
Delft University of Technology  
P.O. Box 5028  
The Netherlands

Copyright © 2010 – 2012 Juan Pablo Mardones

All rights reserved

No parts of this publication may be reproduced, stored in a retrieval system, or transmitted, in any form or by any means, electronic, mechanical, photocopying, recording, or otherwise, without the prior written permission of the author.

## ABSTRACT

This thesis studies the zinc extraction from spinels through hydro and pyrometallurgical processing. Two zinc-bearing spinels are covered: zinc ferrite  $\text{ZnO} \cdot \text{Fe}_2\text{O}_3$  to a limited extent and gahnite  $\text{ZnO} \cdot \text{Al}_2\text{O}_3$  as the main subject, compounds which are found naturally on the Earth's crust as well as in industrial residues from the zinc industry, steel industry and others. Zinc ferrite contains 27 % of Zn and 33 % as ZnO; resource recovery from ferrite has been studied already in the past. On the other hand, the processing of gahnite, containing 35 % of Zn and 44 % as ZnO, is studied more extensively since research in the field of extractive metallurgy is effectively non-existent. Hence, the main objective of the present thesis is finding routes of treatment for this spinel.

Zinc ferrite was produced synthetically at the CiTG/3mE labs by mixing equimolar amounts of ZnO and  $\text{Fe}_2\text{O}_3$  at 1100 °C. Gahnite was produced by an analog method, a mixture of equimolar amounts of ZnO and  $\text{Al}_2\text{O}_3$ .

The first approach was hydrometallurgical. Atmospheric hot acid leaching (4 M, 95 °C, 120 min, L/S 40) was performed with  $\text{H}_2\text{SO}_4$ , HCl and  $\text{HNO}_3$ , resulting in a non-detected dissolution of the compound. Pressure leaching (90 min, L/S 40) was carried out in an autoclave with  $\text{H}_2\text{SO}_4$  and  $\text{HNO}_3$ , resulting in a low (2.9 %; 0.75 M, 140 °C, 3.6 bar) and a moderate extraction (22.2 %; 4.0 M, 250 °C, 39.7 bar) respectively.

The second approach was pyrometallurgical processing (60 min dwell, 10 °C/min heating rate), divided into two sub-routes. A series of carbothermic tests (1:1.25 stoichiometric ratio) successfully led to a full reduction of the spinel at 1300 °C (99.90 % extraction of zinc). Aluminothermic tests (1.5:2 stoichiometric ratio) successfully resulted in a 99.98 % zinc extraction at 1200 °C.

The mix of gahnite and ferrite with carbon at 1300 °C produced a 99.65 % extraction of the metal. Addition of ZnO to the previous mixture resulted in a 100 % extraction, at 1300 °C. Further experiments with gahnite at 1200 °C by adding  $\text{SiO}_2$ , first with carbon and later with aluminium, resulted in a moderate 23.14 % and a low 4.69 % extraction correspondingly. Trials with CaO at 1400 °C created a glass residue and a slag, in each case.

It is thus possible to establish the zinc extraction from gahnite  $\text{ZnO} \cdot \text{Al}_2\text{O}_3$  as follows:

Route	Zinc extraction
Atmospheric acidic leaching	Non-detected
Pressure leaching	Low – Moderate
Reduction with aluminium and silica	Low
Reduction with carbon and silica	Moderate
Carbothermic reduction	Full
Aluminothermic reduction	Full





## ACKNOWLEDGEMENTS

I wish to express my gratitude to Hans de Ruiter (CiTG), a good friend, whose help and support before coming to The Netherlands was fundamental.

I have to thank Dr. Yongxiang Yang (3mE) for providing a challenging thesis subject.

The assistance, care for personal security and kindness of Ron Penners (CiTG), particularly during the pressure leaching work, is more than appreciated.

The lab experience and knowledge on chemistry and thermodynamics shared by Dr. Yulia Meteleva-Fischer (M2i) during the pyrometallurgical work was essential. The discussion of ideas was fruitful and enjoyable, and her encouragement is highly esteemed.

I am grateful for the friendship of Bogdan Necula, Mónica Reulink, Andrea Bojack, Tungky Subroto, Sander Leeftang and Shoshan Abrahams. I was really fortunate to have met them.

*This Master of Science thesis is dedicated to my parents, Nancy and Raúl,  
whose support and love I have received throughout my life, till this very day.  
I cannot thank you enough.*

# TABLE OF CONTENTS

ABSTRACT .....	iii
ACKNOWLEDGEMENTS .....	vi
TABLE OF CONTENTS .....	viii
LIST OF ABBREVIATIONS .....	xi
LIST OF TABLES .....	xii
LIST OF FIGURES .....	xiv
1 INTRODUCTION .....	1
2 LITERATURE REVIEW .....	5
2.1 Overview of metallurgical processing of zinc residues .....	5
2.1.1 Galvanizer's ashes and dross .....	5
2.1.2 EAF dust .....	5
2.2 Overview of metallurgical processing of zinc ferrite .....	6
2.2.1 Leaching .....	7
2.2.2 Iron removal .....	8
2.2.2.1 Jarosite process .....	8
2.2.2.2 VM Goethite process .....	9
2.2.2.3 Paragoethite process .....	10
2.2.2.4 Hematite process .....	12
2.2.3 Comparison of iron removal processes .....	12
2.3 Overview of metallurgical processing of gahnite .....	13
3 THERMODYNAMICS .....	15
3.1 Ellingham diagram .....	15
3.2 Carbothermic reduction of gahnite .....	17
3.3 Aluminothermic reduction of gahnite .....	20
3.4 Additional tests .....	21
3.4.1 Gahnite and carbon and silica .....	21
3.4.2 Gahnite and aluminium and silica .....	22
4 EXPERIMENTAL .....	24
4.1 Raw materials .....	24
4.1.1 Zinc ferrite synthesis .....	24
4.1.2 Gahnite synthesis .....	25
4.1.2.1 XRD pattern of gahnite without full procedure .....	26
4.1.2.2 XRD pattern of gahnite after full procedure .....	27



4.2 Experiments strategy .....	29
4.2.1 Hydrometallurgy plan .....	29
4.2.1.1 Atmospheric leaching (ALX) .....	29
4.2.1.2 Pressure leaching (PLX) .....	29
4.2.1.3 Experimental set-up for PLX .....	31
4.2.2 Pyrometallurgy plan .....	33
4.2.2.1 Plan .....	34
4.2.2.2 Experimental set-up for reduction .....	35
5 RESULTS OF HYDROMETALLURGICAL TREATMENT .....	37
5.1 Atmospheric leaching .....	37
5.2 Pressure leaching .....	38
5.2.1 Pressure leaching with sulphuric acid .....	39
5.2.1.1 H <sub>2</sub> SO <sub>4</sub> 0.50 M .....	39
5.2.1.2 H <sub>2</sub> SO <sub>4</sub> 0.75 M .....	41
5.2.2 Pressure leaching with nitric acid .....	43
5.2.2.1 HNO <sub>3</sub> 0.50 M .....	43
5.2.2.2 HNO <sub>3</sub> 4.00 M .....	44
6 RESULTS OF PYROMETALLURGICAL TREATMENT .....	47
6.1 Reduction of gahnite with carbon .....	47
6.1.1 G + C at 1300 °C .....	47
6.1.2 G + C at 1250 °C .....	49
6.1.3 G + C at 1200 °C .....	51
6.1.4 Tablet G + C at 1300 °C .....	53
6.2 Reduction of gahnite with aluminium .....	55
6.2.1 Aluminium balls .....	55
6.2.2 G + Al at 1200 °C .....	62
6.2.2.1 Tablet .....	62
6.2.2.2 Powder .....	64
6.2.3 G + Al at 1150 °C .....	66
6.2.4 G + Al at 1100 °C .....	68
6.2.5 G + Al at 1000 °C .....	70
6.2.6 G + Al at 950 °C .....	72
6.2.7 G + Al at 900 °C .....	74
6.3 Reduction test for gahnite and ferrite combined .....	76
6.4 Reduction test for gahnite and ferrite and ZnO combined .....	78
6.5 Exploratory reduction tests with addition of SiO <sub>2</sub> .....	80
6.5.1 G + C + SiO <sub>2</sub> .....	80
6.5.2 G + Al + SiO <sub>2</sub> .....	82
6.6 Exploratory reduction tests with addition of SiO <sub>2</sub> and CaO .....	84
6.6.1 G + C + SiO <sub>2</sub> + CaO .....	84
6.6.2 G + Al + SiO <sub>2</sub> + CaO .....	85
7 DISCUSSION .....	86
7.1 Hydrometallurgical treatment .....	86
7.1.1 Atmospheric leaching .....	86

7.1.2 Pressure leaching .....	86
7.2 Pyrometallurgical treatment .....	88
7.2.1 Carbothermic reduction .....	88
7.2.2 Aluminothermic reduction .....	90
7.2.3 Other pyrometallurgical tests .....	92
8 CONCLUSIONS .....	94
8.1 Hydrometallurgical treatment .....	94
8.2 Pyrometallurgical treatment .....	96
8.3 Overall treatment of gahnite .....	99
9 RECOMMENDATIONS .....	100
9.1 Hydrometallurgical treatment .....	100
9.2 Pyrometallurgical treatment .....	102
10 REFERENCES .....	104
APPENDIX: Additional dwell graphs .....	105

## LIST OF ABBREVIATIONS

LX	Leaching
ALX	Atmospheric leaching ( $P = 1 \text{ atm}$ )
PLX	Pressure leaching ( $P > 1 \text{ atm}$ )
CiTG	Faculteit Civiele Techniek en Geowetenschappen
3mE	Faculteit Werktuigbouwkunde, Maritieme Techniek & Technische Materiaalwetenschappen
LMP	Light Metals Processing Group
G	Gahnite
F	Zinc ferrite
ICP	Inductively Coupled Plasma
XRD	X-Ray Diffraction
XRF	X-Ray Fluorescence
EAF	Electric Arc Furnace
EAFD	Electric Arc Furnace Dust
LME	The London Metal Exchange

## LIST OF TABLES

Table 1.1 Chemical composition of gahnite .....	1
Table 1.2 Main zinc ores .....	1
Table 1.3 Zinc demand growth outlook .....	2
Table 1.4 Cash LME Price of Zinc .....	3
Table 1.5 Estimated prices of zinc at the LME .....	3
Table 2.1 Typical EAF dust composition .....	6
Table 2.2 Comparison of iron removal processes for processing of zinc ferrite .....	12
Table 3.1: Thermodynamics calculations for the reduction of gahnite with carbon .....	19
Table 4.1 Tests performed for atmospheric leaching of gahnite .....	29
Table 4.2 Initial plan for pressure leaching of gahnite with $H_2SO_4$ .....	30
Table 4.3 Initial plan for pressure leaching of gahnite with HCl .....	30
Table 4.4 Initial plan for pressure leaching of gahnite with $HNO_3$ .....	30
Table 4.5 Initial plan for pressure leaching of gahnite with NaOH .....	30
Table 4.6 Adjusted plan for pressure leaching of gahnite with $H_2SO_4$ .....	31
Table 4.7 Adjusted plan for pressure leaching of gahnite with $HNO_3$ .....	31
Table 4.8 Initial plan for carbothermic reduction of gahnite .....	34
Table 4.9 Initial plan for aluminothermic reduction of gahnite .....	35
Table 5.1 Tests performed for atmospheric leaching of gahnite .....	37
Table 5.2 Metal extraction with $H_2SO_4$ 0.50 M .....	39
Table 5.3 Metal extraction with $H_2SO_4$ 0.75 M .....	41
Table 5.4 Metal extraction with $HNO_3$ 0.50 M .....	43
Table 5.5 Metal extraction with $HNO_3$ 4.00 M .....	44
Table 7.1 Results from atmospheric leaching of gahnite .....	86
Table 7.2 Results from pressure leaching of gahnite .....	86
Table 7.3 Main results from carbothermic reduction of gahnite .....	88
Table 7.4 Main results from carbothermic reduction of gahnite .....	90
Table 7.5 Other results from aluminothermic reduction of gahnite .....	92
Table 7.6 Results from additional pyrometallurgical tests with gahnite .....	92
Table 8.1 Overall results of hydrometallurgical treatment of gahnite .....	94
Table 8.2 Overall results of pyrometallurgical treatment of gahnite .....	97
Table 8.3 Additional results of pyrometallurgical treatment of gahnite .....	98
Table 9.1 Plan recommended for pressure leaching of gahnite with $HNO_3$ .....	100
Table 9.2 Plan recommended for pressure leaching of gahnite with $H_2SO_4$ or HCl .....	100
Table 9.3 Plan recommended for carbothermic reduction of gahnite changing the heating rate .....	102
Table 9.4 Extended plan recommended for aluminothermic reduction of gahnite .....	102

Table 9.5 Plan recommended for aluminothermic reduction of gahnite changing the heating rate .....	103
--	-----

## LIST OF FIGURES

Figure 1.1 Localities for gahnite .....	2
Figure 1.2 Estimated prices of zinc at the LME (seller price only) .....	3
Figure 2.1 Typical jarosite process flow sheet .....	9
Figure 2.2 VM Goethite process flow sheet .....	10
Figure 2.3 Paragoethite process – general flow sheet .....	11
Figure 3.1 Ellingham diagram for oxides .....	16
Figure 3.2 Equilibrium compositions for thermal decomposition of pure gahnite (linear scale) .....	17
Figure 3.3 Equilibrium compositions in reduction of gahnite with carbon (linear scale) .....	17
Figure 3.4 HSC Chemistry graph for reduction of gahnite with aluminium .....	20
Figure 3.5 HSC Chemistry graph for reduction of gahnite with carbon and addition of SiO <sub>2</sub> .....	21
Figure 3.6 HSC Chemistry graph for decomposition of gahnite and addition of SiO <sub>2</sub> .....	22
Figure 3.7 HSC Chemistry graph for reduction of gahnite with aluminium and addition of SiO <sub>2</sub> .....	23
Figure 4.1 Heat treatment for zinc ferrite synthesis .....	25
Figure 4.2 Heat treatment for gahnite synthesis (close-up at the platinum crucible) .....	25
Figure 4.3 Example 1 of XRD pattern of (impure) gahnite without full procedure .....	26
Figure 4.4 Example 2 of XRD pattern of (impure) gahnite without full procedure .....	27
Figure 4.5 XRF results of pure gahnite .....	27
Figure 4.6 XRD pattern of pure gahnite .....	28
Figure 4.7 A few grams of pure gahnite ready to work experimentally with .....	28
Figure 4.8 Autoclave featuring pressure meter, set of water cooling pipes, external thermocouple and sampling pipe .....	32
Figure 4.9 Close-up at autoclave's pressure meter during an experiment .....	33
Figure 4.10 Autoclave controller and external thermocouple controller .....	33
Figure 4.11 Pure carbon powder (graphite) utilized for the carbothermic reduction experiments .....	34
Figure 4.12 Horizontal furnace, pressure meter, flowmeter, argon gas line .....	35
Figure 5.1 XRF result of the residue from HCl leaching of gahnite .....	37
Figure 5.2 XRD pattern of the residue from HCl atmospheric leaching of gahnite .....	38
Figure 5.3 Atmospheric leaching with HNO <sub>3</sub> , H <sub>2</sub> SO <sub>4</sub> and HCl respectively .....	38
Figure 5.4 Extraction (%) of zinc and aluminium from gahnite with H <sub>2</sub> SO <sub>4</sub> vs time (min) of PLX. Conditions: C=0.50 M, L/S=40, T=235 °C, P=30 bar .....	40
Figure 5.5 XRD pattern of the residue of H <sub>2</sub> SO <sub>4</sub> PLX at 0.5 M, confirming the presence of gahnite .....	40
Figure 5.6 Extraction (%) of zinc and aluminium from gahnite with H <sub>2</sub> SO <sub>4</sub> vs time (min) of PLX. Conditions: C=0.75 M, L/S=40, T=140 °C, P=3.6 bar .....	41
Figure 5.7 XRD pattern of the residue of H <sub>2</sub> SO <sub>4</sub> PLX at 0.75 M, confirming the presence of gahnite .....	42
Figure 5.8 Extraction (%) of zinc and aluminium from gahnite with HNO <sub>3</sub> vs time (min) of PLX. Conditions: C=0.50 M, T=245 °C, P=36 bar .....	44

Figure 5.9 Extraction (%) of zinc and aluminium from gahnite with $\text{HNO}_3$ vs time (min) of PLX. Conditions: C=4.00 M, T=250 °C, P=39 bar .....	45
Figure 5.10 XRD pattern of the residue from PLX with $\text{HNO}_3$ 4.0 M .....	45
Figure 6.1 XRD pattern of the residue for the test G + C at 1300 °C .....	47
Figure 6.2 XRF result of the residue for the test G + C at 1300 °C .....	48
Figure 6.3 Photographs taken before (L) and after the experiment of G + C at 1300 °C .....	48
Figure 6.4 XRD pattern of the residue for the test G + C at 1250 °C .....	49
Figure 6.5 XRF results of the residue for the test G + C at 1250 °C .....	50
Figure 6.6 Photographs taken before (L) and after the experiment of G + C at 1250 °C .....	50
Figure 6.7 XRD pattern of the residue for the test G + C at 1200 °C .....	51
Figure 6.8 XRF results of the residue for the test G + C at 1200 °C .....	52
Figure 6.9 Photographs taken before (L) and after the experiment of G + C at 1200 °C .....	52
Figure 6.10 Photograph showing a perfect single tablet of G + C .....	53
Figure 6.11 XRD pattern of the residue for the test Tablet G + C at 1300 °C .....	54
Figure 6.12 XRF result of the residue for the test Tablet G + C at 1300 °C .....	54
Figure 6.13 XRD pattern of the residue for the test G + Al at 1000 °C (balls) .....	55
Figure 6.14 XRF result of the residue for the test G + Al at 1000 °C (balls) .....	56
Figure 6.15 Optical microscope images before reduction attempt of gahnite at 1000 °C (balls) .....	56
Figure 6.16 Optical microscope images after reduction attempt of gahnite at 1000 °C (balls) .....	57
Figure 6.17 Photographs taken before (L) and after the experiment of G + Al at 1000 °C (balls) .....	57
Figure 6.18 XRD pattern of the residue for the test G + Al at 1000 °C (balls) .....	58
Figure 6.19 XRF result of the residue for the test G + Al at 1000 °C (balls) .....	58
Figure 6.20 Optical microscope images after reduction attempt of gahnite at 1000 °C (balls) .....	59
Figure 6.21 Photographs taken before (L) and after the experiment of G + Al at 1000 °C (balls) .....	59
Figure 6.22 XRD pattern of the residue for the test G + Al at 1200 °C (balls) .....	60
Figure 6.23 XRF result of the residue for the test G + Al at 1200 °C (balls) .....	60
Figure 6.24 Optical microscope images after reduction attempt of gahnite at 1200 °C (ball) .....	61
Figure 6.25 Photographs taken before (L) and after the experiment of G + Al at 1200 °C (balls) .....	61
Figure 6.26 XRD pattern of the residue for the test G + Al at 1200 °C (tablet) .....	62
Figure 6.27 XRF result of the residue for the test G + Al at 1200 °C (tablet) .....	63
Figure 6.28 Photographs taken before (L) and after the experiment of G + Al at 1200 °C (tablet) .....	63
Figure 6.29 XRD pattern of the residue for the test G + Al at 1200 °C (powder) .....	64
Figure 6.30 XRF result of the residue for the test G + Al at 1200 °C (tablet) .....	65
Figure 6.31 Photographs taken before (L) and after the experiment of G + Al at 1200 °C (powder) .....	65
Figure 6.32 XRD pattern of the residue for the test G + Al at 1150 °C .....	66
Figure 6.33 XRF result of the residue for the test G + Al at 1150 °C .....	67
Figure 6.34 Photographs taken before (L) and after the experiment of G + Al at 1150 °C .....	67
Figure 6.35 XRD pattern of the residue for the test G + Al at 1100 °C .....	68
Figure 6.36 XRF results of the residue for the test G + Al at 1100 °C .....	69
Figure 6.37 Photographs taken before (L) and after the experiment of G + Al at 1100 °C .....	69
Figure 6.38 XRD pattern of the residue for the test G + Al at 1000 °C .....	70
Figure 6.39 XRF results of the residue for the test G + Al at 1000 °C .....	71
Figure 6.40 Photographs taken before (L) and after the experiment of G + Al at 1000 °C .....	71
Figure 6.41 XRD pattern of the residue for the test G + Al at 950 °C .....	72
Figure 6.42 XRF results of the residue for the test G + Al at 950 °C .....	73
Figure 6.43 Photographs taken before (L) and after the experiment of G + Al at 950 °C .....	73

Figure 6.44 XRD pattern of the residue for the test G + Al at 900 °C .....	74
Figure 6.45 XRF results of the residue for the test G + Al at 900 °C .....	75
Figure 6.46 Photographs taken before (L) and after the experiment of G + Al at 900 °C .....	75
Figure 6.47 XRD pattern of the residue for the test G + F + C at 1300 °C .....	76
Figure 6.48 XRF results of the residue for the test G + F + C at 1300 °C .....	77
Figure 6.49 Photographs taken before (L) and after the experiment of G + F + C at 1300 °C .....	77
Figure 6.50 XRD pattern of the residue for the test G + F + ZnO + C at 1300 °C .....	78
Figure 6.51 XRF results of the residue for the test G + F + ZnO + C at 1300 °C .....	79
Figure 6.52 Photographs taken before (L) and after the experiment of G + F + ZnO + C at 1300 °C .....	79
Figure 6.53 XRD pattern of the residue for the test G + C + SiO <sub>2</sub> + C at 1200 °C .....	80
Figure 6.54 XRF results of the residue for the test G + C + SiO <sub>2</sub> at 1200 °C .....	81
Figure 6.55 Photographs taken before (L) and after the experiment G + C + SiO <sub>2</sub> at 1200 °C .....	81
Figure 6.56 XRD pattern of the residue for the test G + Al + SiO <sub>2</sub> + C at 1200 °C .....	82
Figure 6.57 XRF results of the residue for the test G + Al + SiO <sub>2</sub> at 1200 °C .....	83
Figure 6.58 Photographs taken before (L) and after the experiment G + Al + SiO <sub>2</sub> at 1200 °C .....	83
Figure 6.59 Photographs taken before (L) and after the experiment G + C + SiO <sub>2</sub> + CaO at 1400 °C .....	84
Figure 6.60 Photographs taken before (L) and after the experiment G + Al + SiO <sub>2</sub> + CaO at 1400 °C .....	85
Figure 7.1 Results of PLX of gahnite with H <sub>2</sub> SO <sub>4</sub> .....	87
Figure 7.2 Results of PLX of gahnite with HNO <sub>3</sub> .....	87
Figure 7.3 Zinc extraction from gahnite through carbothermic treatment in the range 1200 – 1300 °C .....	88
Figure 7.4 Original HSC Chemistry thermodynamic graph combined with real zinc extraction .....	89
Figure 7.5 Zinc extraction from gahnite through carbothermic treatment in the range 1200 – 1300 °C .....	90
Figure 7.6 Original thermodynamic calculation combined with real zinc extraction .....	91
Figure 8.1 Overall results of hydrometallurgical treatment of gahnite .....	95
Figure 8.2 Overall results of pyrometallurgical treatment of gahnite .....	97
Figure 8.3 Additional results of pyrometallurgical treatment of gahnite .....	98
Figure 8.4 Zinc extraction of gahnite .....	99



“The two most important pairs of eyes in the world”

— Salvador Dalí, referring to Vermeer and van Leeuwenhoek  
Delft, 1962



# 1 INTRODUCTION

In previous research at the Light Metals Processing Section of TU Delft, a zinc-based compound called gahnite has been found in residues from the brass <sup>[1]</sup> and zinc industry <sup>[2]</sup>, which no processing technology is known of.

After an extensive review in the literature (books, journals, theses, articles), it was concluded that gahnite has not been studied before in terms of zinc extraction, neither hydro nor pyrometallurgically.

Gahnite is a zinc oxide. Its chemical formula is  $\text{ZnO} \cdot \text{Al}_2\text{O}_3$  but it is usually written as  $\text{ZnAl}_2\text{O}_4$  too. It is referred to as zinc aluminate as well. There are very few reported studies on this compound; for instance, the known properties of this material are just the crystal structure and the optical spectra, and the electronic properties are relatively unknown <sup>[3]</sup>. It was first described in 1807 for an occurrence in the Falun mine, Dalarna, in Sweden, and named after the discoverer of the mineral, the Swedish chemist Johan Gottlieb Gahn (1745-1818) <sup>[4]</sup>.

Gahnite is a zinc spinel. This feature presents major challenges to process it since the crystal structure is very stable, aiming at the extraction of zinc from it <sup>[5]</sup> <sup>[1]</sup>. Its chemical composition is shown below.

Table 1.1 Chemical composition of gahnite.

Compound	%
Zinc	35.66
Aluminium	29.43
Oxygen	34.90
ZnO	44.39
$\text{Al}_2\text{O}_3$	55.61

With this data, the current mineral sources of zinc for industrial production can be updated. The common zinc minerals are given next.

Table 1.2 Main zinc ores.

Mineral	Formula	Zinc content [%]
Zincite	$\text{ZnO}$	80.4
Sphalerite, Zinc blende or Wurtzite	$\text{ZnS}$	67.1
Marmatite	$(\text{Zn}, \text{Fe})\text{S}$	< 67.0
Hydrozincite	$3\text{ZnO} \cdot 2\text{ZnCO}_3 \cdot 3\text{H}_2\text{O}$	59.5
Willemite	$2\text{ZnO} \cdot \text{SiO}_2$	58.7
Hemimorphite	$4\text{ZnO} \cdot 2\text{SiO}_2 \cdot 2\text{H}_2\text{O}$	54.3
Smithsonite or Calamine	$\text{ZnCO}_3$	52.2
<b>Gahnite</b>	<b><math>\text{ZnO} \cdot \text{Al}_2\text{O}_3</math></b>	<b>35.66</b>

This percentage of zinc contained in the spinel represents an important source of the metal and, even though not currently processed anywhere, it can be a feedstock for the industry in the coming future, especially considering the increasing demand, particularly from China, the world's largest zinc consumer.

Gahnite has been found along within zinc orebodies, mainly in the locations of Falun (Sweden), Bavaria (Germany), Calabria (Italia), several states of USA, Brasil, Madagascar, Namibia, and in territories of Australia. Prof. Mike Buxton of CiTG provided remarks about interesting geological findings of gahnite deposits by Anglo American in areas of Africa and Australia, and reaffirming the situation of no knowledge on how to process it.

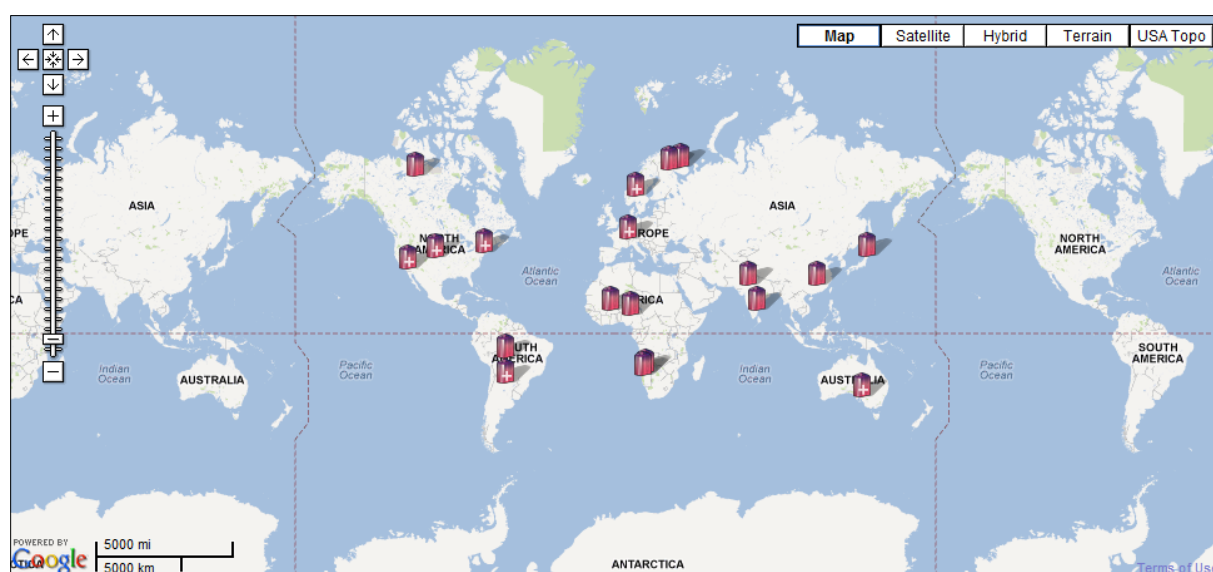


Figure 1.1 Localities for gahnite <sup>[5]</sup>.

China currently consumes about 40 % of the world's annual production, and with the rapid development of its automotive, machinery manufacturing, construction metals and communications industries, its domestic demand of zinc is set to continue to rise.

Moreover, it is likely that China may lose the ability to meet its own supply altogether which will continue the nation standing as a net importer. Going forward, demand is still projected to be above 5 % with China still not quite able to meet all of its need from domestic production sources alone.

Consumption growth rates within China have been above 10 % annually in recent years. This has largely been driven by galvanized steel production growth as well as by demand from newly constructed base metal smelting capacity. Zinc demand growth outlook is shown below.

Table 1.3 Zinc demand growth outlook. Source: Wood Mackenzie.

	2012	2013
<b>Global</b>	6.2 %	5.8 %
<b>China</b>	8.5 %	8.7 %

Canada, China, USA and Perú are significant sources of production and large reserves. Significant large mines are reaching the end of their productive lives with large deposits of lower grade in new mines known but as yet not under construction largely due to financing constraints and lack of investment.

Zinc is traded by undisclosed supply contracts between primary producers and fabricators, upon The London Metal Exchange (LME), between secondary processors and tertiary manufacturers or via traders (as agents and principals). As such, there is not a universal pricing unit though the LME price acts as a daily benchmark with pricing adjustments for regional bonded warehouse locations and inventories being taken into account.

The previous analysis can be visualized by looking at the Cash Price of Zinc at LME.

Table 1.4 Cash LME Price of Zinc.

	<b>2010</b>	<b>2011</b>	<b>2012</b>	<b>2013 (projected)</b>
<b>US\$/lb</b>	98	103	98	<b>111</b>

Finally, utilizing data from the LME, positive prices are observed in the short run as well as in the long run (please note the following table and figure).

Table 1.5 Estimated prices of zinc at the LME.

<b>ZINC</b>	<b>Prompt date</b>	<b>Buyer (US\$/tonne)</b>	<b>Seller (US\$/tonne)</b>
<b>Cash</b>	28/08/2012	1,829.00	1,829.50
<b>3 Months</b>	23/11/2012	1,850.00	1,851.00
<b>December 1</b>	18/12/2013	1,900.00	1,905.00
<b>December 2</b>	17/12/2014	1,938.00	1,943.00
<b>December 3</b>	16/12/2015	1,960.00	1,965.00

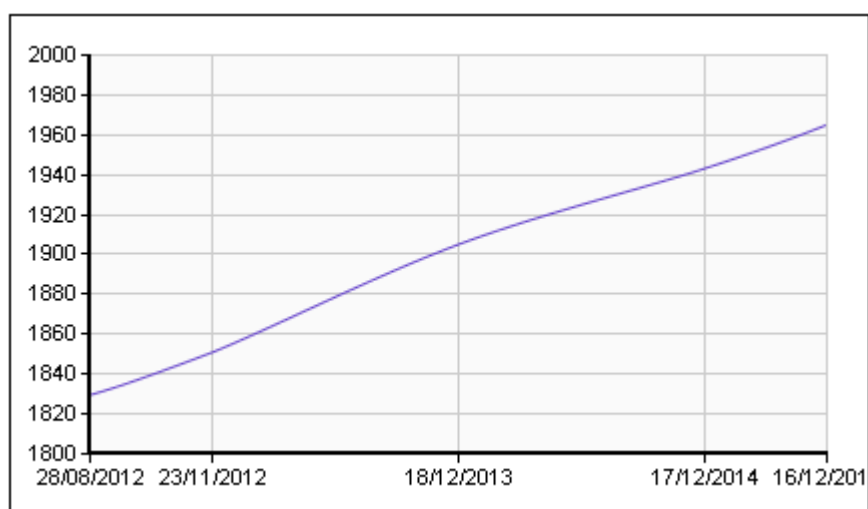


Figure 1.2 Estimated prices of zinc at the LME (seller price only).

It is then concluded that studying the zinc extraction from gahnite is supported by both:

- the inexistent knowledge of its processing, hydro and pyrometallurgically
- the projected increasing demand of the metal, the end of life of current large mines and optimistic price prospects

with relevant insights for the fields of extractive metallurgy and mineral economics.

## 2 LITERATURE

### 2.1 Overview of metallurgical processing of zinc residues

The most important secondary sources of zinc as feed for smelting operation are essentially galvanizer's ashes and dross, as well as electric arc furnace (EAF) dusts from the processing of steel scrap.

Metallic scrap such as diecastings can also be a raw material source but are more commonly recycled either to reconstitute diecasting alloys or used as feed for zinc oxide production.

#### 2.1.1 Galvanizer's ashes and dross

The so called galvanizer's ashes are skimmings from the surface of a hot dip galvanizing bath and are formed by oxidation of the zinc surface, which is accelerated by the dipping and withdrawal of work from the bath. A coating of zinc ammonium chloride flux can be used to reduce oxidation as well as assisting the galvanizing process. Zinc content of ashes is usually between 65 – 75 %, partly as oxide and partly as metal and zinc chloride  $\text{ZnCl}_2$ . Ashes can be de-metallized by ball milling and screening to remove coarse metal prills. Fines can then be added directly to a roasting plant prior to feeding to the leaching section of an electrolytic plant. Roasting serves to eliminate the chloride content. Alternatively, it can be washed with a sodium carbonate solution to extract chloride while retaining zinc in the solids <sup>[6]</sup>.

On the other hand, the so called Galvanizer's dross is a zinc-iron alloy taken from the bottom of a hot dip galvanizing bath. It is ordinarily around 3.5 % Fe and 96 % Zn, which is usually recovered by distillation and is commonly the raw material for the manufacture of zinc oxide  $\text{ZnO}$ .

#### 2.1.2 EAF dust

EAF dust is formed during the melting of scrap steel in an electric arc furnace. It is composed of oxides of iron, zinc and other metals along with volatile chlorides. It also contains fines from other components of the furnace charge such as lime  $\text{CaO}$ , used to form slag.

Around 45 – 50 % of the zinc content exists as  $\text{ZnO}$  while the remainder is primarily zinc ferrite  $\text{ZnO} \cdot \text{Fe}_2\text{O}_3$  and some  $\text{ZnCl}_2$ . Most of the iron is present as ferric oxide  $\text{Fe}_2\text{O}_3$ . Typical composition of EAF dusts is given in Table 2.1.

Processing of EAF dusts attracted considerable attention during the 1990s and a number of processing options were developed. Most of these involved carbothermic reduction and direct condensation of zinc from reduction process gases. Most of these processes failed due to heavy contamination of the condensation operation with dusts and halides. The major treatment method used for EAF dusts remains the Waelz Kiln fuming process <sup>[7]</sup>.

Table 2.1 Typical EAF dust composition.

Element	Range [%]
Zn	10 – 35
Fe	25 – 35
Pb	0.5 – 5
CaO	5 – 20
SiO <sub>2</sub>	3 – 5
Cl	1 – 5
F	0.5 – 1

Alternatively, hydrometallurgical extraction efficiency of zinc from EAF dusts is relatively low due to the high proportion of zinc present as  $\text{ZnO} \cdot \text{Fe}_2\text{O}_3$ , which is insoluble in a dilute acid leach or an alkali leach (atmospheric leaching). Consequently, zinc extraction can be as low as 50 % and is not likely to be more than 70 %. To address this, it is possible to recycle the leach residue to the electric furnace, but this situation requires the zinc extraction plant to be located close to the electric furnace rather than at a central location servicing a number of steel plants. In that case, the plant size is small and any economies of scale are lost<sup>1</sup>. If the leach residue is recycled then it should be mixed with pulverized coal and dried to less than 10 % moisture. Otherwise,  $\text{ZnO} \cdot \text{Fe}_2\text{O}_3$  residue can be leached in hot strong sulfuric acid  $\text{H}_2\text{SO}_4$ , but iron must then be separated from the resulting solution.

## 2.2 Overview of metallurgical processing of zinc ferrite

Zinc ferrite  $\text{ZnO} \cdot \text{Fe}_2\text{O}_3$  is insoluble in dilute sulphuric acid solution and requires elevated temperatures and reasonably strong acid conditions to be attacked. Iron is dissolved as a result and must be then removed from the leach solution before it is suitable for electrolysis.

Any iron present in zinc concentrates combines with zinc oxide during roasting to form zinc ferrite  $\text{ZnO} \cdot \text{Fe}_2\text{O}_3$ . This material is not dissolved during normal dilute acid leaching at temperatures up to 60 °C. Consequently, most of the associated zinc is locked into the leach residue, resulting in zinc recoveries for the total electrolytic zinc process in general between 85 – 90 %, but dependent on the iron content of the concentrate.

Ferrite residues were treated by two principal methods: the Waeltz process and by feeding to a lead smelter. The latter approach was only useful if the residue contained reasonable quantities of lead and silver, in which case zinc may be recovered by fuming from the lead blast furnace slag for return to the zinc plant as zinc oxide. The Waeltz process, which involves the fuming of zinc from the residue in a rotary kiln, was applied primarily to recover

<sup>1</sup> The concept of economies of scale in a production process is understood as when the cost per unit of output declines over the range of output. Then, for instance, the average cost of producing one metric tonne of copper per day must decline as the total metric tonnes of copper per day increases. As a consequence, the marginal cost of producing the last metric tonne of copper in that given day must be less than the average cost. “*Can changes in commodity prices cause Economies of Scale in Mining?*”, Mardones J.P. and Schenkenbach S., Erasmus School of Economics, Rotterdam, 2012.



zinc but also recovered lead and some silver into the zinc oxide fume. However, it was a substantial consumer of coke or high rank coal.

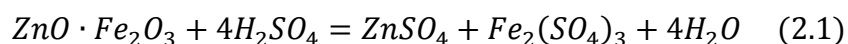
The zinc recovered by these processes was high cost, therefore a more efficient and economical means of extracting zinc from ferrite residues was sought. It had been known since the 1930s that the zinc and iron contents of ferrite residue could be leached in hot sulfuric acid solutions (above 90 °C and above 120 g/L H<sub>2</sub>SO<sub>4</sub>), but the problem had been to devise a means of precipitating iron in a form which could be readily settled, filtered and washed without entraining excessive amounts of zinc. Separation of large amounts of iron as ferric hydroxide by precipitation with zinc oxide was quite impractical in this regard. During the 1960s, efforts were concentrated on the precipitation of iron as a crystalline basic ferric sulfate and it was found that compounds of the form of the mineral 'jarosite' (Na<sub>2</sub>Fe<sub>6</sub>(SO<sub>4</sub>)<sub>4</sub>(OH)<sub>12</sub>) could be formed at temperatures above 90 °C. This led to the development of the jarosite process in which ammonium jarosite was commonly employed as the means of precipitating iron. The process was simultaneously developed by the Electrolytic Zinc Company of Australasia, the Det Norske Zink Co in Norway, and Asturiana de Zink SA in Spain, and was widely and rapidly applied throughout the industry in the late 1960s and early 1970s. The result of this innovation was the improvement of zinc recovery from as low as 85 % to at least 95 % and up to 97 %.

Improvements and variations of the jarosite process have subsequently been made, such as the 'conversion process' developed by Outokumpu Oy in which the leaching of ferrites and precipitation of jarosite take place simultaneously in the same stage.

At almost the same time as the development of the jarosite process, an alternative but similar approach to iron precipitation was developed by Vieille Montagne SA at the Balen plant in Belgium, which involved the separation of iron in the form of the mineral 'goethite' (FeO·OH). This required similar conditions to jarosite and produced a material of higher iron content than jarosite but also of higher zinc content, and did not achieve an overall zinc recovery as high as the jarosite process.

### 2.2.1 Leaching

Zinc ferrite can be successfully dissolved in hot strong sulfuric acid solutions at between 30 and 80 g/L and temperatures of above 90 °C. The basic reaction is given in Equation 2.1.



The acid end point for the hot acid leach is commonly around 30 g/L but can be higher and up to 100 g/L. Ferrite extraction is of the order of 80 % under these conditions giving iron levels in the resulting leach solution commonly in the range of 30 to 40 g/L.

Any residual sulfides contained in leach residues will also be attacked by the ferric iron and extractions of zinc from sulfides will generally be of the order of 50 – 60 %, but dependent on the actual amount present.

## 2.2.2 Iron removal

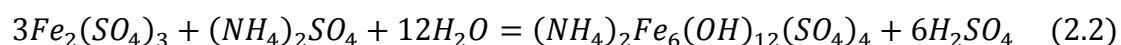
As indicated above, for the removal of any significant quantities of iron from solution (that is above 2 g/L), it is necessary to precipitate the iron in a form that can be readily settled, filtered and washed with minimum entrainment of leach solution. Processes that have been developed rely on the use of three iron compounds – jarosite, goethite and hematite. The jarosite process has many variants and is probably the most cost efficient removal method. Goethite can be produced in two principle ways, one variant known as the goethite process and the other as the paragoethite process. Hematite can only be produced at elevated temperature and pressure and hence involves treatment of solution in an autoclave. In all cases, it is necessary to separate the iron precipitate in as coarse a crystalline form as possible to achieve high settling and filtration rates and to reduce solution entrainment. Generally this requires iron to be precipitated from a low iron concentration in solution in order to minimize nucleation. But in order to promote crystal growth, the addition of seed material in the form of recycle precipitate will clearly assist.

### 2.2.2.1 Jarosite process

This process was developed in the mid 1960s and represented a most significant advance in the electrolytic zinc process <sup>[8]</sup>.

Jarosite is a complex basic iron sulfate represented as  $R_2Fe_6(OH)_{12}(SO_4)_4$  where R may be any of the ions  $K^+$ ,  $NH_4^+$ ,  $Na^+$ ,  $Ag^+$ , or  $R_2$  can be  $Pb_2^+$ . Solution temperatures close to the boiling point are required for the formation of jarosites, and formation is favoured at lower solution acidities.

The reaction for ammonium jarosite formation is given in Equation 2.2.



In order to allow the precipitation reaction to proceed, neutralization of the acid formed is necessary. The addition of ammonia rather than ammonium sulfate will assist, but additional neutralization is required and this is generally achieved by the addition of calcine. In order to reduce zinc loss and quantity of calcine used for jarosite precipitation, it is common practice to use a pre-neutralization step, including thickener, ahead of jarosite precipitation. This aims to reduce residual acidity in hot acid leach solution to a low level in a separate stage which the residue can be separated from for subsequent treatment in the hot acid leach stage with recovery of the ferritic zinc. Another means of reducing zinc losses associated with zinc ferrite contained in the jarosite residue is to subject the residue to an acid re-leach. This is possible because, once formed, jarosite has a higher stability in acid solution than zinc ferrite and is subject to only limited re-solution.

The following scheme gives a generalized jarosite process flow sheet.

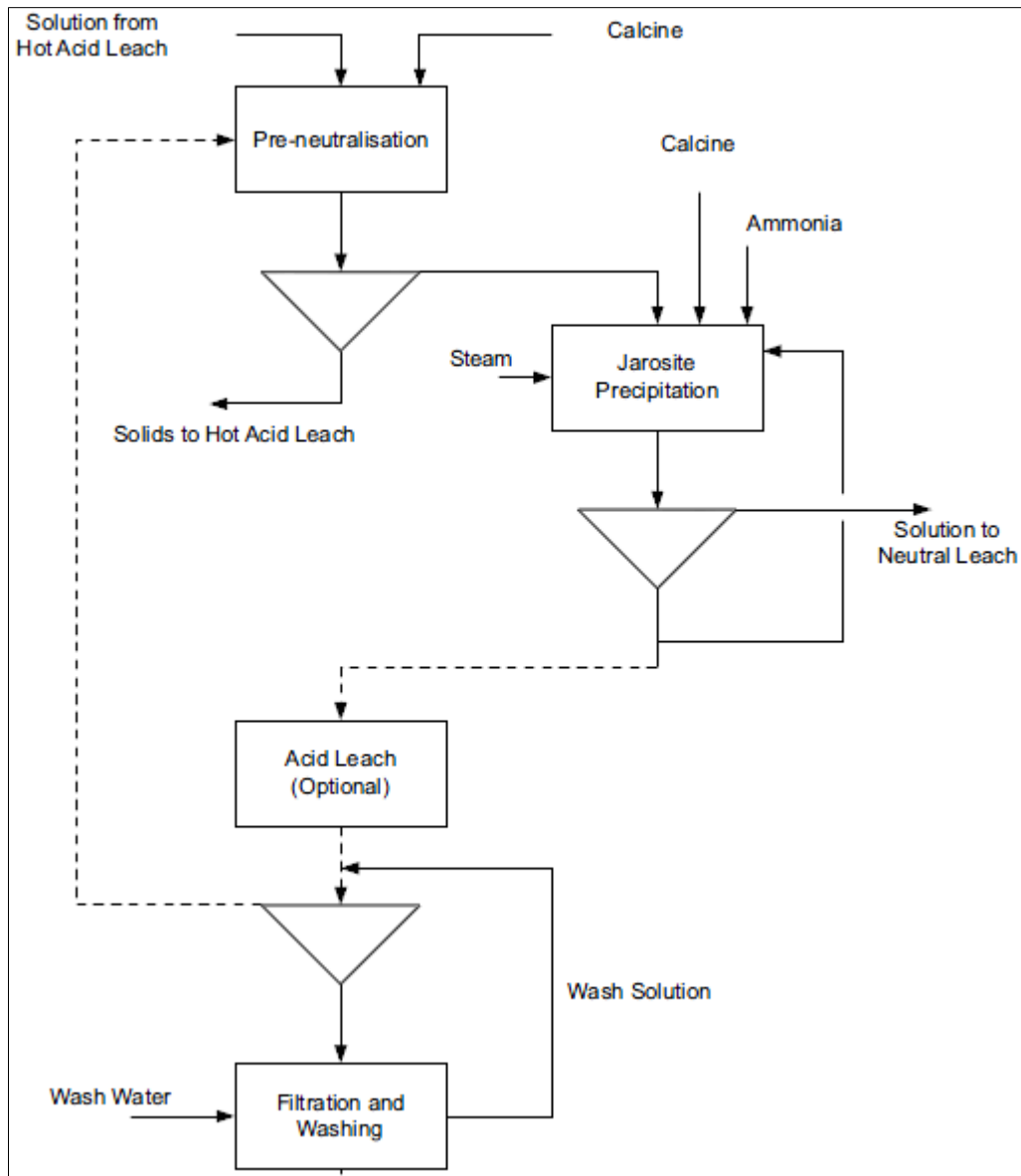
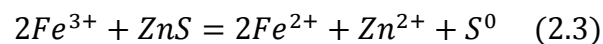


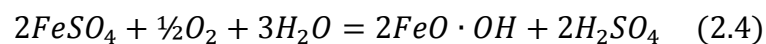
Figure 2.1 Typical jarosite process flow sheet <sup>[6]</sup>.

### 2.2.2.2 VM Goethite process

This process is based in the Goethite process. It was developed by Vieille Montagne at the Balen smelter, Belgium. The first step is to reduce the solution arising from the leaching of ferrites with concentrates according to the following equation:



The residue from the reduction step contains elemental sulfur as well as unreacted sulfides, and is separated and returned to the roasting plant. The resulting solution containing ferrous iron is then re-oxidized to ferric iron using air, and goethite is simultaneously precipitated according to Equation 2.4.



Acid is generated as in jarosite formation and calcine is added to neutralize that acid and maintain the required operating pH.

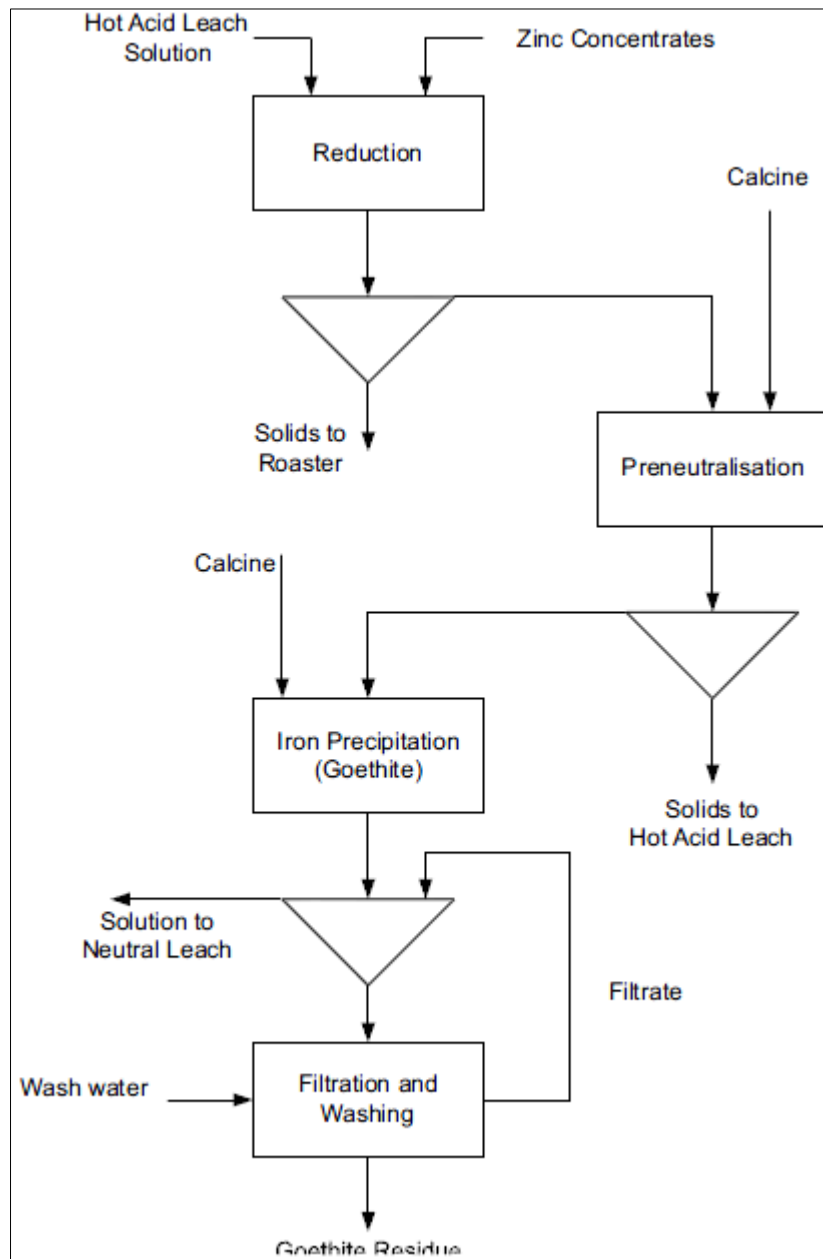


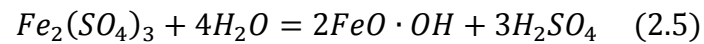
Figure 2.2 VM Goethite process flow sheet <sup>[6]</sup>.

### 2.2.2.3 Paragoethite process

In this case, the low ferric iron concentration necessary for the formation of the goethite structure is achieved by control of the solution flow to the precipitation tanks. It is generally necessary to carry out the precipitation operation in a single stage rather than a series of tanks where there would be a gradation in iron concentration. Hence, very large tanks or a number of single stage tanks operating in parallel are generally used. In this situation, it is particularly difficult to ensure concentration uniformity and the maintenance of ferric iron

concentration. As a result, the form of iron precipitate is not pure goethite but contains hydrated basic sulfate, has poor crystallinity and contains a higher level of entrained zinc than the pure goethite product.

The precipitation reaction is ideally according to Equation 2.5.



A typical flow sheet is shown in Figure 2.3.

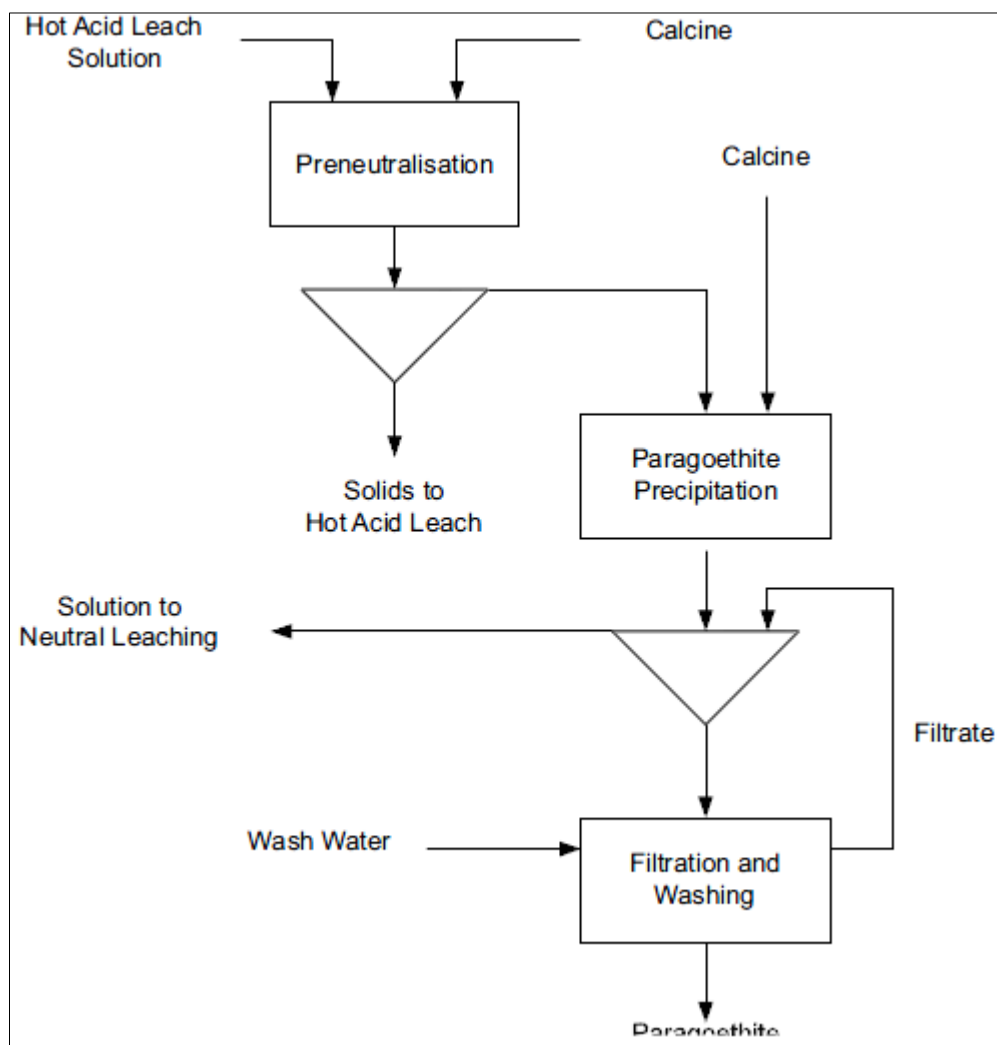
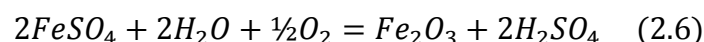


Figure 2.3 Paragoethite process – general flow sheet <sup>[6]</sup>.

Although the paragoethite process simplifies the flow sheet by eliminating the iron reduction stage, it does so at the expense of increased quantities of iron residue and increased zinc losses with lower overall zinc recovery from concentrates. The process is more difficult to control to achieve satisfactory settling and filtration properties and to maintain low levels of entrained zinc in the final residue.

#### 2.2.2.4 Hematite process

In the hematite process, the feed solution is generally reduced as in the VM goethite process to convert all iron to the ferrous state. The solution is heated to between 180 – 200 °C in an autoclave with the addition of oxygen. As a result, ferric iron concentrations can be maintained at a low level ensuring that pure hematite is formed, and acid generation is minimized. The precipitation reaction is as follows:



The acidity is generally allowed to rise to the equilibrium level, which to some extent imposes practical limits on the iron concentration in solution feed to the autoclave. However a particularly high grade iron residue can be produced relatively free of zinc.

The iron content of hematite produced in this way is typically 55 – 60 % and the zinc content is around one per cent, with 1.5 % S. Being free of zinc ferrite residues, in contrast to other iron removal processes, and being inherently low in zinc content, the overall smelter zinc recoveries achieved by use of the hematite process are very high and can exceed 99 % from concentrates. The volume of iron residue produced is also much lower at less than half the quantity produced by the jarosite process.

#### 2.2.3 Comparison of iron removal processes

The various iron removal processes outlined result in significantly different quantities of residue and loss of zinc, as well as different equipment and operating costs. Selection of the most suitable process will depend to a large extent on the options available for residue disposal, and the primary issue may be the quantity of residue produced rather than zinc recovery achieved. The choice of process also impacts on the quantity of secondary leach (or lead–silver) residue produced due to the difference in the quantity of calcine used for iron precipitation. The residue normally associated with that calcine will be incorporated into the iron residue.

The following table gives a comparison of iron removal processes, based on 100 tonne feed.

Table 2.2 Comparison of iron removal processes for processing of zinc ferrite <sup>[6]</sup>.

		Process			
		Jarosite	VM-goethite	Paragoethite	Hematite
Iron residue	Fe content	29.0 %	40.0 %	34.0 %	57.0 %
	Zn content	3.5 %	8.5 %	13.0 %	1.0 %
	Pb content	1.9 %	1.9 %	2.2 %	0 %
Quantity of Fe residue		22.5 t	16.2 t	19.2 t	11.2 t
Zinc loss in Fe residue		1.51 %	2.65 %	4.79 %	0.21 %
Quantity of secondary leach residue		6.0 t	6.5 t	6.0 t	8.0 t
Zinc loss in secondary leach residue		0.58 %	0.63 %	0.58 %	0.77 %
Overall zinc recovery		97.9 %	96.7 %	94.6 %	99.0 %

## 2.3 Overview of metallurgical processing of gahnite

After an extensive search for previous work on the processing of this zinc spinel, it was settled that no research has been performed in the past. For instance, the two major sources consulted in the beginning of the present work, *Resource recovery and recycling from metallurgical wastes* by Rao <sup>[9]</sup> and *The extractive metallurgy of zinc* by Sinclair <sup>[6]</sup> do not even contain the keywords gahnite, zinc aluminate,  $\text{ZnO} \cdot \text{Al}_2\text{O}_3$  or  $\text{ZnAl}_2\text{O}_4$  in the text.

### a) Hydrometallurgical route

In fact, the only known (unsuccessful) attempt to leach gahnite was carried out at the LMP group in which synthetic gahnite was submitted to a hot acid leach at 95 °C with sulphuric acid at 200 g/L for two hours (atmospheric pressure).

Literature references were consulted on compounds close to gahnite, in particular zinc ferrite. Two works were of particular interest for the metallurgical processing.

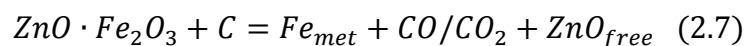
With respect to hydrometallurgical treatment, Havlík *et al.* <sup>[10]</sup> conducted a series of pressure leaching tests with EAF dust for hydrometallurgy recovery of zinc. The material was mainly composed of  $\text{ZnO} \cdot \text{Fe}_2\text{O}_3$ ,  $\text{ZnO}$ ,  $\text{Fe}_3\text{O}_4$ ,  $\text{SiO}_2$ ,  $(\text{ZnMnFe})(\text{FeMn})_2\text{O}_4$  and other complexes. Experiments on a laboratory scale were carried out in the temperature range of 100 – 250 °C and with pressures between 1.0 and 41.0 bar, utilizing sulphuric acid as the leaching agent at 0.4 M, in a 2.0 L autoclave, for 1.0 h and sampling every 15 min.

Extraction curves of zinc were obtained for different working conditions of temperature and pressure, concluding that the optimal parameters were a temperature of 150 °C (4.1 bar) and 0.4 M concentration of  $\text{H}_2\text{SO}_4$  for a 84 % Zn recovery, and that the concentration of the acid is the most important factor for the increase of zinc extraction. Pressure hydrometallurgical recovery of zinc from EAF dust is feasible at a reasonable recovery yield, while iron mostly remains in the solid phase.

This work gave important hints to tackle gahnite hydrometallurgically, in terms of temperature, pressure, L/S ratio, sampling and lixiviant concentration (see Chapter 4).

### b) Pyrometallurgical route

On the other hand, Ye *et al.* <sup>[11]</sup> studied pyrometallurgically the zinc recovery from zinc ferrite  $\text{ZnO} \cdot \text{Fe}_2\text{O}_3$  by a low temperature reduction with carbon where ZnO is liberated according to the following chemical reaction:



This reduction process takes place at 700 – 800 °C and leaves metallic iron as residue. According to thermodynamic calculations, at temperatures below 750 °C, ZnO will not be reduced but the Fe-oxides will be and, at 800 °C, ZnO-reduction will be initiated but at a very low level.

Laboratory scale tests were conducted with three reductants, anthracite, coke breeze and powder graphite, for heat treatment in the range of 2 – 3 h, showing the reduction to metallic iron and ZnO as expected from theoretic calculations, at both 750 °C and 800 °C.

It was also concluded that the residue consists mostly of metallic iron and that higher temperature will give higher reaction rate, achieving over 85 % of zinc extraction by treatment with carbon at 800 °C.

This work showed important insights for this thesis research and exploring the concept with the spinel  $\text{ZnO} \cdot \text{Al}_2\text{O}_3$  (see Chapters 3 and 6).



## 3 THERMODYNAMICS

### 3.1 Ellingham diagram

Gahnite is a very stable compound. Its enthalpy of formation is -495.05 kcal/mol, which is much lower than other zinc-bearing species. For zinc ferrite, zincite and zinc blende the enthalpy of formation is -281.8, -83.772 and -48.518 kcal/mol respectively. This fact could explain difficulties for processing the spinel in question. Most likely, acid leaching would not be as successful as for other zinc compounds due to the high stability. Pyrometallurgical treatment is aimed at reducing zinc from oxides, so analysis of the Ellingham diagram for oxides is applicable (Figure 3.1).

The position of the line for a given reaction on the Ellingham diagram shows the stability of the oxide as a function of temperature. Reactions closer to the top of the diagram are the most “noble” metals (*e.g.*, gold and platinum), and their oxides are unstable and easily reduced. Moving in the opposite direction in the diagram, metals become progressively more reactive and their oxides become harder to reduce.

A given metal can reduce the oxides of all other metals whose lines lie above theirs on the diagram. For reduction of zinc from its oxides all metals below its stability function would be useful: Na, Cr, Mn, V, Si, Ti, Al, U, Li, Mg, Ca.

Taking into account the availability and ease of handling of the metals, aluminium was selected as a reduction agent for experiments. An experimental proof was required, since gahnite contains zinc oxide in a spinel structure with very stable aluminium oxide.

Since the  $2C + O_2 \Rightarrow 2CO$  line is downward-sloping, it cuts across the lines for many of the other metals. This feature makes carbon useful as a reducing agent, because as soon as the carbon oxidation line goes below a metal oxidation line, the carbon can then reduce the metal oxide to metal. So, for example, solid carbon can reduce chromium oxide once the temperature exceeds approximately 1225 °C. The line of the reaction of carbon monoxide formation crosses the line for zinc oxide formation at around 950 °C and was considered as a reduction agent for gahnite as well.

Based on the aforementioned considerations, two routes were explored for the reduction of gahnite: a common reduction treatment with carbon, and reduction with aluminium powder. The aluminothermic reduction was taken as a secondary approach in the beginning of this research (this situation will be explained later on).

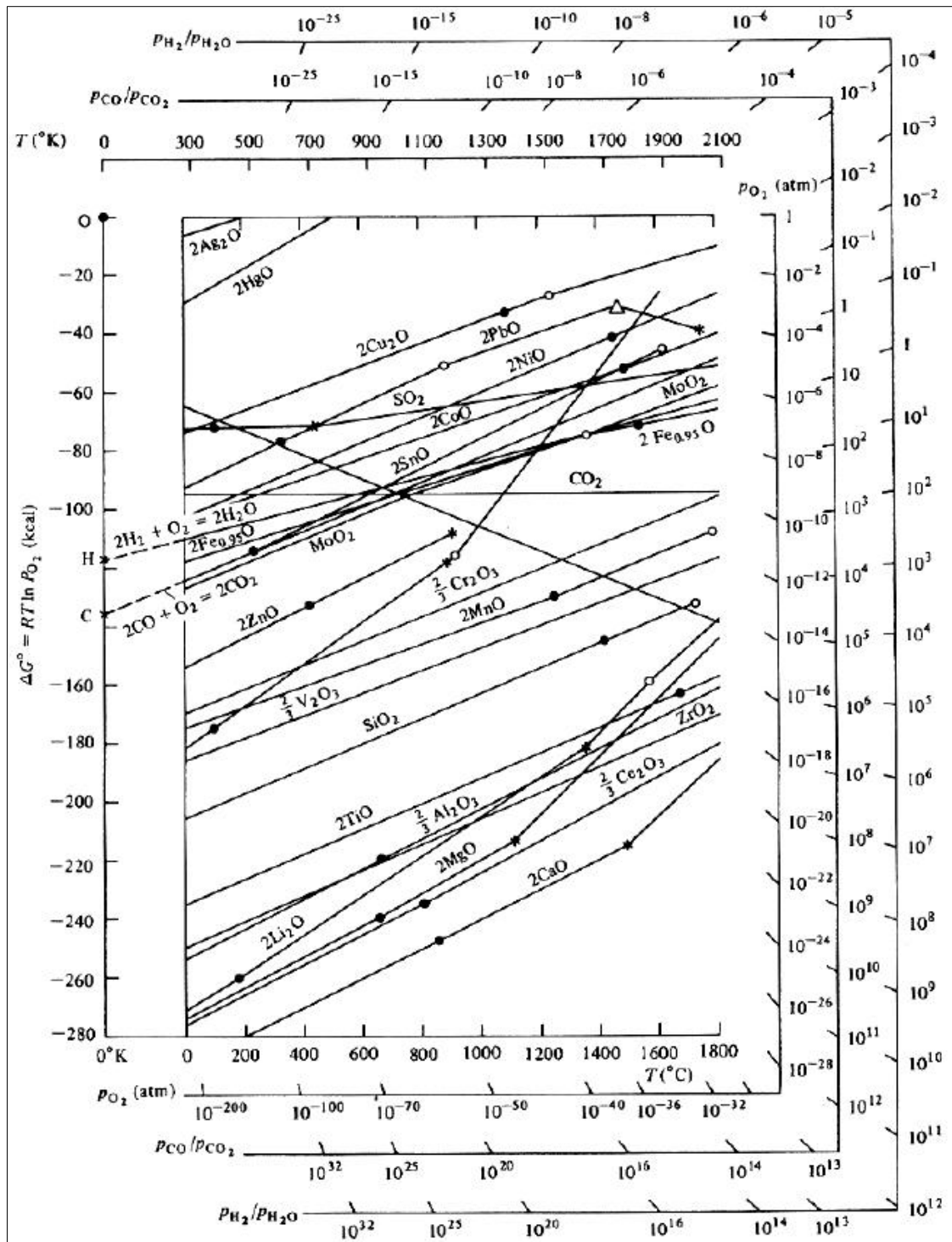


Figure 3.1 Ellingham diagram for oxides.

Prior to experiments, the thermodynamics of the reduction processes was analyzed using HSC Chemistry software. Firstly, a simple experiment of heat treatment of gahnite without any reducing agent was calculated (Figure 3.2). This figure shows that equilibrium concentration of ZnO increases with temperature rise and stability of gahnite decreases. However, at 1500°C equilibrium concentration of gahnite decreased by around 30 % only. In order to get zinc for the released zinc oxide, an additional treatment as acid leaching will be necessary, making the thermal treatment without reduction agent an impractical method.

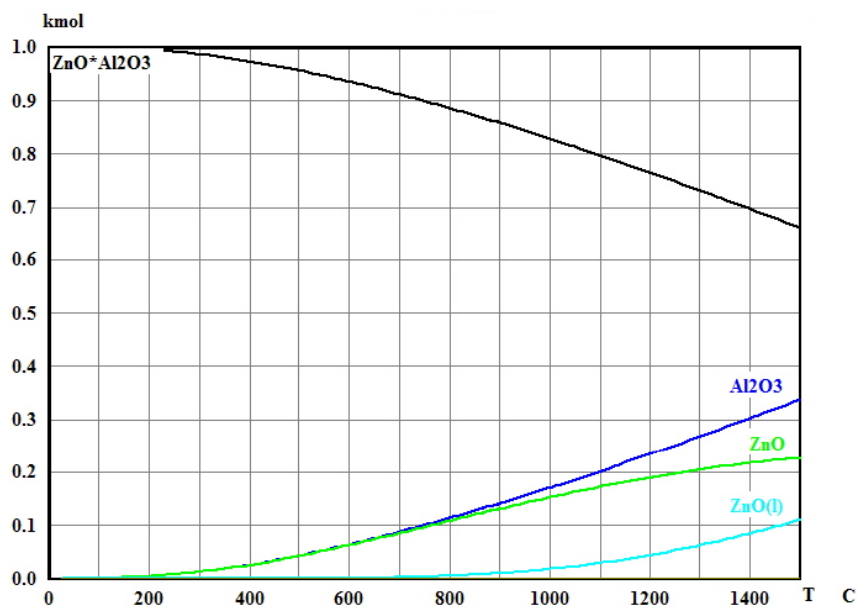


Figure 3.2 Equilibrium compositions for thermal decomposition of pure gahnite (linear scale).

### 3.2 Carbothermic reduction of gahnite

Reduction with carbon was used for treatment of zinc ferrite  $\text{ZnO} \cdot \text{Fe}_2\text{O}_3$  (another relevant zinc spinel, see Chapter 2) by the MEFOS research team<sup>[11]</sup> in Sweden. Thermodynamics of a possible carbothermic reduction of gahnite was analyzed with the same software. Carbon is a cheap and accessible compound widely used for reduction processes.

The following table and graph show equilibrium compositions for the reduction reaction of gahnite with carbon in a 1:1 stoichiometric ratio of the reagents. Full reduction of gahnite can be expected around 1163 – 1164 °C. However, kinetics factors can play a role in heterogeneous reactions.

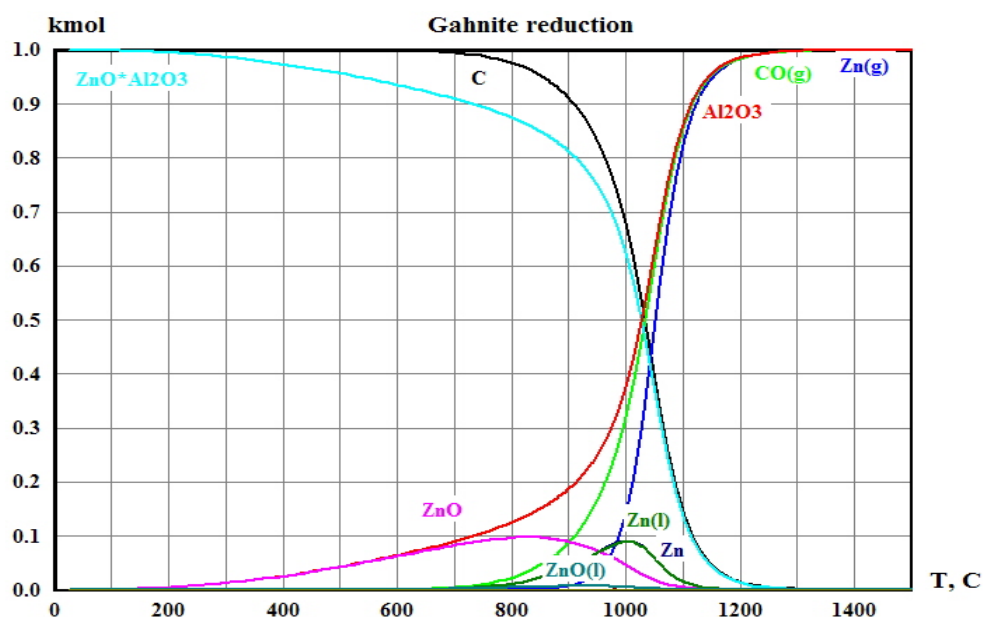


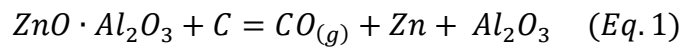
Figure 3.3 Equilibrium compositions in reduction of gahnite with carbon (linear scale).

Gahnite becomes less stable as the temperature rises; a peak of the concentration of ZnO appears at about 800 °C. Zinc starts to be formed around 800 °C, whereas a maximum concentration for Zn<sub>(l)</sub> and Zn<sub>(s)</sub> is at the 1000 °C level.

Above 700 °C, concentration of carbon decreases rapidly, and disappears completely at about 1200 °C. This confirms that carbon acts as a reduction agent for gahnite.

Due to its volatility, the zinc produced will evaporate and form Zn<sub>(g)</sub> and above the 1150 °C level this is the only zinc-bearing compound in the system. Other product of the reaction is Al<sub>2</sub>O<sub>3</sub>.

Complete reduction of gahnite should happen above 1200 °C, with the formation of aluminium oxide and zinc gas (please refer to Eq.1).



Constant of the reaction is above unity around 1100 °C, as it can be seen in Table 3.1, where enthalpy, entropy, Gibbs free energy, constant of the reaction and its logarithmic value are shown.

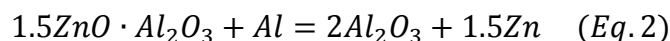
Enthalpy of the reaction decreases slowly with the temperature rise, but the Gibbs energy becomes negative about 1100 °C, showing a probability of the reaction to take place.

In total, carbothermic reduction of gahnite is a feasible route for zinc production. The limiting factor is energy consumption, since temperature above 1100 °C is required.



### 3.3 Aluminothermic reduction of gahnite

Aluminium is an active metal and used too as reduction agent. With HSC Chemistry, the following reaction could take place:



The following graph shows the formation of  $\text{Zn}_{(\text{g})}$  at around 900 °C, which is mainly gas product at higher temperatures.

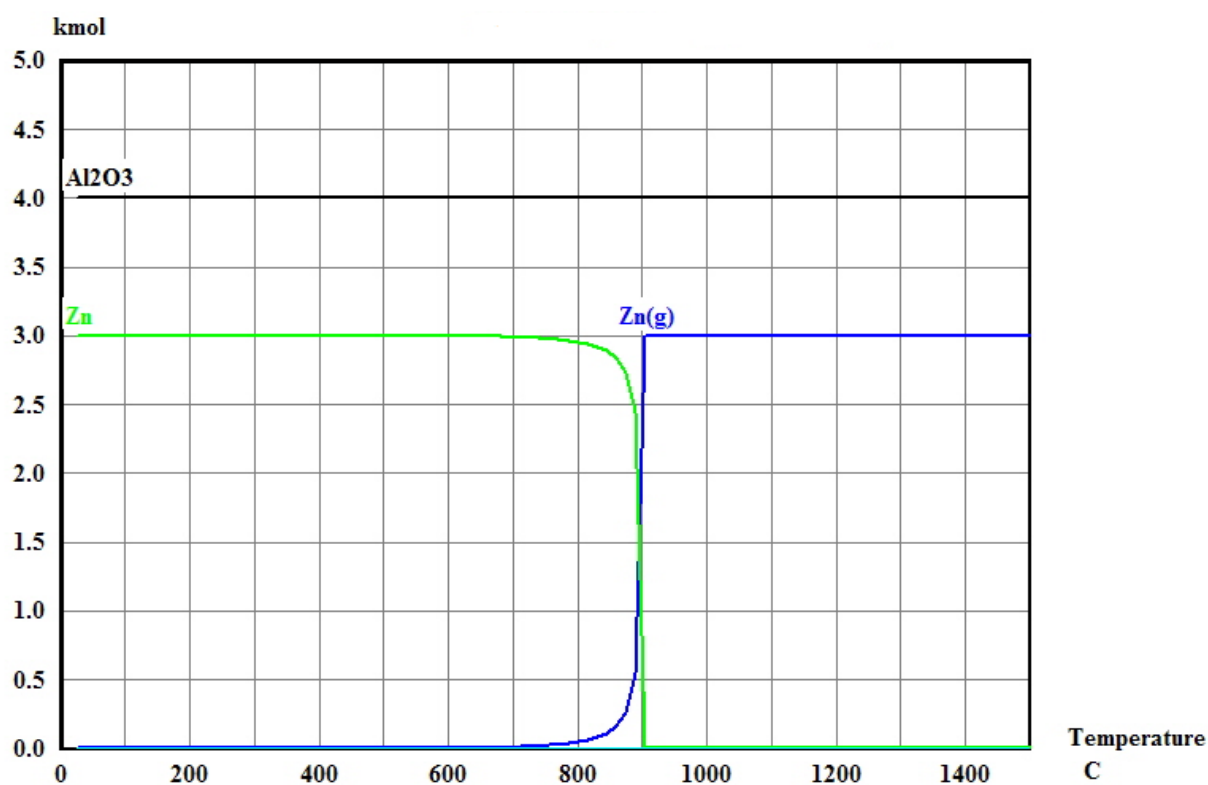


Figure 3.4 HSC Chemistry graph for reduction of gahnite with aluminium.

From Figure 3.4, it can be observed that, in the presence and contact of pure aluminium, zinc in the gas phase starts to appear slowly just below 800 °C, in concordance to the sudden decrement as a solid in the range 850 – 900 °. This situation confirms that aluminium powder is acting as a reducing agent of gahnite. The calculation shows then a high probability that all the zinc contained in the spinel is present only in the gas phase for the range 900 – 1000 °C, while  $\text{Al}_2\text{O}_3$  is observed to remain stable, as a solid, without the presence in any form of zinc higher than that range.

Given this novel approach, it results to be interesting to prove this heat treatment experimentally, at which temperature the reaction actually takes place and thus gahnite can be converted completely. The thermodynamic calculations give only probability of the process and kinetics play an important role in heterogeneous processes.

### 3.4 Additional tests

A new set of additional tests, previously not considered in the early stages of this research, was conducted after running the first attempts to reduce gahnite both carbo and aluminothermically, in order to explore and gather –if possible– more information about the extractive metallurgy of the zinc spinel. Addition of chemical agents such as  $\text{SiO}_2$  and  $\text{CaO}$  was studied.

#### 3.4.1 Gahnite and carbon and silica

This type of experiments will be referenced to as  $\text{G} + \text{C} + \text{SiO}_2$  onwards. In a number of processing studies, a slag formation was found to maybe lower the temperature of reaction and enhance metal recovery. The aim of these experiments is to add  $\text{SiO}_2$  together with adding carbon. Calculations using HSC Chemistry show strong formation of  $\text{Zn(g)}$  and  $\text{CO}$  at 100 °C lower temperature (Fig. 3.4) than for the reaction without silica (please see Fig. 3.2). The reaction with silica addition is fully completed already at around 1150 °C, whereas without silica is at around 1250 °C.

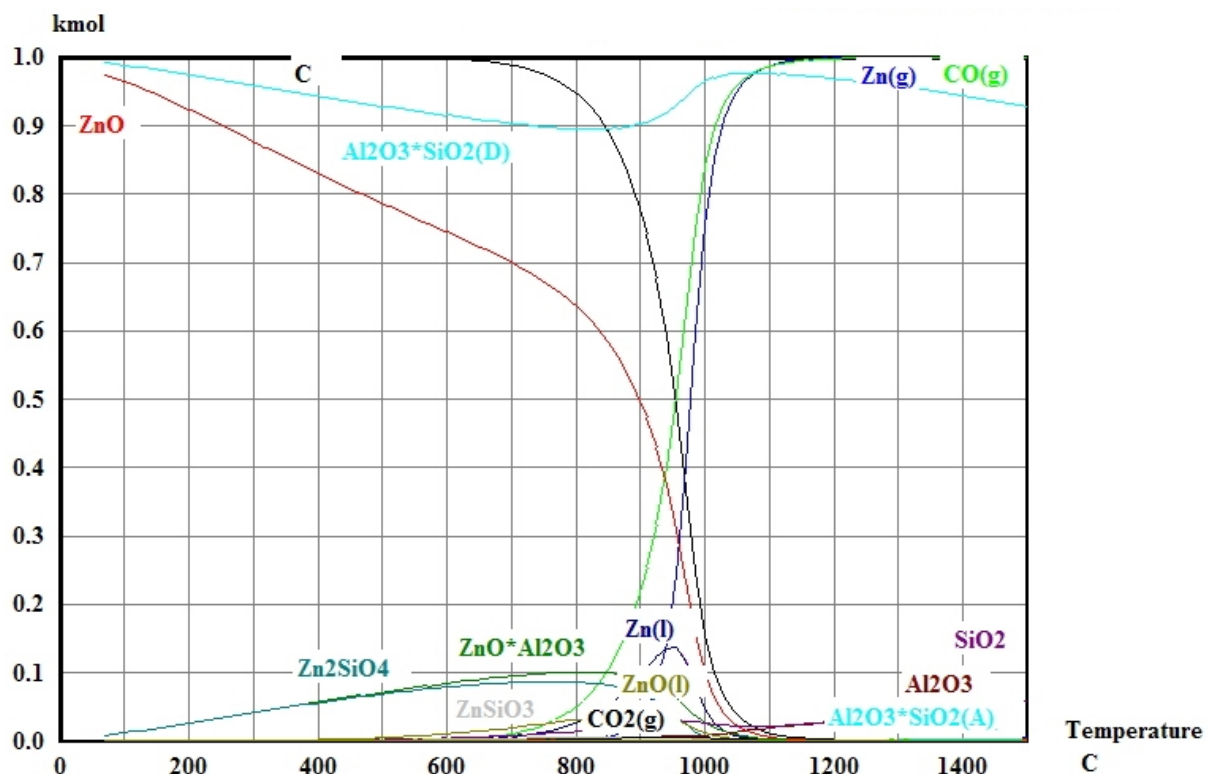


Figure 3.5 HSC Chemistry graph for reduction of gahnite with carbon and addition of  $\text{SiO}_2$ .

The gain in temperature is probably due to formation of a  $\text{Al}_2\text{O}_3 \cdot \text{SiO}_2$  compound, which is thermodynamically more stable than  $\text{ZnO} \cdot \text{Al}_2\text{O}_3$ , according to this calculation.

From around 850 °C, the concentration of  $\text{Zn}_{(g)}$  starts to raise rapidly, being the condition at about 1100 °C ahead more favourable. Just after 600 °C, concentration of C decreases rapidly, and disappears completely between 1100 – 1200 °C. This confirms that carbon is acting as a reductant for gahnite.

Zn produced in this process forms vapour  $\text{Zn}_{(g)}$  and around 1100 °C this is the only zinc-bearing compound in the system.

The mix of gahnite and only silica (referenced to as G +  $\text{SiO}_2$ ) was also studied, finding with HSC Chemistry that, if any reaction of interest takes place, it does high above 1500 °C, making it then impracticable. This can be observed in the following graph.

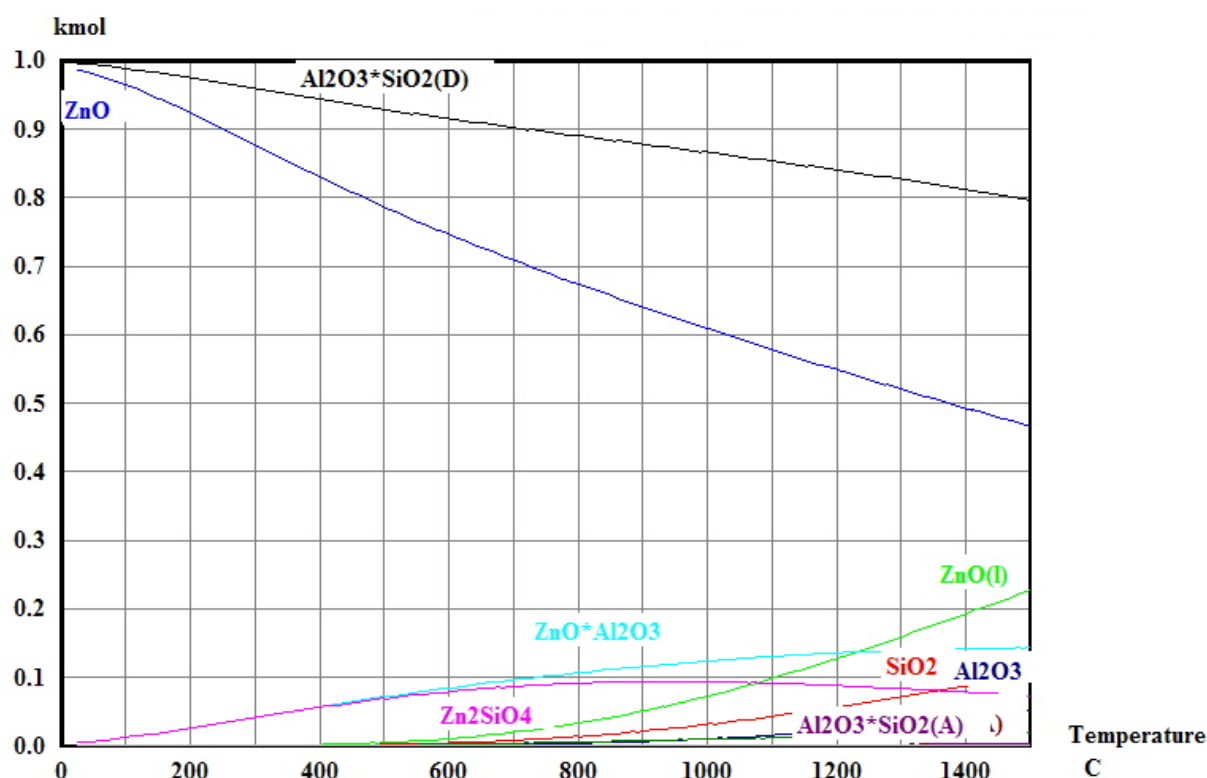


Figure 3.6 HSC Chemistry graph for decomposition of gahnite and addition of  $\text{SiO}_2$ .

### 3.4.2 Gahnite and aluminium and silica

This type of experiments will be referenced to as G + Al +  $\text{SiO}_2$  onwards. Slag formation could lower the reaction temperature and enhance the extraction of zinc from gahnite. In this case, the idea is to form a slag by the addition of  $\text{SiO}_2$  to the mixture of gahnite and aluminium.

The calculations using HSC Chemistry show that an aluminosilicate  $\text{Al}_2\text{O}_3\cdot\text{SiO}_2$  is more stable than gahnite, so that thermodynamically zinc can be formed already at low temperatures (please see Fig. 3.6).



Just below 1000 °C, there is a considerable increase of the concentration of  $\text{Zn}_{(g)}$ , which is the only gas product above 1000 °C.

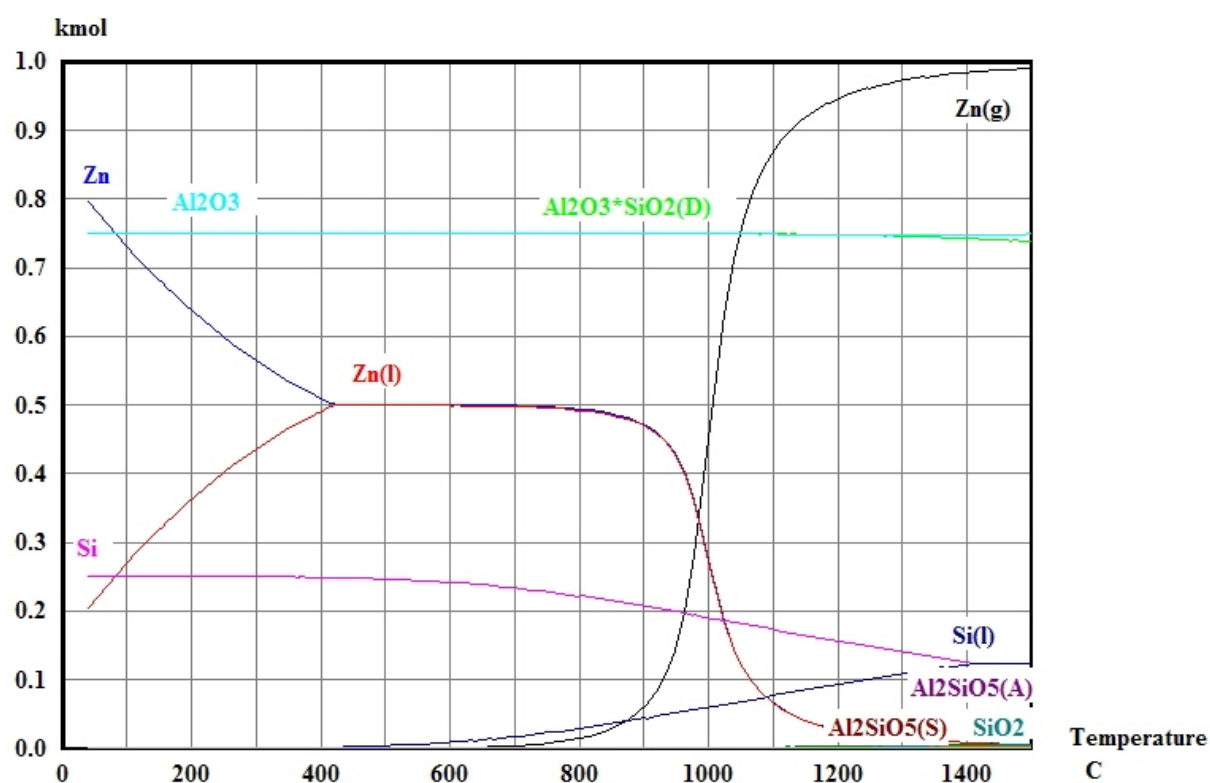


Figure 3.7 HSC Chemistry graph for reduction of gahnite with aluminium and addition of  $\text{SiO}_2$ .

## 4 EXPERIMENTAL

In this section, a description of characteristics such as raw materials, tests plan and experimental set-up is to be given.

### 4.1 Raw materials

The raw materials utilized during most of the relevant experiments were zinc ferrite  $\text{ZnO} \cdot \text{Fe}_2\text{O}_3$  and gahnite  $\text{ZnO} \cdot \text{Al}_2\text{O}_3$ . Even though ferrite is easily available from a number of chemical providers, it was produced synthetically at the CiTG/LMP facilities in order to save costs. On the other hand, gahnite is not available from any provider, and therefore the only option was to conduct a heat treatment for obtaining a synthetic pure compound. The procedure for both cases is explained in sections 4.1.1 and 4.1.2 correspondingly.

Other chemicals involved in the experiments were:

- i) acids as leaching agents: sulphuric acid  $\text{H}_2\text{SO}_4$  (95 – 97 %)  
hydrochloric acid  $\text{HCl}$  ( $\geq 37$  %)  
nitric acid  $\text{HNO}_3$  ( $\geq 65$  %)
- ii) demineralized water (extra filtered) for dilution of acid concentration
- iii) carbon as reducing agent, in the form of fine graphite powder
- iv) aluminium as reducing agent, in the form of small, rough balls
- v) aluminium as reducing agent, in the form of fine powder

#### 4.1.1 Zinc ferrite synthesis

- Equimolar amounts of zinc oxide ( $\text{ZnO}$ ) and ferric oxide ( $\text{Fe}_2\text{O}_3$ ) powders are mixed in an agate mortar and mechanically mixed by a turbula for a period of 30 min.
- The mixed powder is next compacted into briquettes at  $30 \text{ kg/cm}^2$  and heated to  $1100^\circ\text{C}$  for 5 h and then cooled by air.
- The briquettes are afterwards crushed into fine particles ( $<100 \mu\text{m}$ ) by a disk mill in 30 s, and analyzed by XPRD.
- This procedure is based on [2], though it was updated by: use of platinum crucible instead of agate mortar; 6 h instead of 5 h of heat treatment.

Figure 4.1 in the next page is a photograph of the box furnace taken during the procedure.



Figure 4.1 Heat treatment for zinc ferrite synthesis.

#### 4.1.2 Gahnite synthesis

- Equimolar amounts of zinc oxide ( $\text{ZnO}$ ) and aluminium oxide ( $\text{Al}_2\text{O}_3$ ) are thoroughly milled for 5 min in a Retch milling machine.
- After milling, the material is put in an alumina crucible and heated up to  $1000\text{ }^\circ\text{C}$  for 6 h.
- It is then subjected to a dilute solution of sulphuric acid (10 g/L) for 0.5 h to dissolve all the remaining  $\text{ZnO}$ .

This procedure is based on [1], though it was also updated by: use of platinum crucible instead of alumina crucible; heat treatment at  $1100\text{ }^\circ\text{C}$  instead of  $1000\text{ }^\circ\text{C}$ ; acid concentration of 20 g/L instead of 10 g/L; LX time of 1.0 h plus maximum stirring instead of 0.5 h; subsequent thorough water washing of the product for 1.0 h plus maximum stirring.

Figure 4.2 shows an image of the heat treatment, with gahnite inside the Pt crucible.



Figure 4.2 Heat treatment for gahnite synthesis (close-up at the platinum crucible).

#### 4.1.2.1 XRD pattern of gahnite without full procedure

The next two graphs exemplify the product of an unsuccessful synthesis of gahnite.

Figure 4.3 shows clearly the patterns of both synthetic gahnite and zinc oxide ZnO. The presence of ZnO in the product of the procedure indicates that not all the ZnO reacted with the  $\text{Al}_2\text{O}_3$ . This may be due to an interrupted heat treatment, insufficient amount of  $\text{Al}_2\text{O}_3$  in the mix before heat treatment, or insufficient temperature or reaction time for a complete synthesis.

Figure 4.4 shows the pattern of gahnite and also a synthetic gunningita  $\text{Zn}(\text{SO}_4)(\text{H}_2\text{O})$ . Presence of this unusual compound is probably because of an interrupted heat treatment or insufficient reaction time for a full synthesis of the original powders to form gahnite.

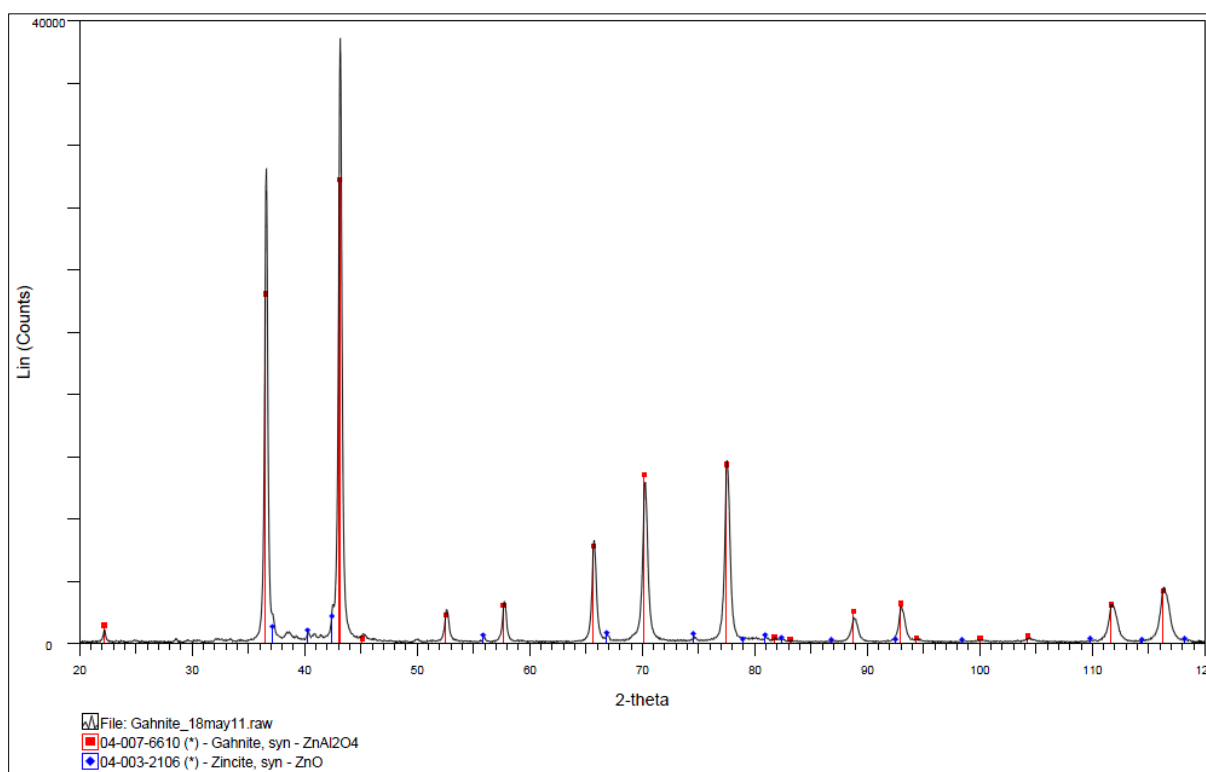


Figure 4.3 Example 1 of XRD pattern of (impure) gahnite without full procedure.

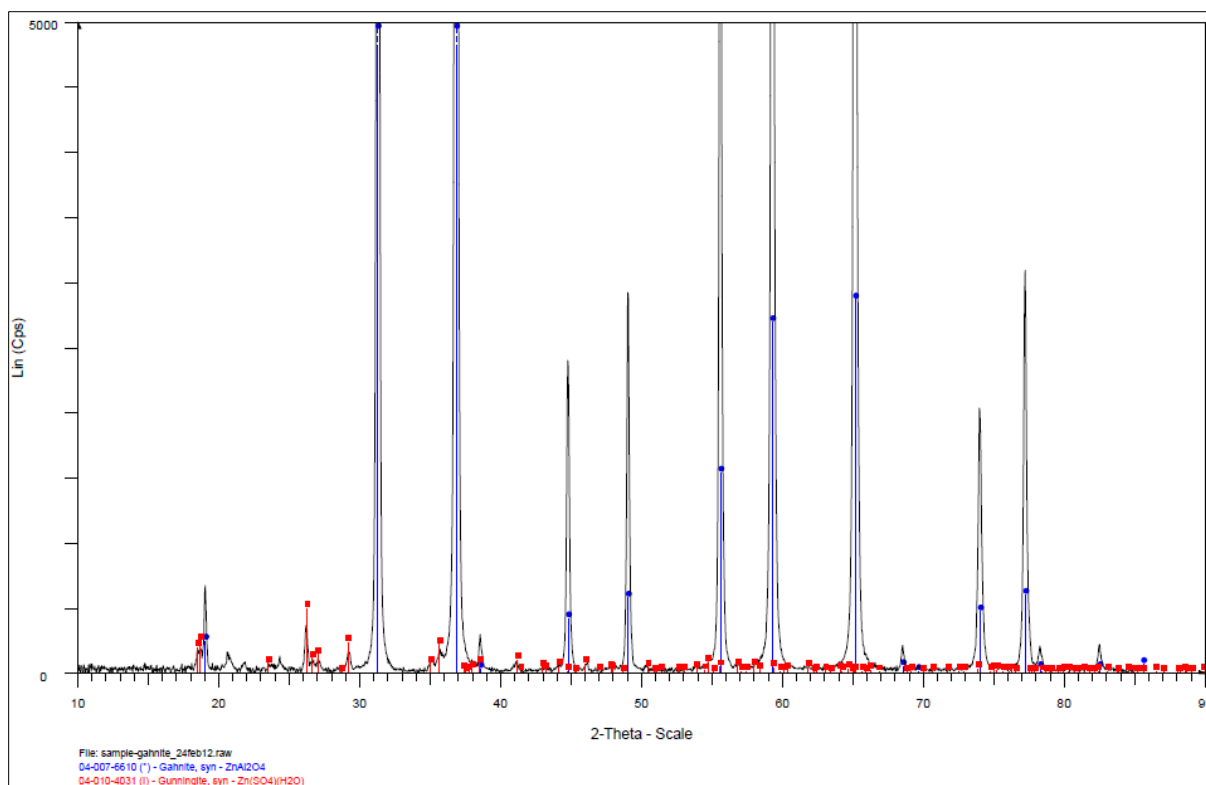


Figure 4.4 Example 2 of XRD pattern of (impure) gahnite without full procedure.

#### 4.1.2.2 XRD pattern of gahnite after full procedure

The graph in the following page shows a perfect pattern for pure gahnite, without the presence of neither any remains of single ZnO or  $\text{Al}_2\text{O}_3$  nor transitional synthetic zinc compounds. This is the gahnite powder that was utilized in all the experiments.

	Compound	Conc.	Absolute
	Name	wt(%)	Error (%)
1	$\text{Al}_2\text{O}_3$	50.9	0.1
2	$\text{Fe}_2\text{O}_3$	0.0247	0.005
3	$\text{SO}_3$	1.57	0.04
4	$\text{SiO}_2$	0.0479	0.007
5	ZnO	47.5	0.1

Figure 4.5 XRF results of pure gahnite.

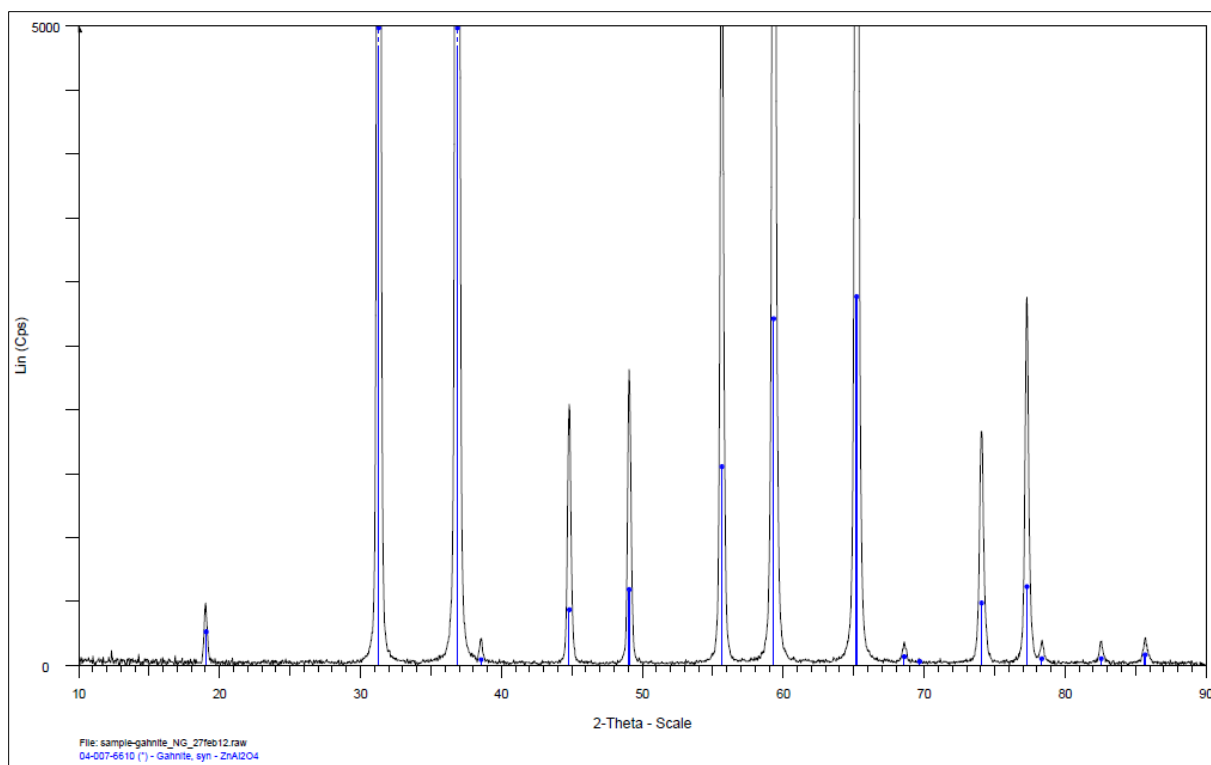


Figure 4.6 XRD pattern of pure gahnite.



Figure 4.7 A few grams of pure synthetic gahnite ready to work experimentally with.

## 4.2 Experiments strategy

The experimental strategy consisted in two stages: the first one entailed two hydrometallurgical attempts to explore the possibilities of acid leaching of gahnite (atmospheric and pressure leaching), while the second one comprised two sets of pyrometallurgical treatment in order to discover the reduction of the spinel in question (carbothermic and aluminothermic reduction).

### 4.2.1 Hydrometallurgy plan

The hydrometallurgical treatment involved first an atmospheric acid leaching which, after exhibiting non-detected dissolution results in terms of zinc extraction, was followed by an acid pressure leaching.

#### 4.2.1.1 Atmospheric leaching (ALX)

Taking usual practices for atmospheric leaching referenced in the Literature Review, the following set of tests was planned and carried out.

Table 4.1 Tests performed for atmospheric leaching of gahnite.

EXPERIMENTS PLAN FOR ATMOSPHERIC LEACHING						
LX agent	Concentration [M]	Gahnite [g]	Pressure [bar]	Temperature [°C]	L/S	Time [min]
H <sub>2</sub> SO <sub>4</sub>	4.0	11.70	1.01	95	10	120
HCl	4.0	10.13	1.01	95	10	120
HNO <sub>3</sub>	4.0	9.93	1.01	95	10	120

Acid concentration was increased in all three cases, as well as keeping reasonably high numbers for temperature, L/S and leaching time, plus continuous stirring. Very small amount of filtered demineralized water was added at a certain point in order to keep the total volume equal to the initial conditions.

Sampling was performed every 15 min so that –ideally– a zinc extraction curve could be established, if. As a result, there were taken eight samples of 5 mL per LX agent: G1.1 to G1.8 for H<sub>2</sub>SO<sub>4</sub>, G2.1 to G2.8 for HCl and G3.1 to G3.8 for HNO<sub>3</sub>.

Additionally, a mass balance between the initial amount of gahnite and the remaining residue after the two hours of leaching was also made. Afterwards, a similar second set of tests would be prepared without diluting the acids.

#### 4.2.1.2 Pressure leaching (PLX)

As stated in Chapter 2, there is not a single reference of attempting to perform a pressure leaching of gahnite. Taken some reference points into account for designing an experimental plan, the following was defined in the beginning:

Table 4.2 Initial plan for pressure leaching of gahnite with H<sub>2</sub>SO<sub>4</sub>.

PLX with H <sub>2</sub> SO <sub>4</sub>						
Temperature [°C]	Pressure [bar]	Concentration [M]	L/S	Mass [g]	Sampling [min]	Stirring rate
100	1.01	0.3 up to 2.0	10 or higher	< 12	5, 15, 30, 45, 60, 90, 120, 150	Maximum and constant
150	4					
200	15					
250	39					
300 ?	?					

Table 4.3 Initial plan for pressure leaching of gahnite with HCl.

PLX with HCl						
Temperature [°C]	Pressure [bar]	Concentration [M]	L/S	Mass [g]	Sampling [min]	Stirring rate
100	1.01	0.3 up to 2.0	10 or higher	< 12	5, 15, 30, 45, 60, 90, 120, 150	Maximum and constant
150	4					
200	15					
250	39					
300 ?	?					

Table 4.4 Initial plan for pressure leaching of gahnite with HNO<sub>3</sub>.

PLX with HNO <sub>3</sub>						
Temperature [°C]	Pressure [bar]	Concentration [M]	L/S	Mass [g]	Sampling [min]	Stirring rate
100	1.01	1.0 up to 6.0	10 or higher	< 12	5, 15, 30, 45, 60, 90, 120, 150	Maximum and constant
150	4					
200	15					
250	39					
300 ?	?					

Table 4.5 Initial plan for pressure leaching of gahnite with NaOH.

PLX with NaOH						
Temperature [°C]	Pressure [bar]	Concentration [M]	L/S	Mass [g]	Sampling [min]	Stirring rate
100	1.01	1.0 up to 2.0	10 or higher	< 12	5, 15, 30, 45, 60, 90, 120, 150	Maximum and constant
150	4					
200	15					
250	39					
300 ?	?					

The values of the pressure variable were only an estimate since the autoclave control box can only adjust temperature. Also, the temperature level of 300 °C was not sure to be reached because it depended on the performance of the device.

As it will be described in the Results Chapter, there were several operational constraints for carrying this plan out fully. First, the use of HCl and NaOH had to be discarded due to corrosion restrictions of the titanium-based container <sup>[12] [13]</sup>. And secondly, only low



concentrations for  $\text{H}_2\text{SO}_4$  and  $\text{HNO}_3$  were possible to be used for the same reasons; this led to prefer a very high liquid-to-solid ratio on one hand, and, on the other, taking special and careful precautions, to try to reach a very high temperature (and consequential pressure) in the vessel during the test itself. Thus, the adjusted plan for pressure leaching of gahnite was the next:

Table 4.6 Adjusted plan for pressure leaching of gahnite with  $\text{H}_2\text{SO}_4$ .

<b>PLX with <math>\text{H}_2\text{SO}_4</math></b>		
<b>Concentration [M]</b>	<b>Gahnite [g]</b>	<b>L/S</b>
0.50	8.52	40
0.75	8.61	40

Table 4.7 Adjusted plan for pressure leaching of gahnite with  $\text{HNO}_3$ .

<b>PLX with <math>\text{HNO}_3</math></b>		
<b>Concentration [M]</b>	<b>Gahnite [g]</b>	<b>L/S</b>
0.50	8.33	40
4.00	8.28	40

#### 4.2.1.3 Experimental set-up for PLX

PLX tests were performed in a Parr 4841 autoclave of one litre of capacity. According to the manufacturer, this device can operate up to  $400^\circ\text{C}$  and up to 600 PSI (approximately 41.3 bar). It includes an internal container made up of titanium in which the solution to be leached is placed (it is recommended not to fill it completely). On the middle top of this container a stirrer is located to provide the appropriate stirring to the solution during the experiments. Also, on top of the reactor, the pressure meter is placed along an external (secondary) thermocouple for independent temperature readings. Adjacent to it, a sampling device is available by opening and closing small valves which allow the entry of solution and subsequent semi cooling for the actual sampling in one of the extremes.

A simple set of pipes was also installed in order to deliver fast cooling of the autoclave when needed, especially in risky circumstances such as unexpected pressure or temperature rises.

This set-up was given maintenance and tested by Mr. Jan van Os of the Process & Energy Department at TU Delft, with the autoclave working at maximum pressure with hot water during a full week, detecting no leaks. Figures 4.8 and 4.9 show the set-up put in place at the Hydrometallurgy Lab and a close-up of the pressure meter respectively, both during real experiments.



Figure 4.8 Autoclave featuring pressure meter, set of water cooling pipes, external thermocouple and sampling pipe.

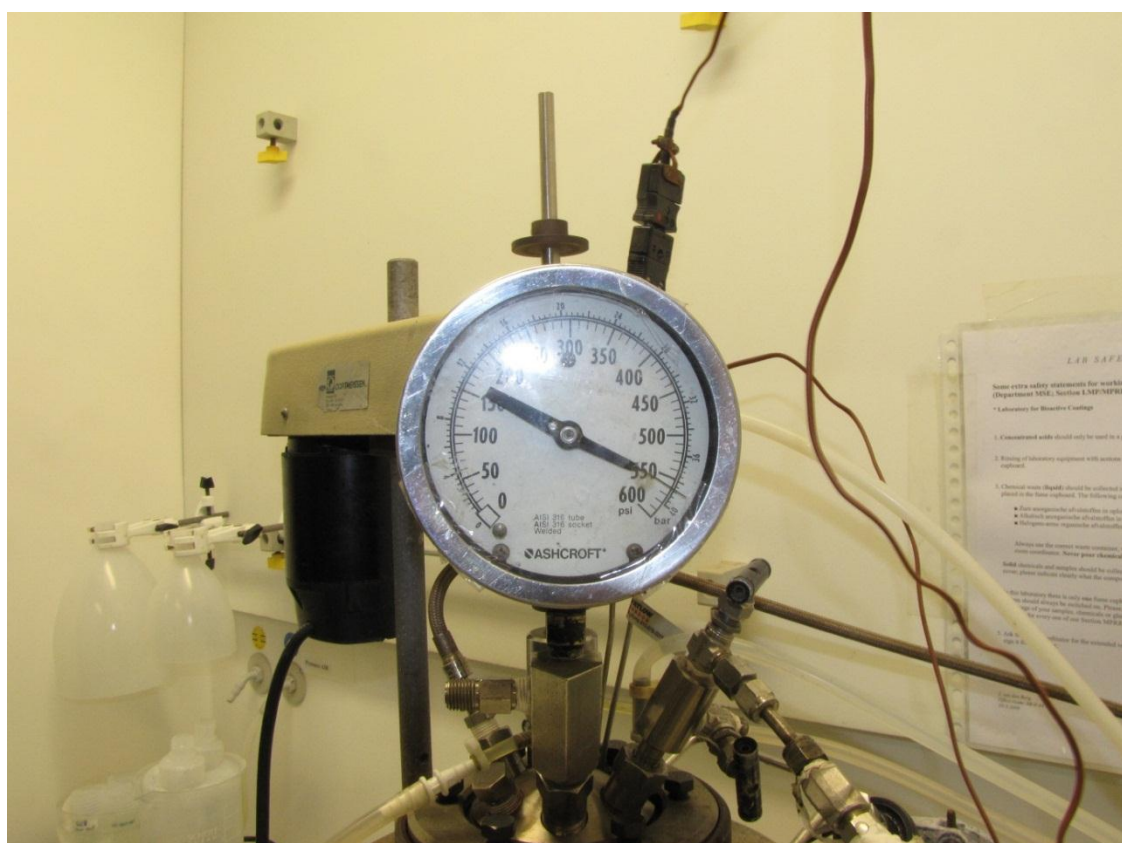


Figure 4.9 Close-up at autoclave's pressure meter during an experiment.

The following photograph shows the controller of the autoclave, by which the temperature of the vessel and the stirring speed can be manually controlled.



Figure 4.10 Autoclave controller and external thermocouple controller.

#### 4.2.2 Pyrometallurgy plan

The following plan was prepared in order to conduct a set of pyrometallurgical experiments with gahnite  $\text{ZnO} \cdot \text{Al}_2\text{O}_3$ , aiming at achieving a reduction with carbon C.

The state of this gahnite is a whitish, fine powder, as can be seen in the Figure 4.7.

This material was produced synthetically and purified at the LMP facilities during previous stages (as described in section 4.1.2). XRD and XRF analyses confirm the state of the compound (please refer to Figures 4.5 and 4.6).

On the other hand, carbon is available as graphite also as a fine powder (the provider is Fluka Chemika).



Figure 4.11 Pure carbon powder (graphite) utilized for the carbothermic reduction experiments.

#### 4.2.2.1 Plan

The first route was studied through a series of tests with pure carbon powder at different temperatures, taking into account the thermodynamics analysis of Chapter 3, starting at 1300 °C and going down every 50 °C as low as any reduction would take place. Initially, it was planned to run these experiments with a 1:1 stoichiometric ratio between gahnite and carbon, however it was later decided to add a small extra amount of reductant, resulting in 1:1.25 experiments. Also, at first a few tests were carried out for two hours, yet as results were being obtained only one hour proved to be an appropriate duration for heat treatment. The value for heating rate reflects common practice for lab scale pyrometallurgical tests and the mixing of the powders with the Retsch machine during half an hour was seen adequate. Argon injection was set as to make sure to fill the furnace with gas at a constant flow rate without spreading the already mixed (loose) powder contained in the crucible.

Table 4.8 Initial plan for carbothermic reduction of gahnite.

Carbothermic reduction					
Temperature [°C]	Stoichiometric ratio	Retsch mixing [min]	Dwell time [h]	Heating rate [°C/min]	Argon injection [L/min]
1300	1:1	30	2.0	10.0	~ 3.0
1250					
1200					
1150					
1100	1:1.25	30	1.0	10.0	~ 3.0
1050					
1000					

As it would turn out later, the experiments below 1200 °C were not performed (see Chapter 6). Since almost no carbon was encountered in the residues, no higher amount of reductant was considered for further tests, staying with the 1:1.25 proportion.



For the second route, a slightly different plan was defined as no previous reference was available. Taking into consideration the thermodynamic calculations from Chapter 3, the initial temperature for these experiments was set to 1200 °C, going down every 50 °C until the expected lower limit for a successful reduction with aluminium powder. Two ratios between gahnite and aluminium were considered in the beginning, although results would later lead to the 1.5:2 stoichiometric ratio. Dwell time was straightly decided to be one hour. Several of the other operational variables were taken directly from the carbothermic route, as no other orientation was at hand. Observation and careful analyses proved to be relevant for studying this novel approach.

Table 4.9 Initial plan for aluminothermic reduction of gahnite.

Aluminothermic reduction					
Temperature [°C]	Stoichiometric ratio	Retsch mixing [min]	Dwell time [h]	Heating rate [°C/min]	Argon injection [L/min]
1200	1.5:1	30	1.0	10.0	~ 3.0
1150					
1100					
1050					
1000	1.5:2				
950					
900					

#### 4.2.2.2 Experimental set-up for reduction

The following photograph shows the set-up that was used for all the reduction tests, carbothermic and aluminothermic.

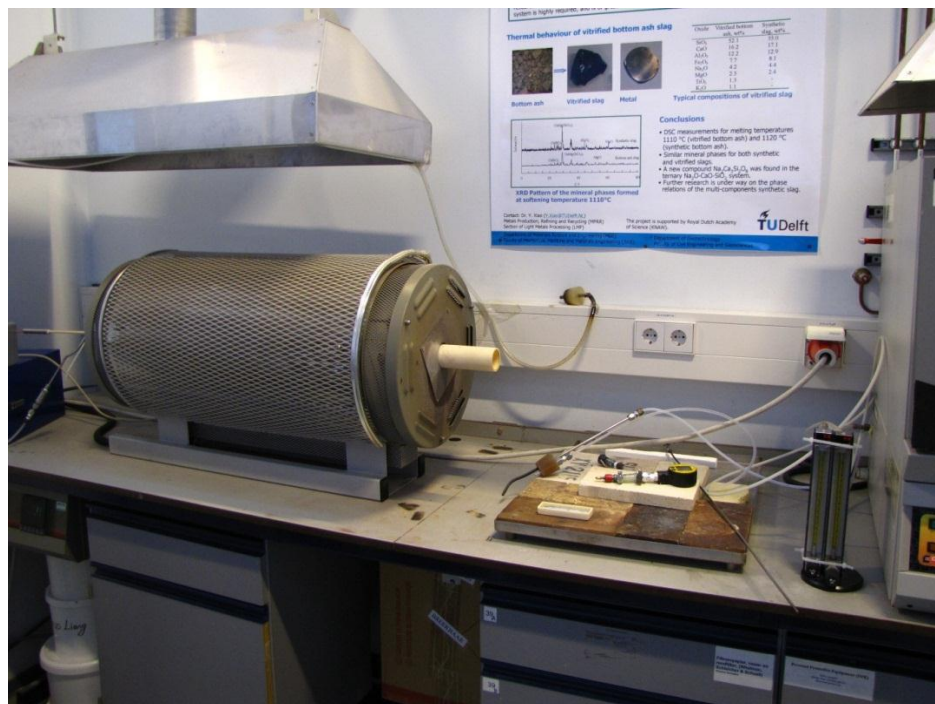


Figure 4.12 Horizontal furnace, pressure meter, flowmeter, argon gas line.

The main device of the set-up was a horizontal furnace with working capabilities up to 1500 °C and incorporating an internal horizontal tube in which the material was placed at the centre. Two corks (stoppers) were located in each extreme of the tube so as to make it as tight as possible and thus avoid heat losses, gas leaks or oxygen entering. In one extreme, argon gas was injected and controlled by a flowmeter. Also, a pressure meter was attached in order to monitor the pressure behaviour during some of the aluminothermic trials. In the other extreme, an independent thermocouple was placed along with an exit for the horizontal tube. Temperature and heating rate were configured in the furnace controller. As it would turn out, no significant difference was detected between the temperature set at the controller and the readings from the separate thermocouple.

## 5 RESULTS OF HYDROMETALLURGICAL TREATMENT

### 5.1 Atmospheric leaching

Results from this first set of hydrometallurgical tests were a non-detected dissolution under the working conditions. Regardless of an adequate time for leaching and somehow high levels of acids concentration, temperature and L/S in comparison to a standard atmospheric procedure (plus continuous stirring), no dissolution of the gahnite was detected and no zinc was extracted. For each leaching agent, sampling was performed every 15 min so that an extraction curve could be established for zinc with ICP results at hand. However, before that, a simple mass balance was done between the initial gahnite and the residue left after each test, which in all three cases turned out to show no significant change. The following table summarizes this outcome.

Table 5.1 Tests performed for atmospheric leaching of gahnite.

RESULTS OF ATMOSPHERIC LEACHING OF GAHNITE							
LX agent	Concentration [M]	Gahnite [g]		Pressure [atm]	Temperature [°C]	L/S	Time [min]
		Before	After				
H <sub>2</sub> SO <sub>4</sub>	4.0	11.70	11.66	1	95	10	120
HCl	4.0	10.13	10.10	1	95	10	120
HNO <sub>3</sub>	4.0	9.93	9.91	1	95	10	120

The marginal loss in the mass balance is probably due to sampling and sample handling, and not to any reaction. This is supported by XRD and XRF analysis of the residue, as can be observed in the following figures for the HCl leaching attempt. No zinc compound was found. The XRF result is quite similar to that of pure gahnite (see Figure 4.6). With respect to this set of temperature and acid concentration, there was no further evident of leaching.

	Compound	Conc.	Absolute
	Name	wt(%)	Error (%)
1	Al <sub>2</sub> O <sub>3</sub>	55	0.2
2	CaO	0.025	0.005
3	Cl	0.038	0.006
4	Fe <sub>2</sub> O <sub>3</sub>	0.046	0.006
5	NiO	0.015	0.004
6	SO <sub>3</sub>	0.028	0.005
7	SiO <sub>2</sub>	0.2	0.01
8	ZnO	45	0.1

Figure 5.1 XRF result of the residue from HCl leaching of gahnite.

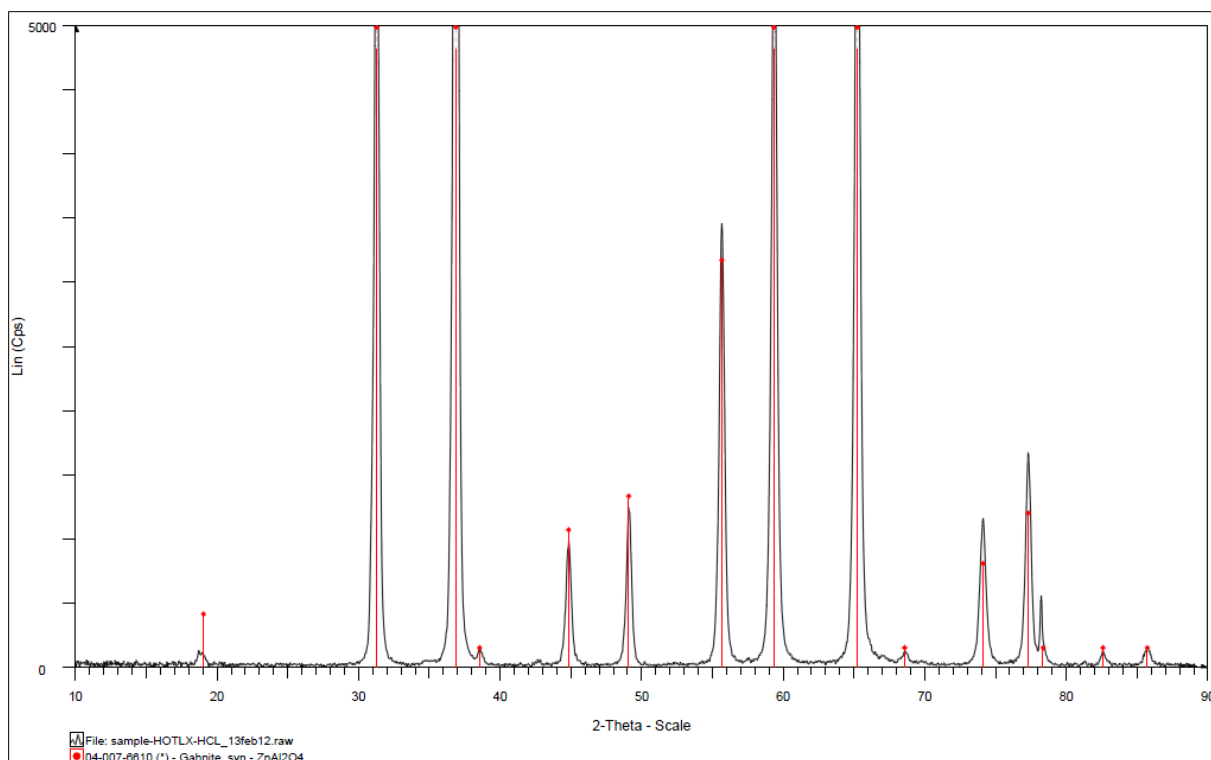


Figure 5.2 XRD pattern of the residue from HCl atmospheric leaching of gahnite.

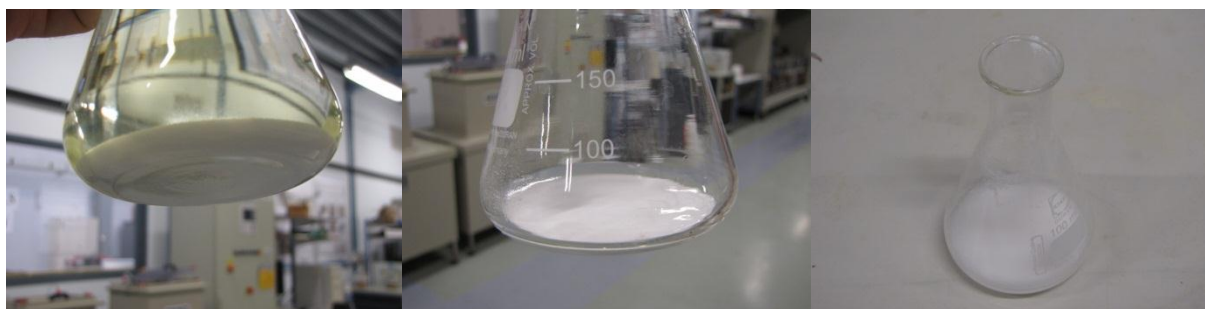


Figure 5.3 Atmospheric leaching with  $\text{HNO}_3$ ,  $\text{H}_2\text{SO}_4$  and  $\text{HCl}$  respectively.

## 5.2 Pressure leaching

High hopes were put on to possible better results for leaching the compound under more aggressive conditions, *i.e.* higher temperature and higher pressure.

As described in the previous chapter, these pressure tests were performed in a Parr 4841 1 L autoclave which allows a continuous mechanical stirring and sampling during the course of an ongoing experiment.

During all the tests performed, it must be noted that controlling the temperature (and consequently, pressure) was hard and laborious. This situation resulted in a number of failed tests, which had to be repeated. Increments of temperature had to be done very smoothly in order to achieve a stable condition of temperature/pressure. However, sudden pressure rises did happen and water cooling was required more than once. Safety precautions were



assumed from beginning to end of each pressure test, both personally and for the surroundings. Another reason for unsatisfactory tests was that the pressure of the vessel also affected the pressure inside the external sampling pipe and a few samples were lost, resulting in having to reprise the whole experiment until sampling was performed in the scheduled lapses of time, keeping in mind the objective of establishing a zinc extraction curve.

An adjusted plan for pressure leaching of gahnite is shown in Tables 4.6 and 4.7, whose results are given next.

### 5.2.1 Pressure leaching with sulphuric acid

#### 5.2.1.1 H<sub>2</sub>SO<sub>4</sub> 0.50 M

This first test of pressure leaching was carried out with sulphuric acid at a concentration of 0.50 M, considering the material restrictions of the Ti<sub>4</sub>-based container of the autoclave. The total capacity of it is 1.0 L, though it was filled with only a third with the solution of diluted acid for allowing a proper, thorough stirring of the mix at all times.

L/S was set quite high, 40. Mass of gahnite put in the autoclave was 8.51 g. Total leaching time was 1.5 h. Samples of 5 mL each were taken after 5, 10, 15, 30, 45, 60, 75 and 90 min, an sent for ICP analysis at the Process & Energy Department. Temperature was taken as high as it was seen stable as well as safe (especially), and then a certain pressure was obtained.

Table 5.2 shows the results of this test, in terms of zinc extraction, represented graphically in Figure 5.4.

Table 5.2 Metal extraction with H<sub>2</sub>SO<sub>4</sub> 0.50 M.

<b>ZnO·Al<sub>2</sub>O<sub>3</sub> + H<sub>2</sub>SO<sub>4</sub> 0.50 M</b>			
SAMPLE		METAL EXTRACTION [%]	
PLX time [min]	Name	Al	Zn
5	PLX A5 f	2.10	1.69
10	PLX A10 f	3.01	2.41
15	PLX A15 f	2.37	1.90
30	PLX A30 f	2.84	2.33
45	PLX A45 f	2.45	2.04
60	PLX A60 f	2.13	1.80
75	PLX A75 f	2.51	2.14
90	PLX A90 f	2.84	2.55

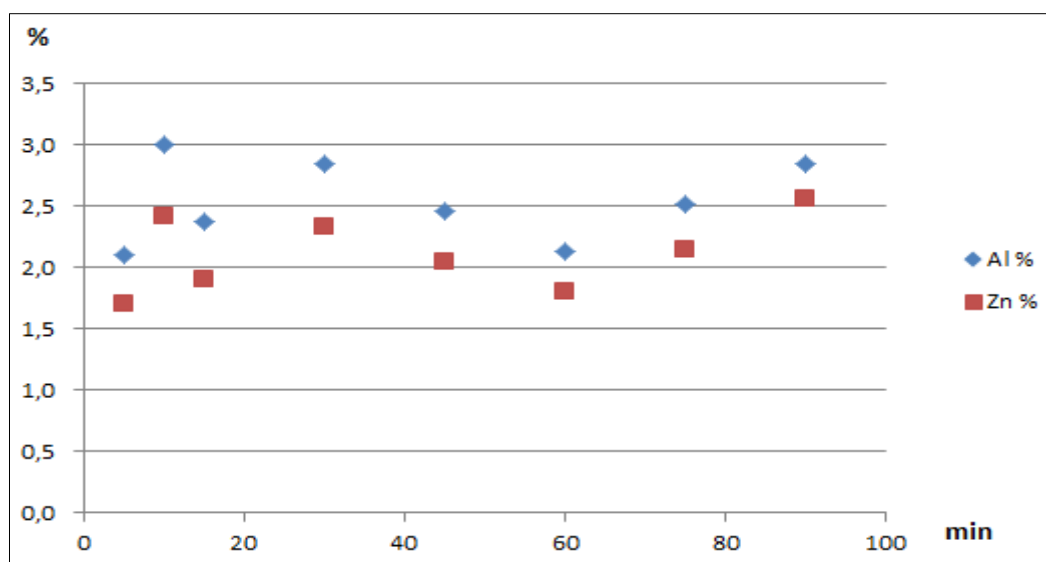


Figure 5.4 Extraction (%) of zinc and aluminium from gahnite with  $\text{H}_2\text{SO}_4$  vs time (min) of PLX.  
Conditions:  $C=0.50$  M,  $L/S=40$ ,  $T=235$  °C,  $P=30$  bar

From the graph, it can be observed that, from the first sample taken at 5 min up to the last one at 90 min, there is a slight tendency to a slow increment of zinc extraction, yet it is not quite conclusive. In any case, the result of this test was very low, achieving only a value of 2.5 % Zn extraction after 90 min, under a pressure of 30.625 bar and at a temperature of 235 °C. This is due more to the refractory spinel than to the leaching time. The next test consisted then in increasing acid concentration. The presence of gahnite in the residue of this test is confirmed by the following XRD result. It also shows the unfortunate occurrence of  $\text{TiO}_2$ , due to a very minor corrosion of the container caused by the use of  $\text{H}_2\text{SO}_4$ .

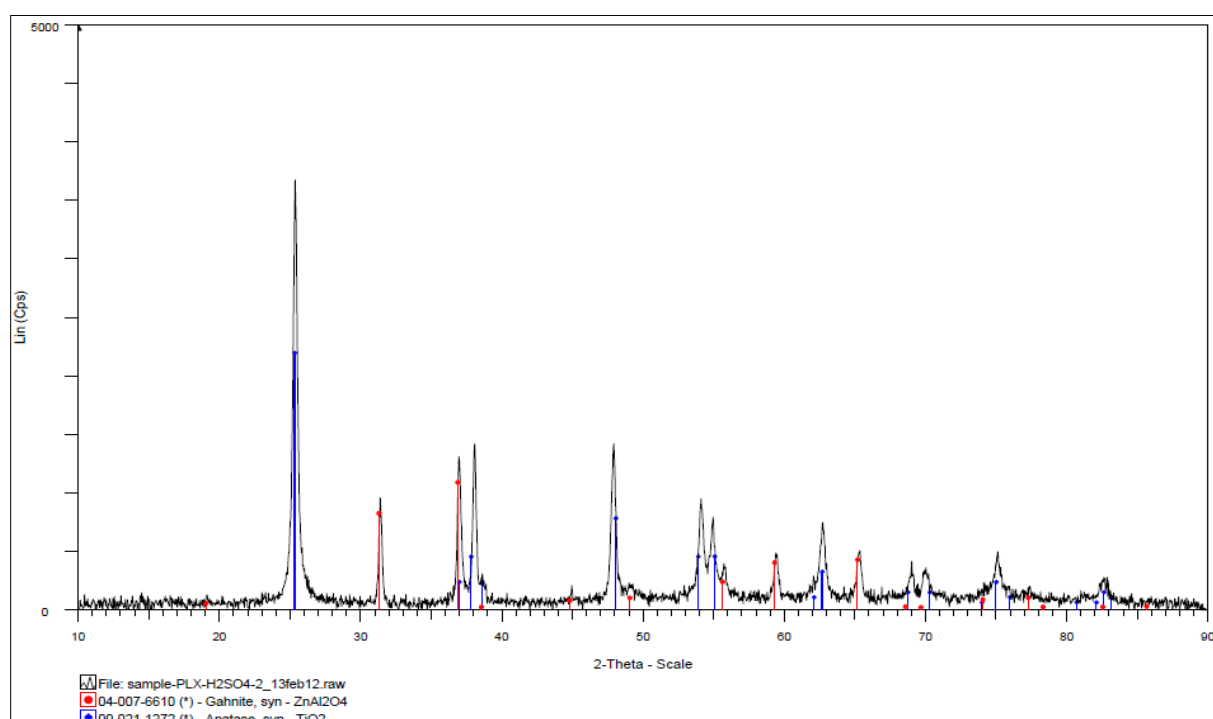


Figure 5.5 XRD pattern of the residue of  $\text{H}_2\text{SO}_4$  PLX at 0.5 M, confirming the presence of gahnite.

### 5.2.1.2 H<sub>2</sub>SO<sub>4</sub> 0.75 M

This test was performed with a slightly higher concentration of the leaching agent, considering the materials restrictions. The amount of gahnite mixed with the solution was 8.6 g, for a L/S of 40. The container was filled up to a third only, so that a thorough mixing was achieved by the mechanical stirrer. Total leaching time was 90 min. Sampling was performed at 5, 10, 15, 30, 45, 60, 75 and 90 min, taken a 5 mL sample each time, and then sent for ICP analysis.

Zinc extraction was low as well, showing only a very small increment after 90 min with respect to the test at 0.50 M. Conditions in this case were a final temperature of 140 °C and a stable pressure of 3.6154 bar. Table 5.3 shows the results of this test, in terms of zinc extraction, represented graphically in Figure 5.6.

Table 5.3 Metal extraction with H<sub>2</sub>SO<sub>4</sub> 0.75 M.

<b>ZnO·Al<sub>2</sub>O<sub>3</sub> + H<sub>2</sub>SO<sub>4</sub> 0.75 M</b>			
SAMPLE		METAL EXTRACTION [%]	
PLX time [min]	Name	Al	Zn
5	PLX B5 f	2.34	1.89
10	PLX B10 f	3.34	2.71
15	PLX B15 f	3.38	2.73
30	PLX B30 f	3.38	2.79
45	PLX B45 f	3.08	2.57
60	PLX B60 f	2.57	2.19
75	PLX B75 f	2.85	2.46
90	PLX B90 f	3.21	2.93

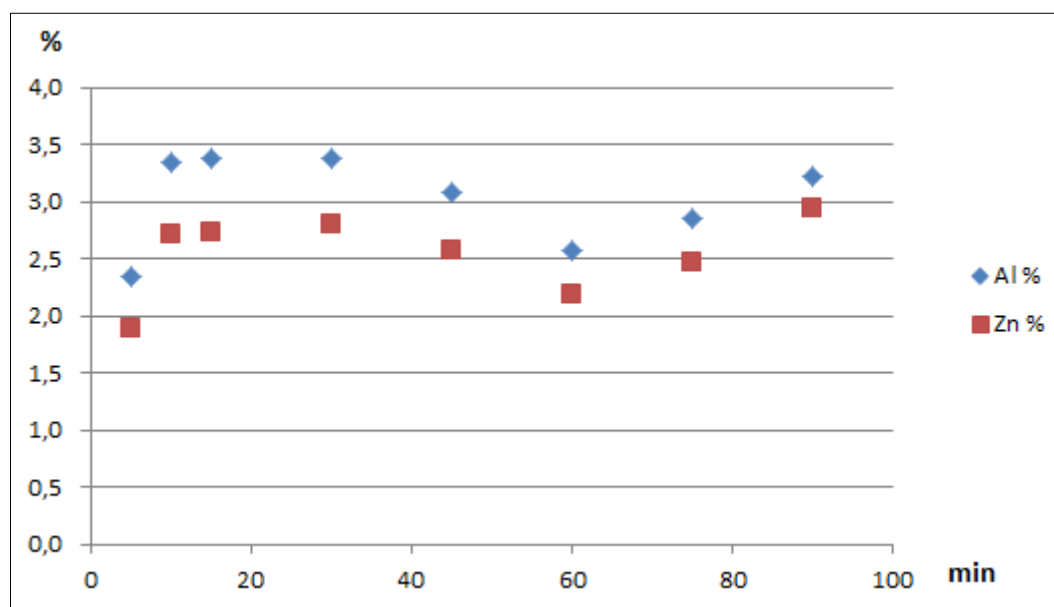


Figure 5.6 Extraction (%) of zinc and aluminium from gahnite with H<sub>2</sub>SO<sub>4</sub> vs time (min) of PLX.  
Conditions: C=0.75 M, L/S=40, T=140 °C, P=3.6 bar

From the graph, it can be observed that the zinc extraction curve for 0.75 M is somehow similar to that at 0.50 M, yet slightly higher. This is due to the increment of the sulphuric acid concentration. From initial point (5 min) to final point (90 min), there is a certain tendency to achieve a metal extraction, however the overall curve is not quite conclusive.

It was intended to run more tests with sulphuric acid at higher concentrations, but it was not possible due to the corrosion restrictions of the container<sup>[12] [13]</sup>. Prof. Michiel Makkee from the Chemical Engineering Department was contacted to explore the possibilities to conduct such tests, but there was no other material available at those facilities that could stand such hard conditions of leaching: a simultaneous combination of high acid concentration, high temperature and high pressure.

According to literature review carried out at this point, maybe a container made of borosilicate glass, fluorocarbons or fluoro-elastomers could resist such a harsh environment, but is not available at the facilities. Therefore, it was decided to stop working with sulphuric acid and perform tests with nitric acid.

The presence of gahnite in the residue of this test was confirmed by an XRD analysis. Also  $\text{TiO}_2$  is present as effect of very minor corrosion of the container due to the use of sulphuric acid.

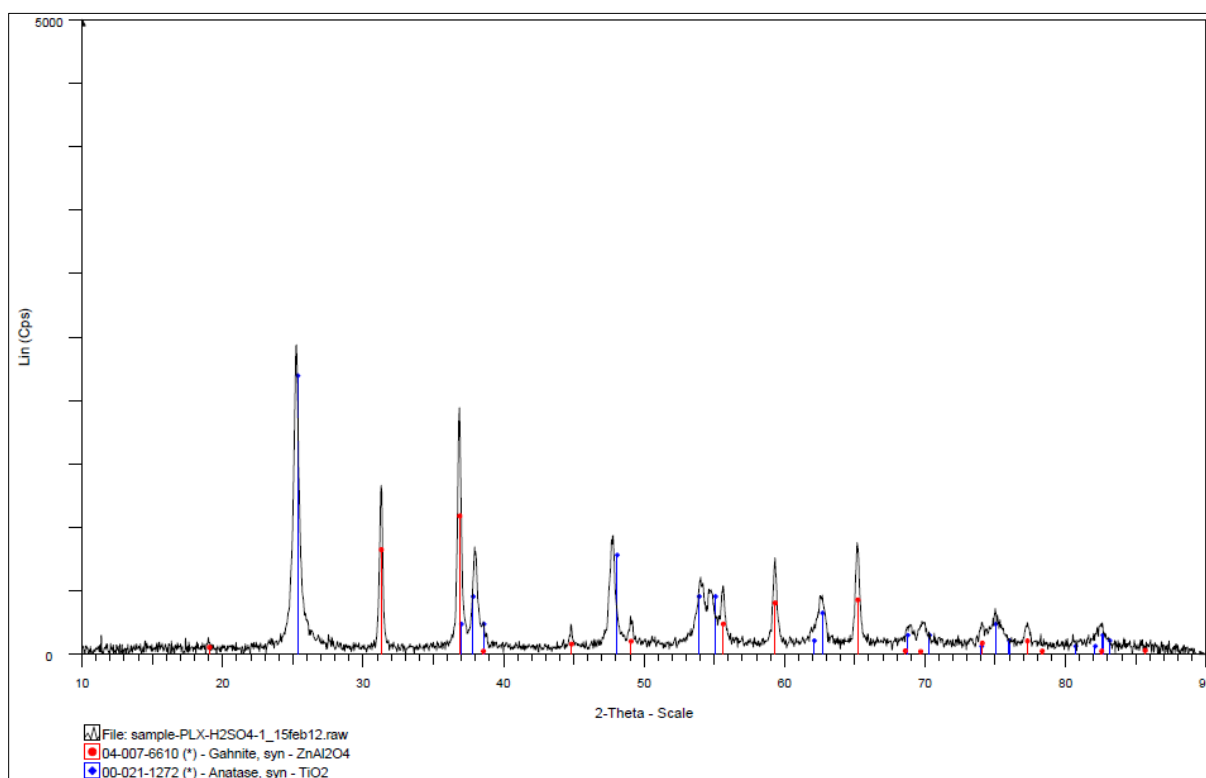


Figure 5.7 XRD pattern of the residue of  $\text{H}_2\text{SO}_4$  PLX at 0.75 M, confirming the presence of gahnite.

### 5.2.2 Pressure leaching with nitric acid

The use of  $\text{HNO}_3$  as leaching agent for the pressure experiments was the next step at this stage after obtaining very low results with  $\text{H}_2\text{SO}_4$ . Corrosion limits allowed higher concentrations of this acid <sup>[12]</sup> <sup>[13]</sup>. First, a value of 0.5 M was used, followed directly by a second trial at 4.0 M.

#### 5.2.2.1 $\text{HNO}_3$ 0.50 M

For this test, the amount of gahnite to be leached was 8.3 g, for a L/S of 40. Total leaching time was set to 90 min, and sampling was performed every 15 min, by taking a 5 mL sample that was sent for ICP analysis later. Again the container was filled only up to a third of its volume to allow a thorough mixing by means of the continuous mechanical stirring. Results of this trial are given below in Table 5.4.

Table 5.4 Metal extraction with  $\text{HNO}_3$  0.50 M.

<b><math>\text{ZnO} \cdot \text{Al}_2\text{O}_3 + \text{HNO}_3</math> 0.50 M</b>			
SAMPLE		METAL EXTRACTION [%]	
PLX time [min]	Name	Al	Zn
15	PLX Y15 f	10.99	12.88
30	PLX Y30 f	12.03	14.23
45	PLX Y45 f	12.04	13.94
60	PLX Y60 f	15.69	18.26
75	PLX Y75 f	17.79	20.69
90	PLX Y90 f	16.99	19.95

Results of zinc extraction proved to be better than working with  $\text{H}_2\text{SO}_4$ . The best outcome was obtained at 75 min of leaching time, for a 20.7 % zinc extraction; although low for an industrial application, still interesting in comparison to the ones with sulphuric acid. Conditions of the autoclave were in this case 245 °C and 36.512 bar.

It must be noted too that working with  $\text{HNO}_3$  was in some way less complicated than with  $\text{H}_2\text{SO}_4$ , in terms of pressure/temperature control. A very high level of pressure was achieved, for a higher temperature than that of  $\text{H}_2\text{SO}_4$ , stable in the duration of the experiment.

Figure 5.8 shows a graph of the results for this pressure test. A small clearer tendency towards leaching in time is observed, in comparison to working with sulphuric acid. Taking this into account, it was decided to jump directly to a higher concentration of nitric acid, and run a test at 4.0 M.

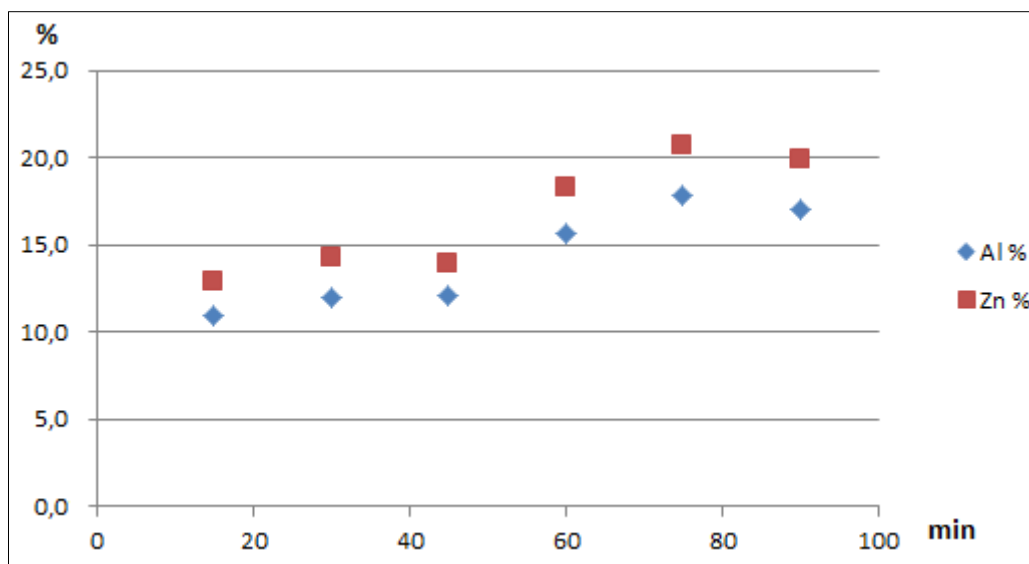


Figure 5.8 Extraction (%) of zinc and aluminium from gahnite with  $\text{HNO}_3$  vs time (min) of PLX.  
Conditions:  $C=0.50$  M,  $T=245$  °C,  $P=36$  bar

#### 5.2.2.2 $\text{HNO}_3$ 4.00 M

The experiment with  $\text{HNO}_3$  at 0.5 M concentration provided better results than working with  $\text{H}_2\text{SO}_4$ , at 0.5 M or 0.75 M. An experiment at a higher concentration then was run, skipping trials at intermediate concentrations of the nitric acid.

A test at 4.0 M concentration was carried out, mixing 8.3 g of pure gahnite with the acid solution by means of a thorough, constant mechanical stirring, for a L/S of 40. Once again, leaching time was set to 90 min, and sampling was done every 15 min by taking a 5 mL sample to be sent afterwards for ICP analysis. The results of this test are given below.

Table 5.5 Metal extraction with  $\text{HNO}_3$  4.00 M.

<b><math>\text{ZnO} \cdot \text{Al}_2\text{O}_3 + \text{HNO}_3</math> 4.00 M</b>			
SAMPLE		METAL EXTRACTION [%]	
PLX time [min]	Name	Al	Zn
15	PLX Z15 f	12.36	14.56
30	PLX Z30 f	12.91	15.34
45	PLX Z45 f	13.75	15.98
60	PLX Z60 f	17.17	19.98
75	PLX Z75 f	19.10	22.08
90	PLX Z90 f	19.08	22.20

The best result was achieved at 90 min leaching time for a 22.2% Zn extraction. Working conditions of the autoclave were 250 °C and 39.762 bar. Only a minor increment in the extraction was obtained, regardless of the high addition of acid. This end results proves that this zinc spinel is in fact quite refractory to a leaching treatment.

Figure 5.9 shows a graph generated with the previous data. There is a slow tendency of leaching in time. Extraction curves are rather similar to the results of the test at 0.5 M.

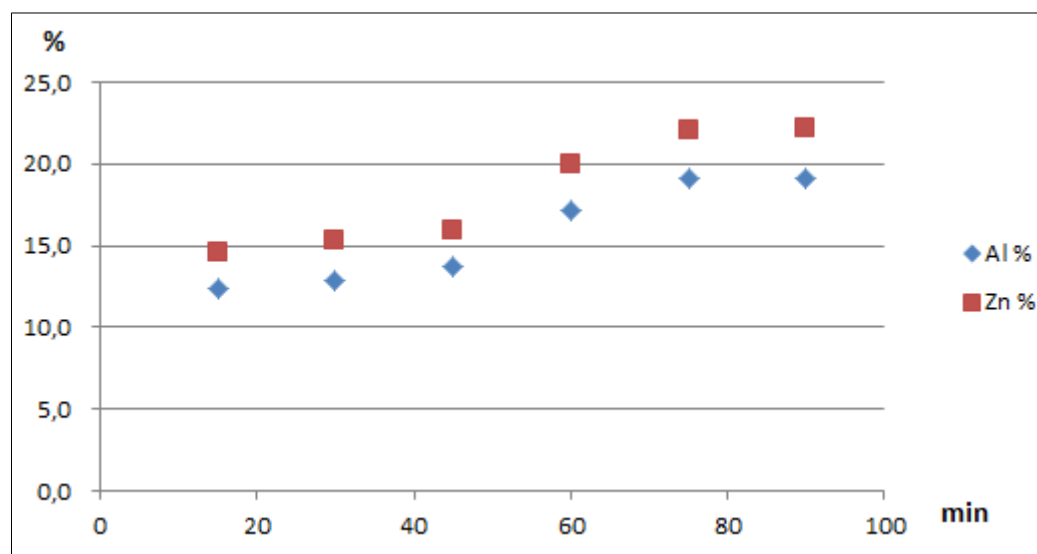


Figure 5.9 Extraction (%) of zinc and aluminium from gahnite with  $\text{HNO}_3$  vs time (min) of PLX.  
Conditions: C=4.00 M, T=250 °C, P=39 bar

Figure 5.10 shows the XRD pattern of the residue from pressure leaching with  $\text{HNO}_3$  at 4.0 M. It clearly shows the presence of gahnite in the remainder.

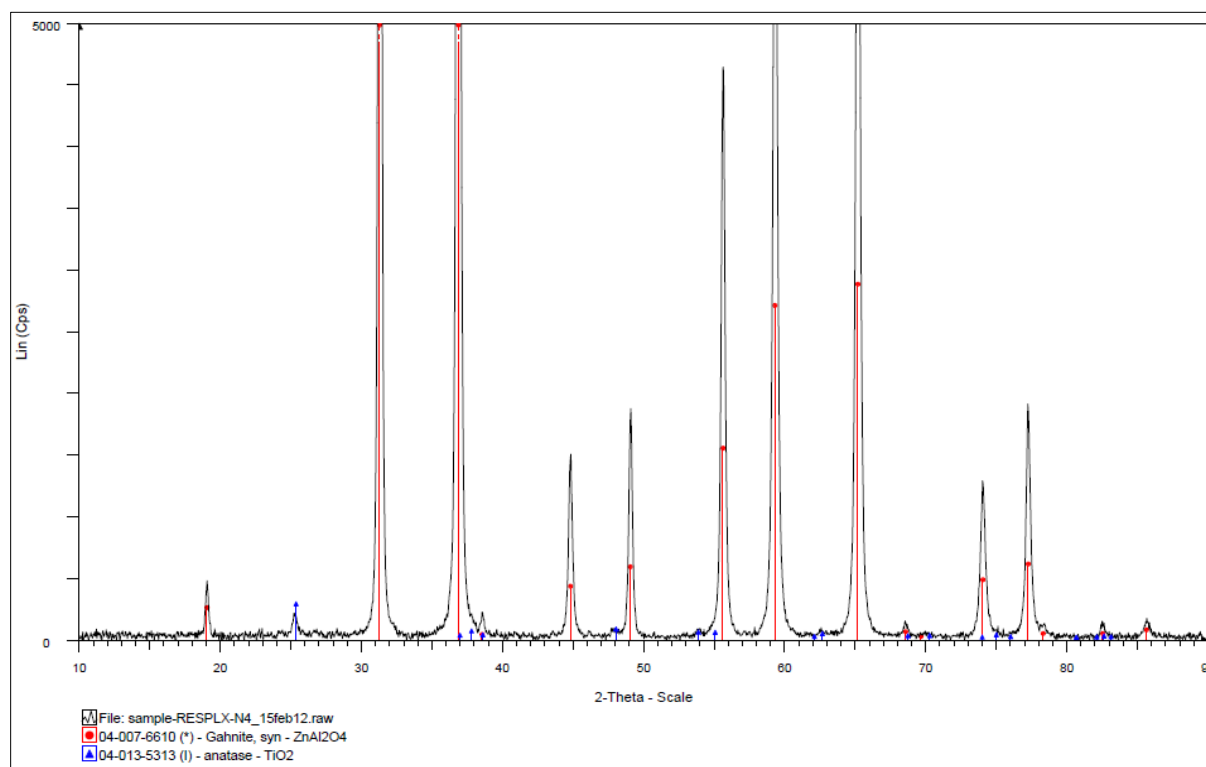


Figure 5.10 XRD pattern of the residue from PLX with  $\text{HNO}_3$  4.0 M.

Though working with nitric acid seemed more promising than using sulphuric acid as a leaching agent, it was decided to stop this hydrometallurgical approach since an extended leach is not practicable in the industrial run-through.

With this findings, the hydrometallurgical treatment was closed and the research moved to explore pyrometallurgical possibilities for the treatment of gahnite  $\text{ZnO} \cdot \text{Al}_2\text{O}_3$ .



## 6 RESULTS OF PYROMETALLURGICAL TREATMENT

### 6.1 Reduction of gahnite with carbon

The following set of experiments commenced at 1300 °C, a temperature level known which gahnite would be reduced fully at, according to preceding thermodynamic calculations. When that was confirmed, the same test was explored but lowering the temperature 50 ° and 100 °C. Temperature measured with an independent, external thermocouple from the one set in the furnace controller is in parentheses.

#### 6.1.1 G + C at 1300 °C (1302 °C)

This test was conducted with a thorough mix for 30 min at full stirring rate in the Retsch machine of 9.17 g of pure gahnite powder and 0.75 g of pure graphite powder, for a 1:1.25 stoichiometric ratio and a total mass of 9.92 g in crucible. Furnace temperature was set to 1300 °C at a heating rate of 10 °C/min for a dwell of 2.0 h. Argon gas injection was set fixed to a 3.0 L/min flowrate.

After heat treatment, mass of the residue amounted 5.40 g, meaning a loss of 4.52 g or 45.6 %.

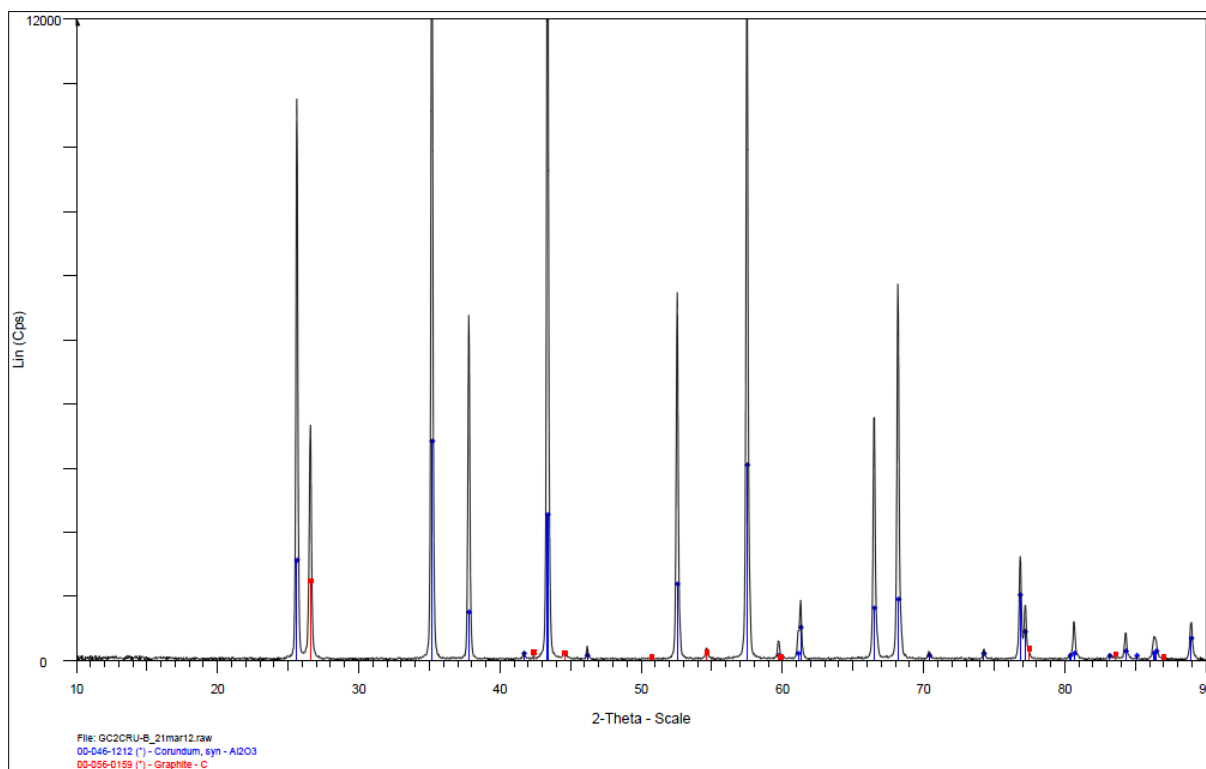


Figure 6.1 XRD pattern of the residue for the test G + C at 1300 °C.

From the previous XRD pattern of the residue, it can be observed that it exclusively consists of  $\text{Al}_2\text{O}_3$  as expected, and marginal carbon. Neither gahnite nor any form of zinc compound is found in the residue.

The XRF result that follows confirms the reducing action of carbon by leaving in the residue a negligible amount of ZnO, only 0.0719 %. Most of the remainder is  $\text{Al}_2\text{O}_3$  as expected, amounting 99.7 %.

	Compound	Conc.	Absolute
	Name	wt(%)	Error (%)
1	$\text{Al}_2\text{O}_3$	(99.7)	
2	CaO	0.00631	0.002
3	$\text{Cr}_2\text{O}_3$	0.00709	0.003
4	CuO	0.00336	0.002
5	$\text{Fe}_2\text{O}_3$	0.0595	0.007
6	$\text{Ga}_2\text{O}_3$	0.00537	0.002
7	K <sub>2</sub> O	0.0104	0.003
8	NiO	0.00434	0.002
9	P <sub>2</sub> O <sub>5</sub>	0.00817	0.003
10	PtO <sub>2</sub>	0.0138	0.004
11	SO <sub>3</sub>	0.0159	0.004
12	SiO <sub>2</sub>	0.0624	0.007
13	ZnO	0.0719	0.008

Figure 6.2 XRF result of the residue for the test G + C at 1300 °C.

From calculations, the 0.0719 % of ZnO detected by XRF analysis corresponds to less than 0.004 g of ZnO left in the residue versus the 4.07 g of ZnO in the original gahnite, or 0.003 g of Zn versus 3.27 g of Zn respectively. This represents a 99.90 % Zn extraction performance, a full reduction process.

The following pictures show the state of the G + C powder mix before and after heat treatment. Not much change is observed as to colour, yet some disruptions in the distribution of the powder are probably due to the release of carbon and zinc both in the gas phase during the process.



Figure 6.3 Photographs taken before (L) and after the experiment of G + C at 1300 °C.

### 6.1.2 G + C at 1250 °C (1243 °C)

After the successful test at 1300 °C and full reduction achieved, the next step was to explore the process at a lower temperature.

This trial was conducted again with a thorough mix for 30 min at full stirring rate in the Retsch machine of 9.19 g of pure gahnite powder and 0.76 g of pure graphite powder, for a 1:1.25 stoichiometric ratio and a total mass of 9.95 g in crucible. Furnace temperature was set to 1250 °C at a heating rate of 10 °C/min for a dwell of 1.0 h this time. Argon gas injection was set fixed to a 3.0 L/min flowrate.

After heat treatment, mass of the residue amounted 7.38 g, meaning a loss of 2.57 g or 25.8 %.

The next XRD pattern of the residue shows the presence of gahnite along with zinc aluminium oxide, a transition phase of the compound. No  $\text{Al}_2\text{O}_3$  is found. All the previous indicates that the gahnite was not reduced completely. This is due to temperature level and not reaction time. This result was expected in concordance with thermodynamic calculations.

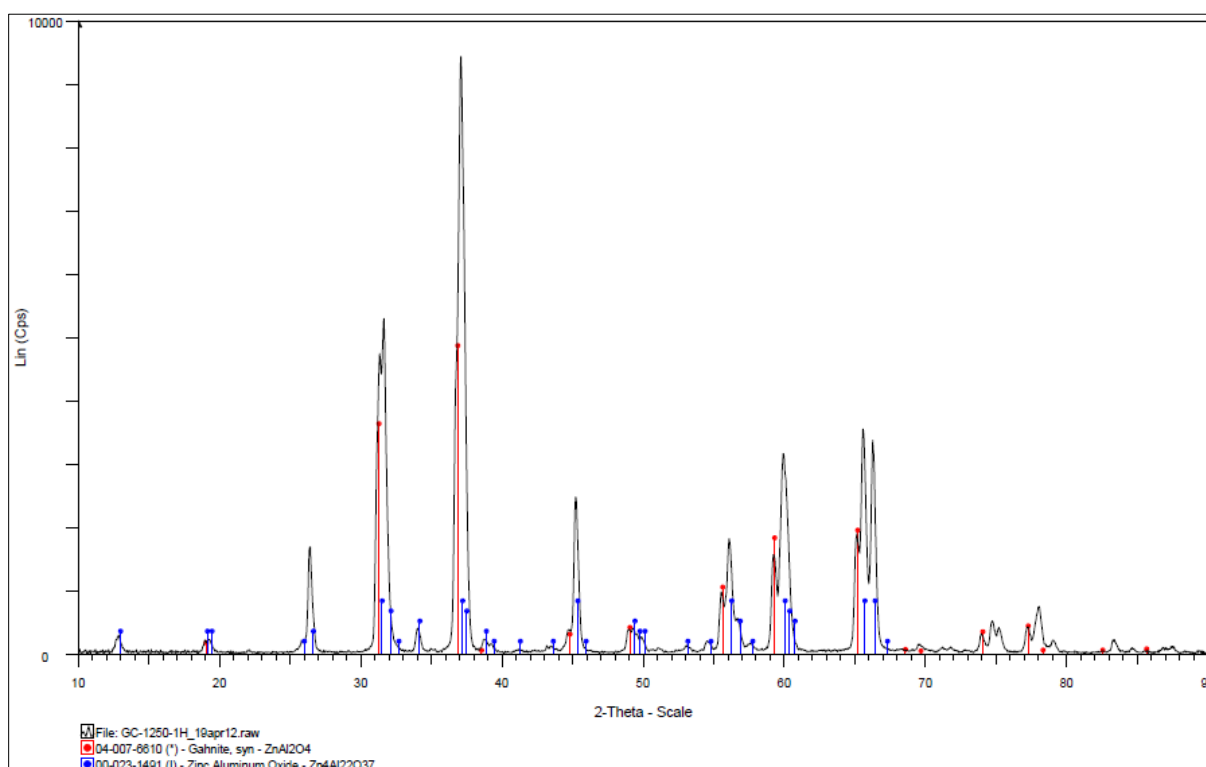


Figure 6.4 XRD pattern of the residue for the test G + C at 1250 °C.

Additionally, the following XRF analysis of the residue confirms the incomplete reduction at this temperature. ZnO amounts 32.9 % which represents 2.43 g of ZnO left in the residue versus the 4.08 g of ZnO in the original gahnite, or 1.95 g of Zn versus 3.28 g of Zn respectively. These figures represent a 40.43 % extraction performance, a moderate reduction.

	Compound	Conc.	Absolute
	Name	wt(%)	Error (%)
1	Al <sub>2</sub> O <sub>3</sub>	66.8	0.2
2	Cr <sub>2</sub> O <sub>3</sub>	0.00762	0.003
3	CuO	0.00808	0.003
4	Fe <sub>2</sub> O <sub>3</sub>	0.0756	0.008
5	Ga <sub>2</sub> O <sub>3</sub>	0.0242	0.005
6	SO <sub>3</sub>	0.0373	0.006
7	SiO <sub>2</sub>	0.0693	0.008
8	ZnO	32.9	0.1

Figure 6.5 XRF results of the residue for the test G + C at 1250 °C.

The following pictures show the state of the G + C powder mix before and after heat treatment. Not much change is observed as to colour and shape.



Figure 6.6 Photographs taken before (L) and after the experiment of G + C at 1250 °C.

### 6.1.3 G + C at 1200 °C (1197 °C)

Taking into account the moderate reduction results at 1250 °C and the earlier thermodynamic calculations, a final experiment was conducted at 1200 °C so that this temperature level was confirmed to be the lower limit for carbothermic reduction of gahnite.

A thorough mix for 30 min at full stirring rate in the Retsch machine of 9.18 g of pure gahnite powder and 0.76 g of pure graphite powder, for a 1:1.25 stoichiometric ratio and a total mass of 9.94 g in crucible, was subjected to heat treatment. Furnace temperature was set to 1200 °C at a heating rate of 10 °C/min for a dwell of 1.0 h. Argon gas was injected constantly at a 3.0 L/min flowrate.

After heat treatment, mass of the residue amounted 8.78 g, meaning a loss of only 1.16 g or 11.7 %.

The following XRD pattern of the residue shows the presence of gahnite as well as ZnO along with (unreacted) carbon, implying that a reduction process was not complete or even did not occur.

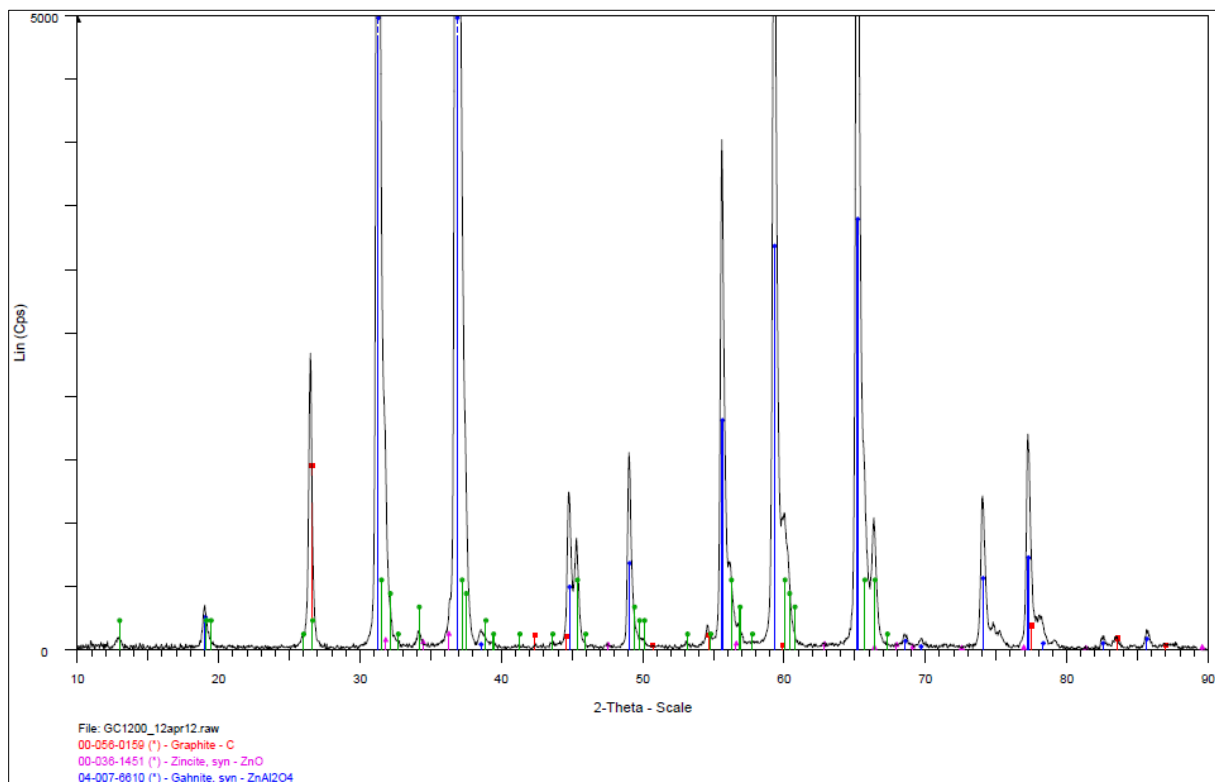


Figure 6.7 XRD pattern of the residue for the test G + C at 1200 °C.

Indeed, the XRF result of the residue shows pretty much the same composition as pure gahnite: 52.6 % of  $\text{Al}_2\text{O}_3$  and 47.2 % of ZnO, implying that a reduction process did not take place in this experiment at 1200 °C.

	Compound	Conc.	Absolute
	Name	wt(%)	Error (%)
1	Al <sub>2</sub> O <sub>3</sub>	52.6	0.2
2	Cr <sub>2</sub> O <sub>3</sub>	0.0135	0.003
3	Fe <sub>2</sub> O <sub>3</sub>	0.106	0.01
4	SO <sub>3</sub>	0.0214	0.004
5	SiO <sub>2</sub>	0.0687	0.008
6	ZnO	47.2	0.1

Figure 6.8 XRF results of the residue for the test G + C at 1200 °C.

This 47.2 % of ZnO detected in the residue indicates that the amount of ZnO (and thus Zn) found in the residue is the same as the ZnO (and Zn in turn) contained in the original gahnite.

Once again, the following pictures show the state of the G + C powder mix before and after heat treatment. Not much change is observed as to shape, however the surface looks whitish.



Figure 6.9 Photographs taken before (L) and after the experiment of G + C at 1200 °C.



#### 6.1.4 Tablet G + C at 1300 °C (1303 °C)

An additional carbothermic test was performed in order to find if any important reduction difference existed between loose powder and pressure tablet.

A thorough mix for 30 min at full stirring rate in the Retsch machine of 9.17 g of pure gahnite powder and 0.75 g of pure graphite powder, for a 1:1.25 stoichiometric ratio and a total mass of 9.92 g in crucible, was subjected to heat treatment. Furnace temperature was set to 1300 °C, a temperature already proved to be the optimum condition for a full extraction of zinc (please see Section 6.1.1) at a heating rate of 10 °C/min for a dwell of 1.0 h. Argon gas was injected constantly at a 3.0 L/min flowrate.

The mixture was put in the crucible as one single perfect tablet after a simple pressing procedure. The following photograph shows how it looks.



Figure 6.10 Photograph showing a perfect single tablet of G + C.

After heat treatment, mass of the residue amounted 5.38 g, meaning a loss of 4.54 g or 45.8 %.

The following XRD pattern of the residue shows the presence of mainly  $\text{Al}_2\text{O}_3$ , and also some remnant Zn and ZnO that did not react.

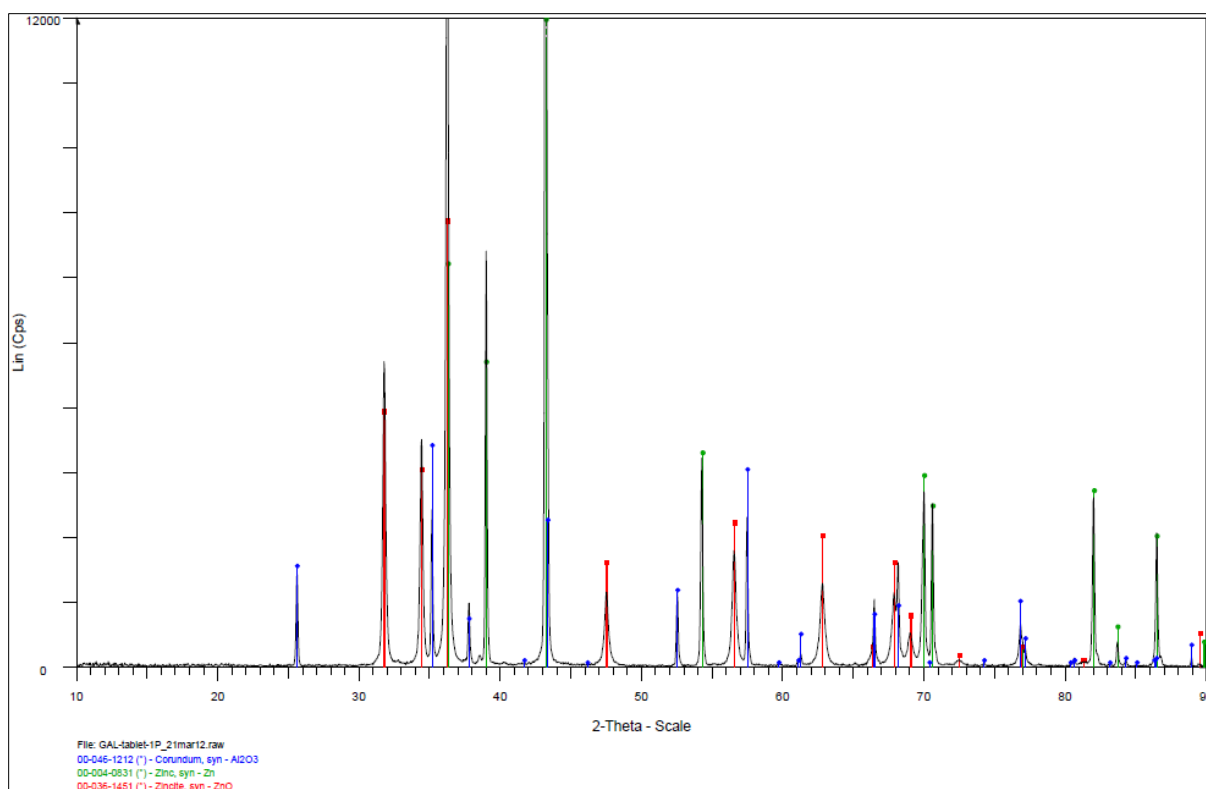


Figure 6.11 XRD pattern of the residue for the test Tablet G + C at 1300 °C.

The XRF result that follows confirms the full reducing action of carbon at this temperature by leaving in the residue a negligible amount of ZnO, only 0.97 %. Most of the remainder is  $\text{Al}_2\text{O}_3$  as expected, amounting 98.7 %.

	Compound	Conc.	Absolute
	Name	wt(%)	Error (%)
1	$\text{Al}_2\text{O}_3$	(98.7)	
2	$\text{Bi}_2\text{O}_3$	0.00164	0.001
3	$\text{CaO}$	0.0157	0.004
4	$\text{Cr}_2\text{O}_3$	0.012	0.003
5	$\text{CuO}$	0.0031	0.002
6	$\text{Fe}_2\text{O}_3$	0.0716	0.008
7	$\text{Ga}_2\text{O}_3$	0.00559	0.002
8	$\text{K}_2\text{O}$	0.00601	0.002
9	$\text{NiO}$	0.0171	0.004
10	$\text{PtO}_2$	0.0185	0.004
11	$\text{SO}_3$	0.0213	0.004
12	$\text{SiO}_2$	0.175	0.01
13	$\text{ZnO}$	0.97	0.03

Figure 6.12 XRF result of the residue for the test Tablet G + C at 1300 °C.

From calculations, the 0.97 % of ZnO detected by XRF analysis corresponds to 0.052 g of ZnO left in the residue versus the 4.07 g of ZnO in the original gahnite, or 0.042 g of Zn versus 3.27 g of Zn respectively. This represents a 98.72 % Zn extraction performance, a full reduction process for this test with tablet.



## 6.2 Reduction of gahnite with aluminium

In the case of aluminothermic reduction of gahnite, experiments started at a temperature of 1200 °C, taking into account the thermodynamic calculations performed with HSC Chemistry earlier (please see Chapter 3). When a full reduction of the spinel was confirmed, tests were executed every 50 °C down to 900 °C, level which was expected to be the lower limit of a successful process according to formerly referred calculations. Temperature measured with an independent, external thermocouple from the one set in the furnace controller is in parentheses.

As stated in Chapter 4, aluminium powder was not readily available in the beginning. A few initial tests were carried out though with the material accessible at that point, small aluminium balls. When this was concluded, tests with pure, fine aluminium powder were performed, obtaining evidently much better and interesting results.

### 6.2.1 Aluminium balls

The first test of this kind was conducted with a thorough mix for 30 min at full stirring rate in the Retsch machine of 13.7503 g of pure gahnite powder and 1.349 g of small aluminium balls, for a 1.5:1 stoichiometric ratio and a total mass of 15.0993 g in crucible. Furnace temperature was set to 1000 °C at a heating rate of 10 °C/min for a dwell of 1.0 h. Argon gas injection was set fixed to a 3.0 L/min flowrate.

After heat treatment, residue mass amounted 13.99 g, meaning a loss of only 1.11 g or 7.3 %.

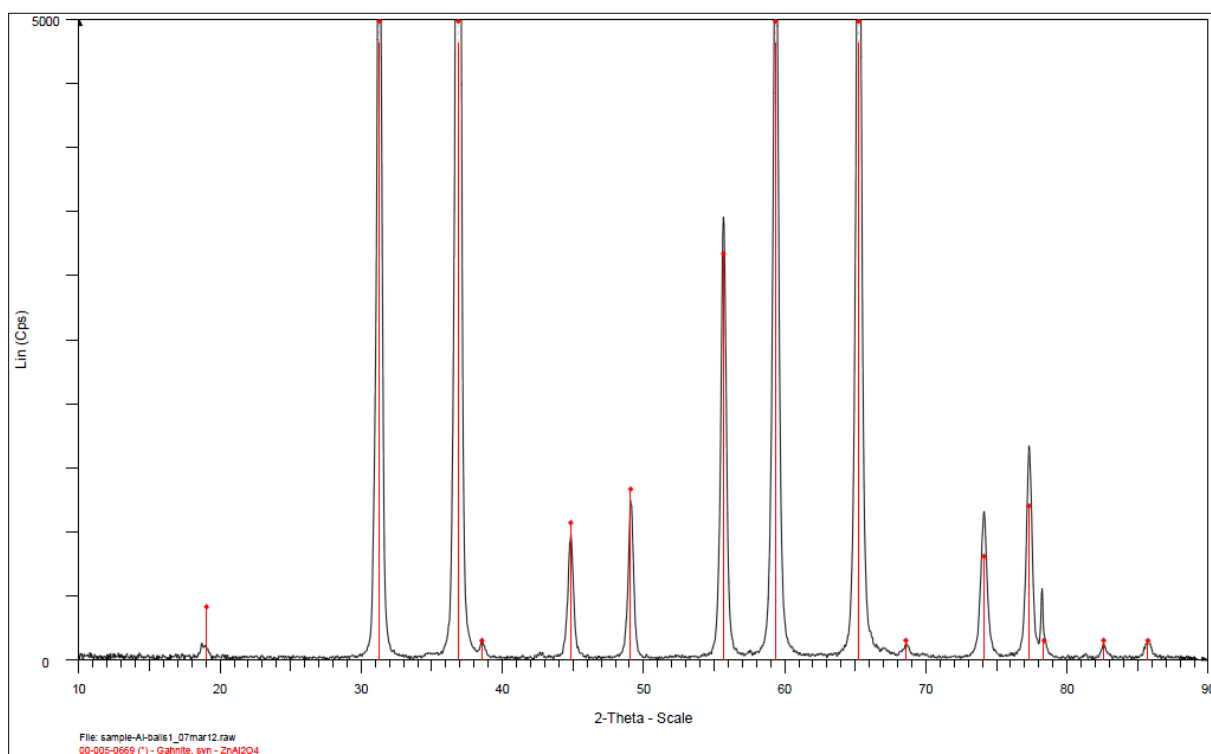


Figure 6.13 XRD pattern of the residue for the test G + Al at 1000 °C (balls).

From the previous XRD pattern of the residue, it is observed that it consists of gahnite exclusively. This is evidence that no reduction, in any grade, took place for this first test.

Below, XRF analysis of the residue further confirms the result. The composition is rather similar to pure gahnite, 44 % ZnO and 56 %  $\text{Al}_2\text{O}_3$ . No reduction of the spinel occurred.

	Compound	Conc.	Absolute
	Name	wt(%)	Error (%)
1	$\text{Al}_2\text{O}_3$	56	0.2
2	CaO	0.015	0.004
3	CuO	0.012	0.003
4	$\text{Fe}_2\text{O}_3$	0.075	0.008
5	NiO	0.012	0.003
6	$\text{SO}_3$	0.027	0.005
7	$\text{SiO}_2$	0.057	0.007
8	ZnO	44	0.1

Figure 6.14 XRF result of the residue for the test G + Al at 1000 °C (balls).

Even so, while waiting for XRD/XRF results, samples of the residue were studied with an optical microscope at the 3ME laboratory facilities. Figure 6.15 and Figure 6.16 show photographs of the mix before and after the reduction attempt at 1000 °C respectively. Some attachment of very fine powder is observed in the surface of aluminium balls, however not big changes in the shape of them are found. Such form alteration would have meant some reduction probably, since certain amount of aluminium would have been used as reducing agent. It was not the case.

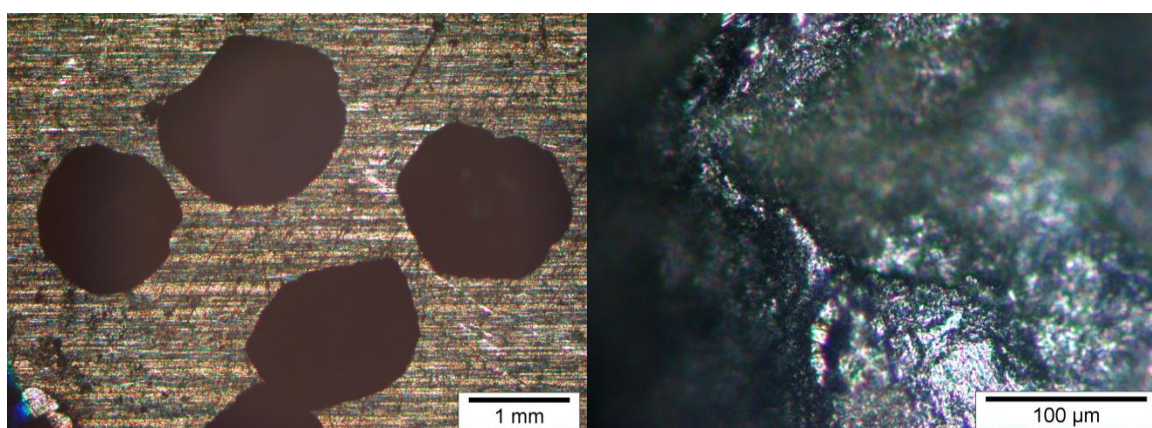


Figure 6.15 Optical microscope images before reduction attempt of gahnite at 1000 °C (balls).

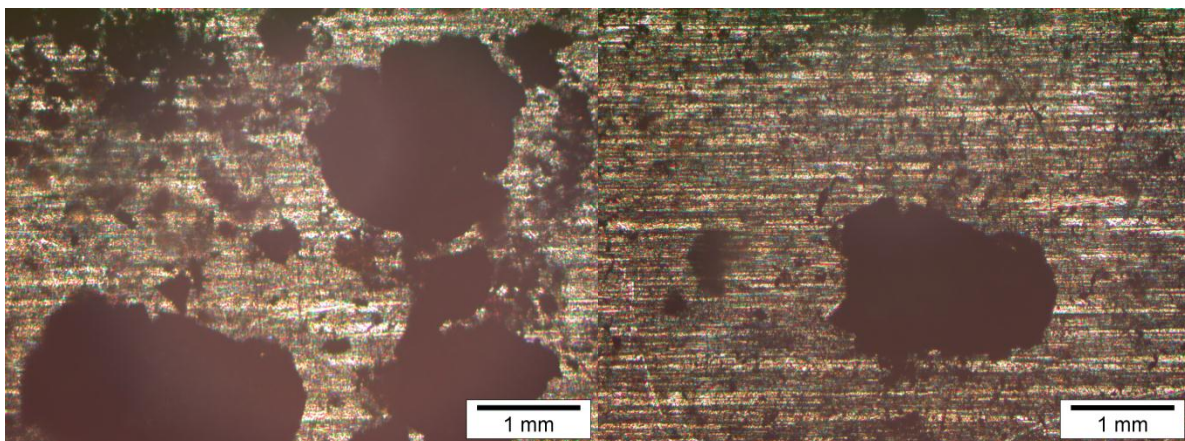


Figure 6.16 Optical microscope images after reduction attempt of gahnite at 1000 °C (balls).

Figure 6.17 shows the state of the mix before and after this first experiment. No changes in colour can be seen. However, some aluminium balls emerged from the mix after heat treatment.



Figure 6.17 Photographs taken before (L) and after the experiment of G + Al at 1000 °C (balls).

A second trial was performed increasing the ratio of aluminium. Now, a thorough mix for 30 min at full stirring rate in the Retsch machine of 13.7503 g of pure gahnite powder and 2.698 g of small aluminium balls, for a 1.5:2 stoichiometric ratio and a total mass of 16.4483 g in crucible, was put for heat treatment. Furnace temperature was set to 1000 °C at a heating rate of 10 °C/min for a dwell of 1.0 h. Argon gas injection was set fixed to a 3.0 L/min flowrate.

After heat treatment, mass of the residue amounted 16.24 g, meaning a loss of only 0.21 g or 1.3 %.

The following XRD pattern of the residue shows again the presence of gahnite (suggesting no reduction) but  $\text{Al}_2\text{O}_3$  as well (suggesting some reduction).

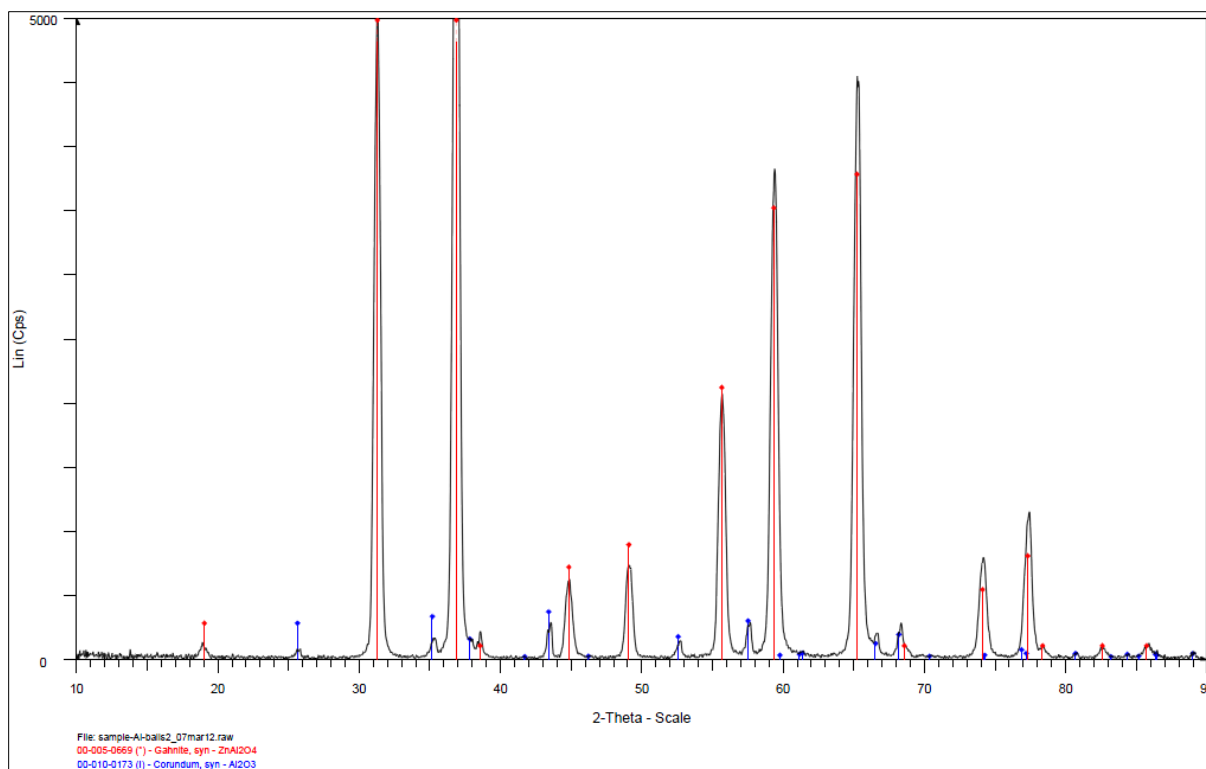


Figure 6.18 XRD pattern of the residue for the test G + Al at 1000 °C (balls).

XRF analysis of the residue presents only a minimal increase in the ZnO, only 47 %, compared to the previous test.  $\text{Al}_2\text{O}_3$  amounts 53 %. This composition is again quite similar to pure gahnite. Virtually no reduction took place.

	Compound	Conc.	Absolute
	Name	wt(%)	Error (%)
1	$\text{Al}_2\text{O}_3$	53	0.1
2	CaO	0.012	0.003
3	CuO	0.011	0.003
4	$\text{Fe}_2\text{O}_3$	0.05	0.007
5	$\text{K}_2\text{O}$	0.061	0.007
6	NiO	0.01	0.003
7	$\text{SO}_3$	0.026	0.005
8	$\text{SiO}_2$	0.073	0.008
9	ZnO	47	0.1

Figure 6.19 XRF result of the residue for the test G + Al at 1000 °C (balls).

Photographs taken with optical microscope after heat treatment show the same result as before, no changes.



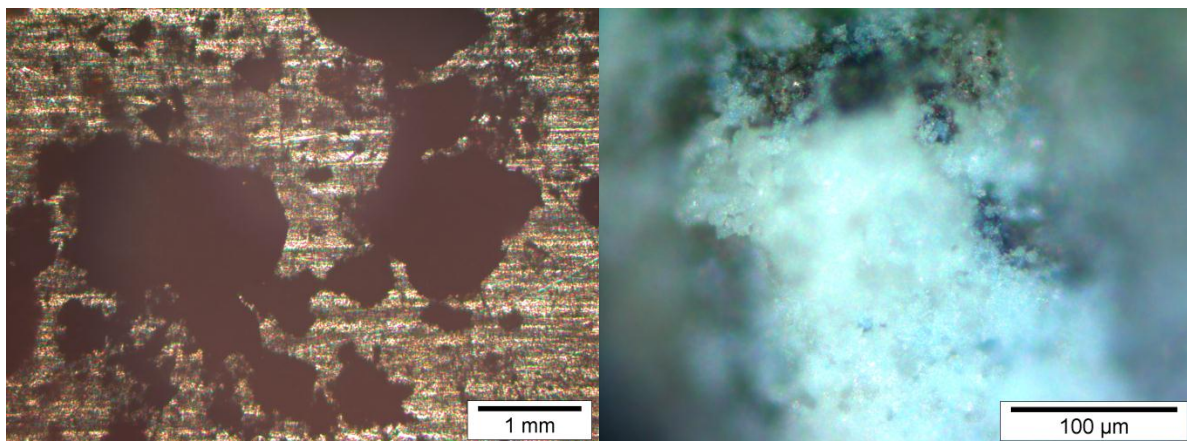


Figure 6.20 Optical microscope images after reduction attempt of gahnite at 1000 °C (balls).

Figure 6.21 shows the state of the mix before and after this second experiment. No changes in colour can be seen, remaining whitish. However, some aluminium balls emerged from the mix after heat treatment, as in the first test.



Figure 6.21 Photographs taken before (L) and after the experiment of G + Al at 1000 °C (balls).

A final attempt with balls was done, keeping ratio but increasing temperature. This test was conducted with a thorough mix for 30 min at full stirring rate in the Retsch machine of 9.01 g of pure gahnite powder and 1.77 g of small aluminium balls, for a 1.5:2 stoichiometric ratio and a total mass of 10.78 g in crucible. Furnace temperature was set this time to 1200 °C at a heating rate of 10 °C/min for a dwell of 1.0 h. Argon gas injection was set fixed to a 3.0 L/min flowrate.

After heat treatment, mass of the residue amounted 10.11 g, meaning a loss of only 0.65 g or 6.0 %.

XRD pattern of the residue below show the presence of gahnite (suggesting no reduction) but again  $\text{Al}_2\text{O}_3$  (suggesting some reduction).

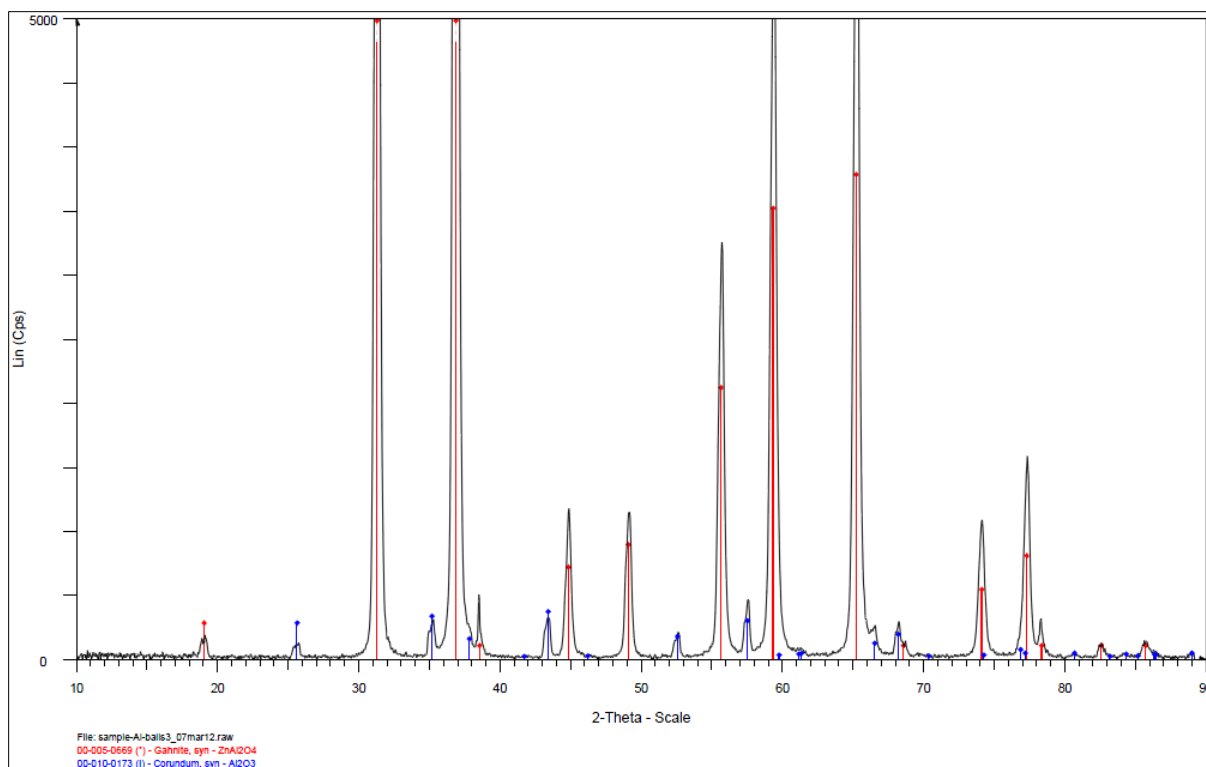


Figure 6.22 XRD pattern of the residue for the test G + Al at 1200 °C (balls).

XRF analysis of the residue shows once again essentially the same composition as pure gahnite, 44 % ZnO and 56 %  $\text{Al}_2\text{O}_3$ , implying that no reduction of the spinel followed.

	Compound	Conc.	Absolute
	Name	wt(%)	Error (%)
1	$\text{Al}_2\text{O}_3$	56	0.1
2	CuO	0.013	0.003
3	$\text{Fe}_2\text{O}_3$	0.056	0.007
4	$\text{K}_2\text{O}$	0.057	0.007
5	MgO	0.2	0.01
6	MnO	0.014	0.004
7	$\text{SO}_3$	0.0087	0.003
8	$\text{SiO}_2$	0.083	0.009
9	ZnO	44	0.1

Figure 6.23 XRF result of the residue for the test G + Al at 1200 °C (balls).

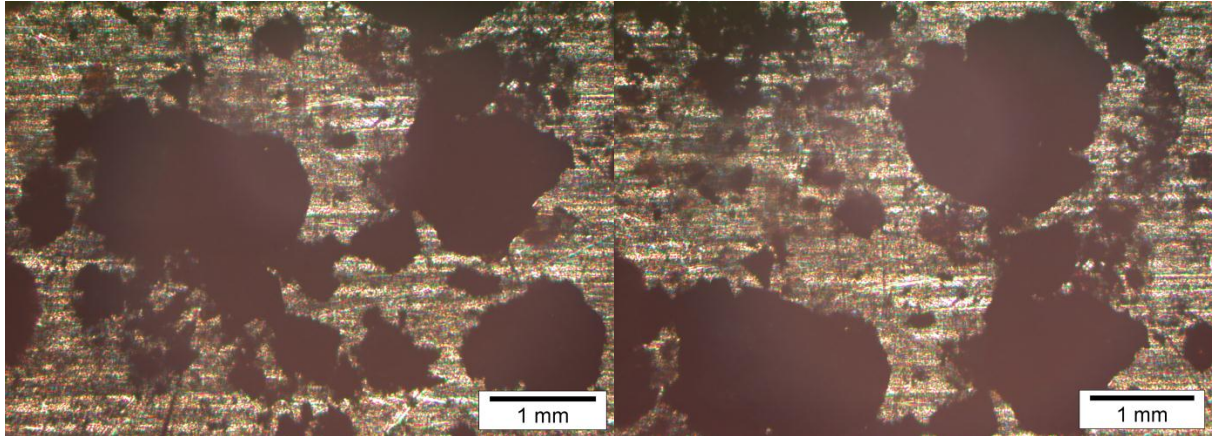


Figure 6.24 Optical microscope images after reduction attempt of gahnite at 1200 °C (balls).

Optical microscope pictures of the residue show once again the same situation as before, some minor powder agglomeration next to aluminium balls, but no major shape change of them.

On the other hand, working at 1200 °C produced that, in the residue, more aluminium balls emerged to the surface of the mix after heat treatment. Colour of the powder part remained the same.



Figure 6.25 Photographs taken before (L) and after the experiment of G + Al at 1200 °C (balls).

With this last test of reduction with aluminium balls obtaining null results, this type of experiments concluded. Having now aluminium powder available, a new series of tests was conducted, as explained from Section 6.2.2 onwards.

### 6.2.2 G + Al at 1200 °C (1194 °C)

Two tests were conducted at this temperature, one with the mix of gahnite and aluminium as loose powder and the other as a tablet (pressed powder).

#### 6.2.2.1 Tablet

This test was conducted with a thorough mix for 30 min at full stirring rate in the Retsch machine of 9.01 g of pure gahnite powder and 1.77 g of pure aluminium powder, for a 1.5:2 stoichiometric ratio and a total mass of 10.78 g in crucible. Furnace temperature was set to 1200 °C at a heating rate of 10 °C/min for a dwell of 1.0 h. Argon gas injection was set fixed to a 3.0 L/min flowrate.

The mixture was put in the crucible as one single perfect tablet after a simple pressing procedure.

After heat treatment, mass of the residue amounted 7.49 g, meaning a loss of 3.29 g or 30.5 %.

From the following XRD pattern of the residue, it can be observed that it exclusively consists of  $\text{Al}_2\text{O}_3$  and marginal aluminium. Neither gahnite nor any form of zinc aluminium oxide is found in the residue. No zinc compound is detected whatsoever.

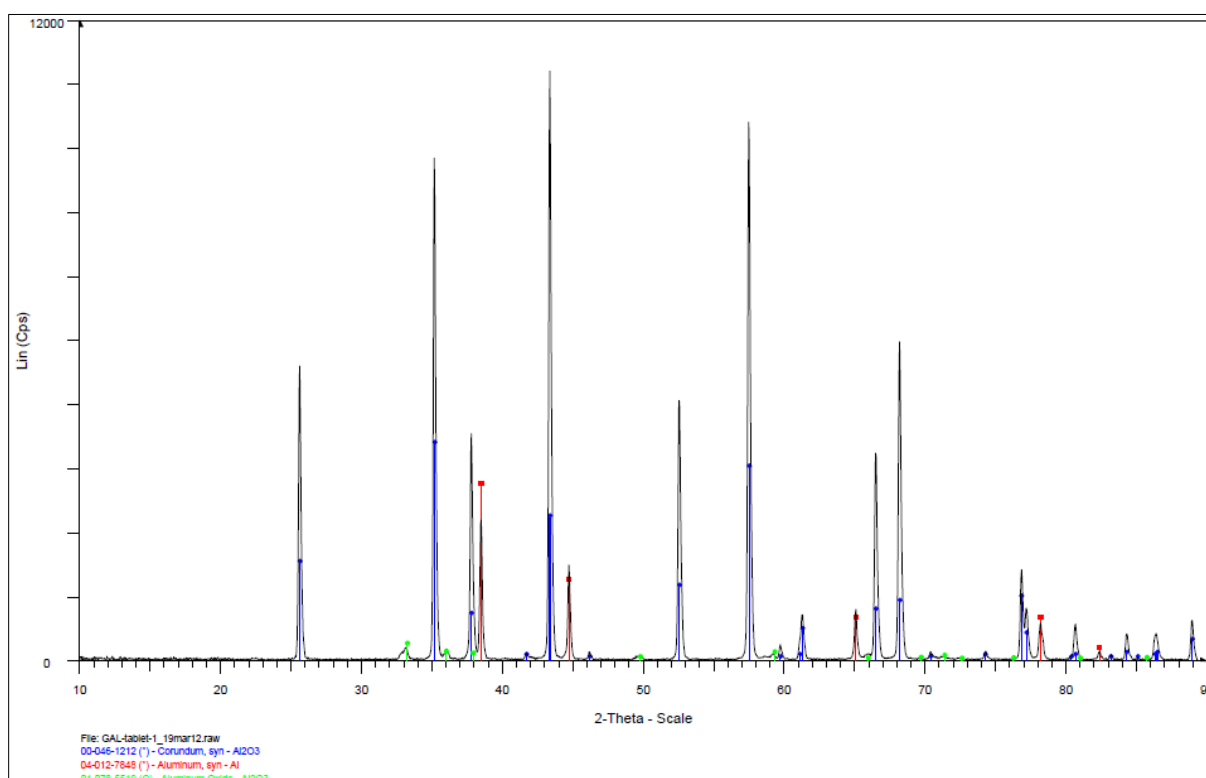


Figure 6.26 XRD pattern of the residue for the test G + Al at 1200 °C (tablet).



The following XRF result of the residue confirms that there is virtually no zinc left, and that  $\text{Al}_2\text{O}_3$  is the single compound prevailing, both as expected at this temperature according to previous thermodynamic calculations.

	Compound	Conc.	Absolute
	Name	wt(%)	Error (%)
1	$\text{Al}_2\text{O}_3$	(99.6)	
2	$\text{CaO}$	0.0149	0.004
3	$\text{Cr}_2\text{O}_3$	0.00942	0.003
4	$\text{CuO}$	0.0156	0.004
5	$\text{Fe}_2\text{O}_3$	0.176	0.01
6	$\text{Ga}_2\text{O}_3$	0.0057	0.002
7	$\text{PtO}_2$	0.0116	0.003
8	$\text{SO}_3$	0.097	0.009
9	$\text{SiO}_2$	0.0732	0.008
10	$\text{ZnO}$	0.0109	0.003

Figure 6.27 XRF result of the residue for the test G + Al at 1200 °C (tablet).

XRD/XRF results confirm that aluminium acted as a reducing agent of gahnite and that practically all the zinc contained in the spinel was extracted.

From calculations, the 0.0109 % of ZnO detected by XRF analysis corresponds to less than 0.001 g of ZnO left in the residue versus the 4.0 g of ZnO in the original gahnite, or 3.21 g of Zn versus less than 0.001 g of Zn respectively. This represents a 99.98 % Zn extraction performance, a full reduction process.

The following pictures show the state of the G + Al tablet before and after heat treatment. Not much change is observed as to shape and colour.



Figure 6.28 Photographs taken before (L) and after the experiment of G + Al at 1200 °C (tablet).

### 6.2.2.2 Powder

In view of the excellent results of the previous test at 1200 °C with the G + Al mix as a single perfect tablet, a similar trial was performed but with the mix as a powder.

The test was conducted with a thorough mix for 30 min at full stirring rate in the Retsch machine of 9.01 g of pure gahnite powder and 1.77 g of pure aluminium powder, for a 1.5:2 stoichiometric ratio and a total mass of 10.78 g in crucible. Furnace temperature was set to 1200 °C at a heating rate of 10 °C/min for a dwell of 1.0 h. Argon gas injection was set fixed to 3.0 L/min.

After heat treatment, mass of the residue amounted 7.56 g, meaning a loss of 3.22 g or 29.9 %.

Neither gahnite nor any zinc compound at all is observed in the following XRD pattern of the residue. As expected, only  $\text{Al}_2\text{O}_3$  is found, plus a minimal Al.

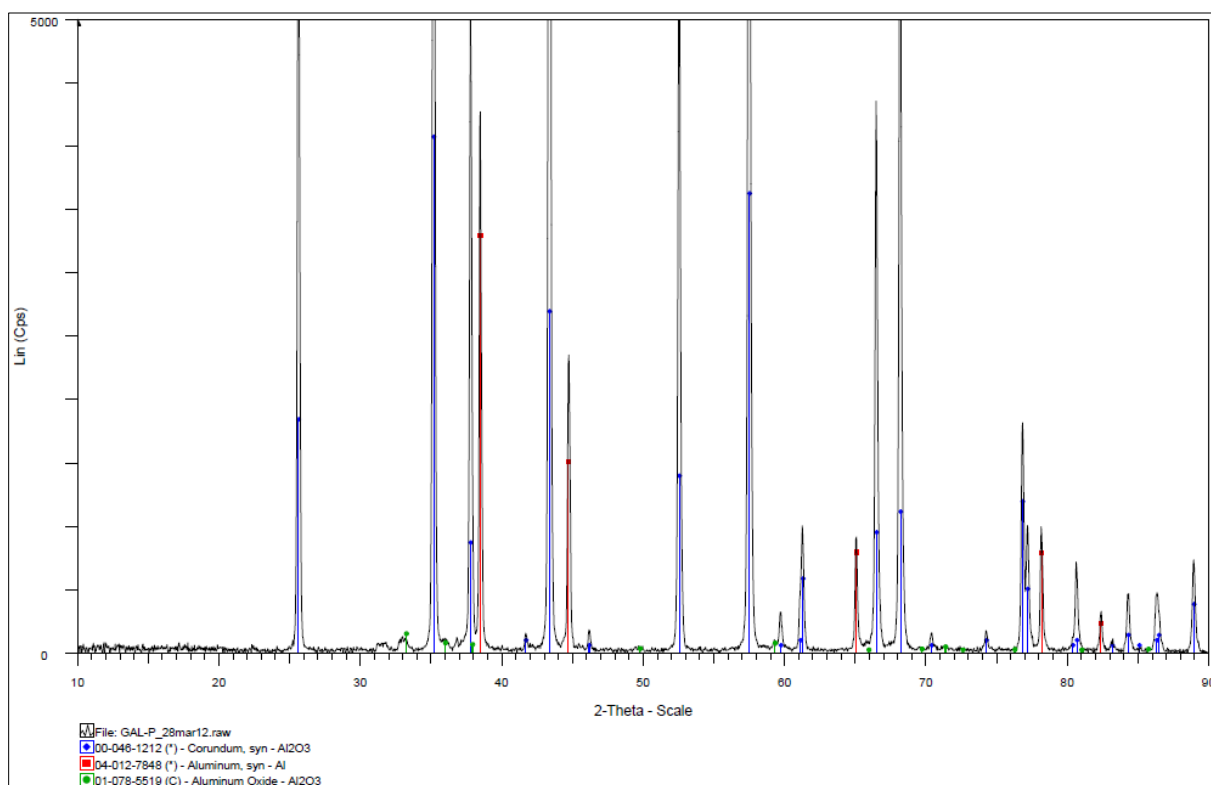


Figure 6.29 XRD pattern of the residue for the test G + Al at 1200 °C (powder).

The following XRF result of the residue confirms that practically there is no zinc left, and that  $\text{Al}_2\text{O}_3$  is the single compound existing after heat treatment (99.6 %).

	Compound	Conc.	Absolute
	Name	wt(%)	Error (%)
1	Al <sub>2</sub> O <sub>3</sub>	(99.6)	
2	Ca	0.00785	0.003
3	Cu	0.00355	0.002
4	Fe	0.115	0.01
5	Ga	0.00457	0.002
6	Ni	0.0033	0.002
7	Pt	0.00821	0.003
8	S	0.0363	0.006
9	Si	0.0514	0.007
10	Ti	0.000753	0.0008
11	Zn	0.169	0.01

Figure 6.30 XRF result of the residue for the test G + Al at 1200 °C (tablet).

From calculations, the 0.169 % of ZnO detected by XRF analysis corresponds to 0.01 g of ZnO left in the residue versus the 4.0 g of ZnO in the original gahnite, or 0.01 g of Zn versus 3.21 g of Zn respectively. This represents a 99.68 % Zn extraction performance, again a full reduction process.

One more interesting observation is that there appears to be not much difference between tablet and powder as of extraction results during the reduction process (99.98 % vs 99.68 % respectively).

The following pictures show the state of the G + Al powder before and after heat treatment. Not much change is perceived in shape and colour.



Figure 6.31 Photographs taken before (L) and after the experiment of G + Al at 1200 °C (powder).

### 6.2.3 G + Al at 1150 °C (1148 °C)

Now that the full reducing action of aluminium was confirmed by the previous two trials at 1200 °C, the strategy was followed to lower that condition gradually and explore the results in terms of zinc extraction so that an extraction curve could be established.

A test was conducted 50 °C lower.

After thorough mix for 30 min at full stirring rate in the Retsch machine of 9.01 g of pure gahnite powder and 1.77 g of pure aluminium powder, for a 1.5:2 stoichiometric ratio and total mass of 10.78 g in crucible. Furnace temperature was set to 1150 °C at a heating rate of 10 °C/min for a dwell of 1.0 h. Argon gas injection was set fixed to 3.0 L/min.

This time, the mix was put in the crucible as a powder.

After heat treatment, mass of the residue amounted 7.84 g, meaning a 2.94 g loss or 27.3 %.

From the following XRD pattern of the residue, it can be observed that it consists of  $\text{Al}_2\text{O}_3$  only. No zinc compound is detected in any form.

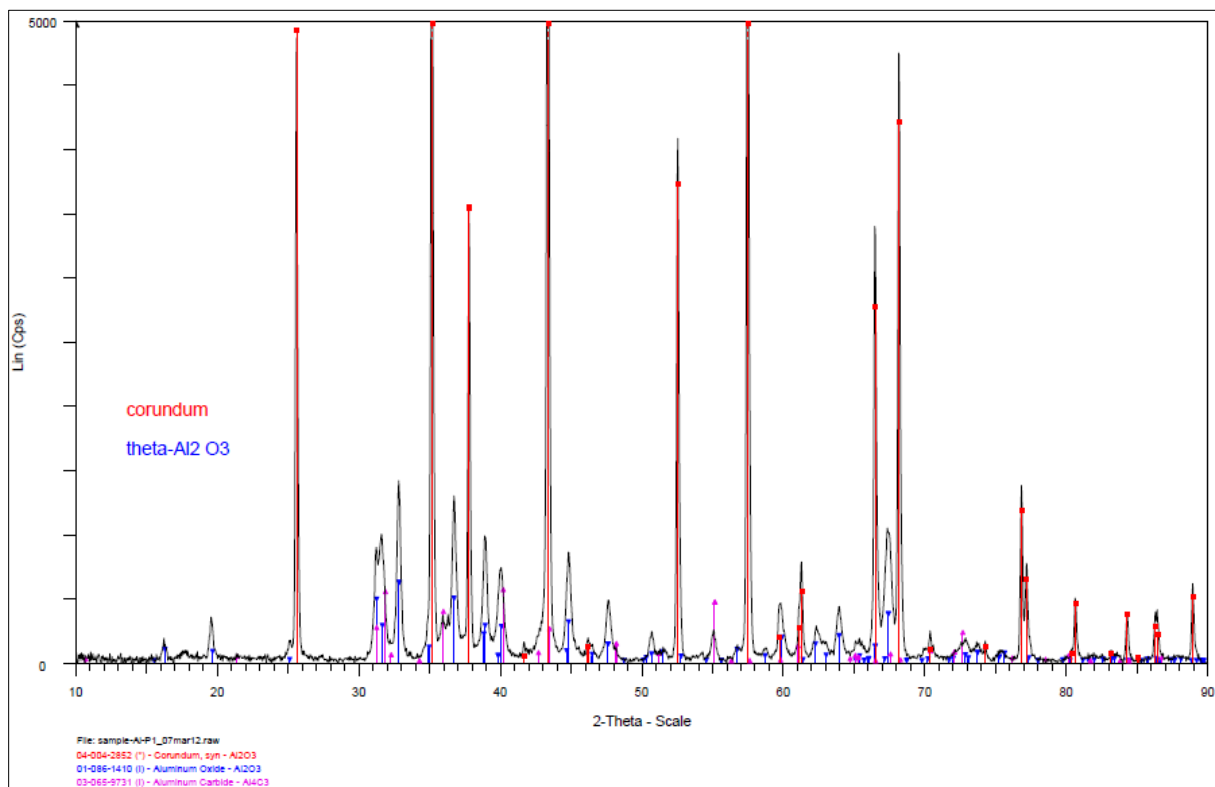


Figure 6.32 XRD pattern of the residue for the test G + Al at 1150 °C.

XRF result confirms that, at this temperature, practically all zinc is extracted from gahnite, leaving only an aluminium oxide residue, as expected.

	Compound	Conc.	Absolute
	Name	wt(%)	Error (%)
1	Al <sub>2</sub> O <sub>3</sub>	95	0.1
2	Br	0.00096	0.0009
3	CaO	0.014	0.004
4	CuO	0.0065	0.002
5	Fe <sub>2</sub> O <sub>3</sub>	0.22	0.01
6	Ga <sub>2</sub> O <sub>3</sub>	0.0044	0.002
7	K <sub>2</sub> O	0.017	0.004
8	MnO	0.02	0.004
9	NiO	0.0062	0.002
10	PtO <sub>2</sub>	0.02	0.004
11	SO <sub>3</sub>	1.1	0.03
12	SiO <sub>2</sub>	0.27	0.02
13	ZnO	3	0.05

Figure 6.33 XRF result of the residue for the test G + Al at 1150 °C.

From calculations, the 3.0 % of ZnO detected by XRF analysis corresponds to only 0.235 g of ZnO left in the residue versus the 4.0 g of ZnO in the original gahnite, or 0.189 g of Zn versus 3.21 g of Zn respectively. This represents a 94.11 % Zn extraction performance, an almost full reduction process at 1150 °C.

The following pictures show the state of the G + Al powder before and after heat treatment. The residue has a darker colour. No major changes in the distribution of the powder along the crucible are perceived.



Figure 6.34 Photographs taken before (L) and after the experiment of G + Al at 1150 °C.

#### 6.2.4 G + Al at 1100 °C (1093 °C)

A new test was carried out 50 °C lower than the previous one.

Again, after a thorough mix for 30 min at full stirring rate in the Retsch machine of 9.03 g of pure gahnite powder and 1.79 g of pure aluminium powder, for a 1.5:2 stoichiometric ratio and a total mass of 10.82 g in the crucible. Furnace temperature was set this time to 1100 °C at a heating rate of 10 °C/min for a dwell of 1.0 h. Argon gas injection was set fixed to 3.0 L/min flowrate.

The mix was put in the crucible as a powder.

After heat treatment, mass of the residue amounted 7.80 g, meaning a 3.02 g loss or 27.9 %.

From the following XRD pattern of the residue, again it can be observed that it solely consists of  $\text{Al}_2\text{O}_3$ . No zinc compound is detected.

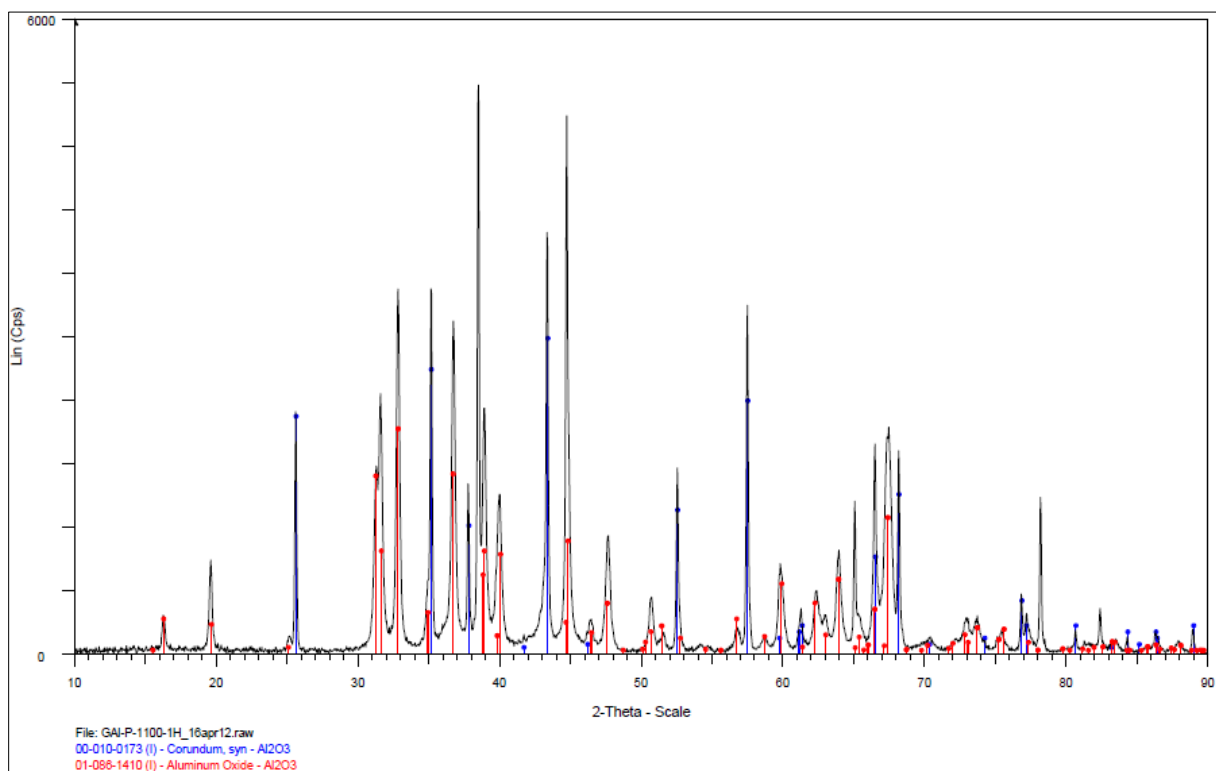


Figure 6.35 XRD pattern of the residue for the test G + Al at 1100 °C.

XRF result confirms that, at this temperature, practically all zinc is extracted from gahnite, leaving only an aluminium oxide residue, as expected.



	Compound	Conc.	Absolute
	Name	wt(%)	Error (%)
1	Al <sub>2</sub> O <sub>3</sub>	94.7	0.1
2	CaO	0.0112	0.003
3	Cr <sub>2</sub> O <sub>3</sub>	0.0127	0.003
4	CuO	0.0056	0.002
5	Fe <sub>2</sub> O <sub>3</sub>	0.212	0.01
6	Ga <sub>2</sub> O <sub>3</sub>	0.00798	0.003
7	Na <sub>2</sub> O	0.237	0.02
8	PtO <sub>2</sub>	0.0261	0.005
9	SO <sub>3</sub>	0.488	0.02
10	SiO <sub>2</sub>	0.0762	0.008
11	ZnO	4.2	0.06

Figure 6.36 XRF results of the residue for the test G + Al at 1100 °C.

From calculations, the 4.2 % of ZnO detected by XRF analysis corresponds to only 0.328 g of ZnO left in the residue versus the 4.01 g of ZnO in the original gahnite, or 0.263 g of Zn versus 3.22 g of Zn respectively. This represents a 91.82 % Zn extraction performance, a rather complete reduction process at 1100 °C.

The following pictures show the state of the G + Al powder before and after heat treatment. The residue has a darker colour. No major changes in the distribution of the powder along the crucible are perceived.



Figure 6.37 Photographs taken before (L) and after the experiment of G + Al at 1100 °C.

### 6.2.5 G + Al at 1000 °C (993 °C)

Taking into account the excellent results from the previous experiments, the temperature was lowered again, this time to 1000 °C.

After a thorough mix for 30 min at full stirring rate in the Retsch machine of 9.02 g of pure gahnite powder and 1.78 g of pure aluminium powder, for a 1.5:2 stoichiometric ratio and a total mass of 10.80 g in the crucible. Furnace temperature was set this time to 1100 °C at a heating rate of 10 °C/min for a dwell of 1.0 h. Argon gas injection was set fixed to 3.0 L/min flowrate.

The mix was put in the crucible as a powder.

After heat treatment, mass of the residue amounted 8.01 g, meaning a 2.79 g loss or 25.8 %.

From the following XRD pattern, it can be observed that even though the main component of the residue is  $\text{Al}_2\text{O}_3$ , some zinc and zinc aluminate transition compound are found. The explanation for this is that the temperature is not high enough for a full reduction of gahnite. This situation was expected, after thermodynamic calculations in Chapter 3.

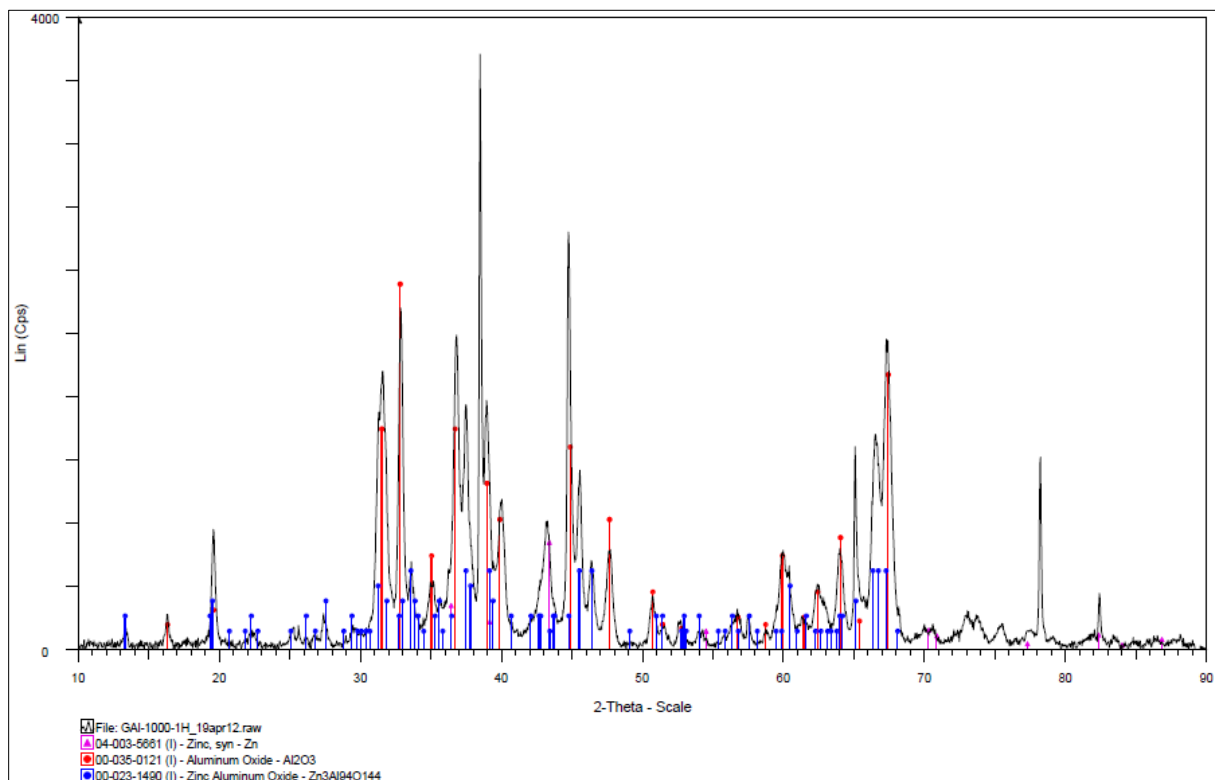


Figure 6.38 XRD pattern of the residue for the test G + Al at 1000 °C.

However, XRF analysis below shows that, on one side  $\text{Al}_2\text{O}_3$  is effectively the major compound in the residue with a 92.6 %, and on the other ZnO only amounts 6.48 %.



From calculations, this 6.48 % of ZnO detected corresponds to only 0.519 g of ZnO left in the residue versus the 4.00 g of ZnO in the original gahnite, or 0.417 g of Zn versus 3.22 g of Zn respectively. This represents a 87.03 % Zn extraction performance, still a good result for the reduction process at 1000 °C.

	Compound	Conc.	Absolute
	Name	wt(%)	Error (%)
1	Al <sub>2</sub> O <sub>3</sub>	92.6	0.1
2	CaO	0.00937	0.003
3	Cr <sub>2</sub> O <sub>3</sub>	0.0135	0.003
4	Fe <sub>2</sub> O <sub>3</sub>	0.227	0.01
5	Ga <sub>2</sub> O <sub>3</sub>	0.00674	0.002
6	NiO	0.00927	0.003
7	PtO <sub>2</sub>	0.0335	0.005
8	SO <sub>3</sub>	0.482	0.02
9	SiO <sub>2</sub>	0.116	0.01
10	WO <sub>3</sub>	0.0531	0.007
11	ZnO	6.48	0.07

Figure 6.39 XRF results of the residue for the test G + Al at 1000 °C.

The following pictures show the state of the G + Al powder before and after heat treatment. The residue has a darker colour. No major changes in the distribution of the powder along the crucible are perceived.



Figure 6.40 Photographs taken before (L) and after the experiment of G + Al at 1000 °C.

### 6.2.6 G + Al at 950 °C (956 °C)

Considering the thermodynamic calculations carried out in Chapter 3, stating that the reducing action of aluminium is yet occurring below the 1000 °C level, another experiment was performed 50 °C lower.

After a thorough mix for 30 min at full stirring rate in the Retsch machine of 4.12 g of pure gahnite powder and 0.82 g of pure aluminium powder, for a 1.5:2 stoichiometric ratio and a total mass of 4.63 g in the crucible. Furnace temperature was set this time to 950 °C at a heating rate of 10 °C/min for a dwell of 1.0 h. Argon gas injection was set fixed to 3.0 L/min flowrate.

The mix was put in the crucible as a powder.

After heat treatment, mass of the residue amounted 3.66 g, meaning a 0.97 g loss or 21.0 %.

From the following XRD pattern, it can be observed that even though the main component of the residue is  $\text{Al}_2\text{O}_3$ , gahnite is found present. Again, the explanation for this is that the temperature is not high enough for a full reduction of the spinel. This situation was expected at this somehow low temperature, after thermodynamic calculations in Chapter 3.

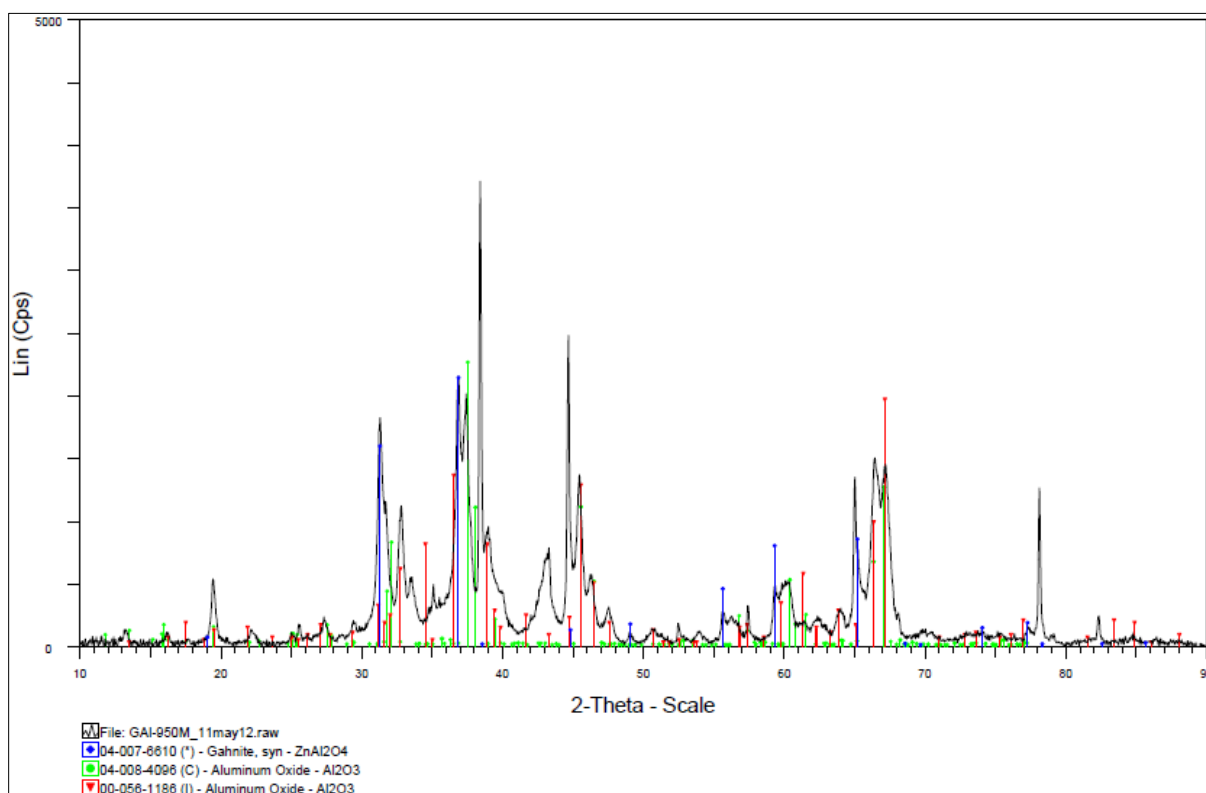


Figure 6.41 XRD pattern of the residue for the test G + Al at 950 °C.

XRF results confirm the predominant presence of  $\text{Al}_2\text{O}_3$  in the residue, as expected, and some ZnO (9.372 %) bound to the gahnite detected by XRD.

	Compound	Conc.	Absolute
	Name	wt(%)	Error (%)
1	Al <sub>2</sub> O <sub>3</sub>	89.114	0.1
2	Bi <sub>2</sub> O <sub>3</sub>	0.003	0.002
3	CaO	0.013	0.003
4	Fe <sub>2</sub> O <sub>3</sub>	0.205	0.01
5	Ga <sub>2</sub> O <sub>3</sub>	0.011	0.003
6	NiO	0.05	0.007
7	PtO <sub>2</sub>	0.042	0.006
8	SO <sub>3</sub>	1.018	0.03
9	SiO <sub>2</sub>	0.171	0.01
10	ZnO	9.372	0.09

Figure 6.42 XRF results of the residue for the test G + Al at 950 °C.

From calculations, this 9.372 % of ZnO detected corresponds to only 0.343 g of ZnO left in the residue versus the 1.83 g of ZnO in the original gahnite, or 0.276 g of Zn versus 1.47 g of Zn respectively. This represents a 81.23 % Zn extraction performance, still a good result for the reduction process at 950 °C.

The following pictures show the state of the G + Al powder before and after heat treatment. No major changes are observed.



Figure 6.43 Photographs taken before (L) and after the experiment of G + Al at 950 °C.

### 6.2.7 G + Al at 900 °C (904 °C)

Since the extraction results of the previous experiments were accordingly becoming lower as the temperature was being decreased, a final test for this aluminothermic reduction process was defined, at 900 °C, also keeping in mind the thermodynamic calculations in Chapter 3.

After a thorough mix for 30 min at full stirring rate in the Retsch machine of 9.03 g of pure gahnite powder and 1.78 g of pure aluminium powder, for a 1.5:2 stoichiometric ratio and a total mass of 10.81 g in the crucible. Furnace temperature was set this time to 900 °C at a heating rate of 10 °C/min for a dwell of 1.0 h. Argon gas injection was set fixed to 3.0 L/min flowrate.

The mix was put in the crucible as a powder.

After heat treatment, mass of the residue amounted 8.74 g, meaning a 2.07 g loss or 19.1 %.

From the following XRD pattern, it can be observed that the as expected the main component of the residue is  $\text{Al}_2\text{O}_3$ , however ZnO is found as well as gahnite along with some aluminium, due to the low reaction temperature, causing that not all the aluminium powder reacted with the gahnite powder. This is consistent with the thermodynamic calculations in Chapter 3.

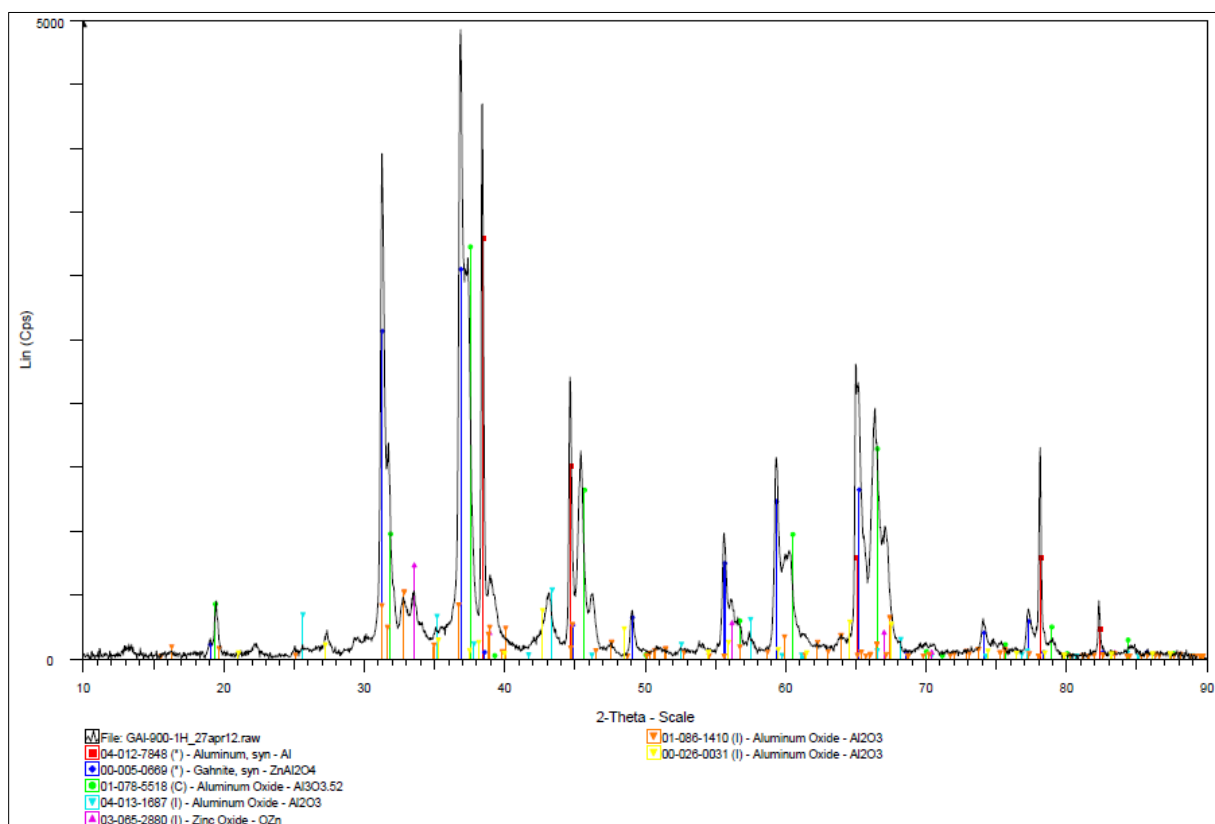


Figure 6.44 XRD pattern of the residue for the test G + Al at 900 °C.

On the other hand, XRF result confirms the leading presence of  $\text{Al}_2\text{O}_3$  in the residue, as expected, and ZnO (12.368 %) bound to the gahnite detected by XRD, the lowest extraction result in the G + Al series.

	Compound	Conc.	Absolute
	Name	wt(%)	Error (%)
1	$\text{Al}_2\text{O}_3$	86.852	0.1
2	CaO	0.015	0.004
3	$\text{Cr}_2\text{O}_3$	0.01	0.003
4	$\text{Fe}_2\text{O}_3$	0.175	0.01
5	$\text{Ga}_2\text{O}_3$	0.011	0.003
6	NiO	0.008	0.003
7	$\text{SO}_3$	0.39	0.02
8	$\text{SeO}_2$	0.002	0.001
9	$\text{SiO}_2$	0.17	0.01
10	ZnO	12.368	0.1

Figure 6.45 XRF results of the residue for the test G + Al at 900 °C.

From calculations, this 12.368 % of ZnO detected corresponds to 1.080 g of ZnO left in the residue versus the 4.01 g of ZnO in the original gahnite, or 0.869 g of Zn versus 3.22 g of Zn respectively. This represents a 73.03 % Zn extraction performance, still an interesting result for the reduction process at such a low temperature, 900 °C.

The following pictures show the state of the G + Al powder before and after heat treatment. The residue powder has changed to a whitish appearance, while no major changes are observed in the distribution of the powder inside the boat crucible.



Figure 6.46 Photographs taken before (L) and after the experiment of G + Al at 900 °C.

### 6.3 Reduction test for gahnite and ferrite combined

This test was conducted in the very final phase of the research. The idea was to examine the reduction result for the mixture of gahnite  $\text{ZnO} \cdot \text{Al}_2\text{O}_3$  and ferrite  $\text{ZnO} \cdot \text{Fe}_2\text{O}_3$ , a combination of zinc spinels that has been found in industrial residues.

This test is referred to as G + F + C.

A thorough mix for 30 min at full stirring rate in the Retsch machine was executed of 4.58 g of pure gahnite powder and 6.03 g of pure ferrite powder and 0.75 g of pure carbon powder (graphite), for a 1:1:1 stoichiometric ratio and a total mass of 11.36 g in crucible. Furnace temperature was set for this particular test to 1300 °C at a heating rate of 10 °C/min for a dwell of 1.0 h. Argon gas injection was set fixed to 3.0 L/min flowrate. Temperature measured with an independent, external thermocouple from the one set in the furnace controller was 1301 °C.

The mix was put in the crucible as a powder.

After heat treatment, mass of the residue amounted 5.73 g, meaning a 5.63 g loss or 49.6 %.

From the following XRD pattern, it can be observed that the sole compound present in the residue is a transition phase of zinc iron aluminium oxide. Neither gahnite nor ferrite are found, suggesting an almost complete reduction of the mix.

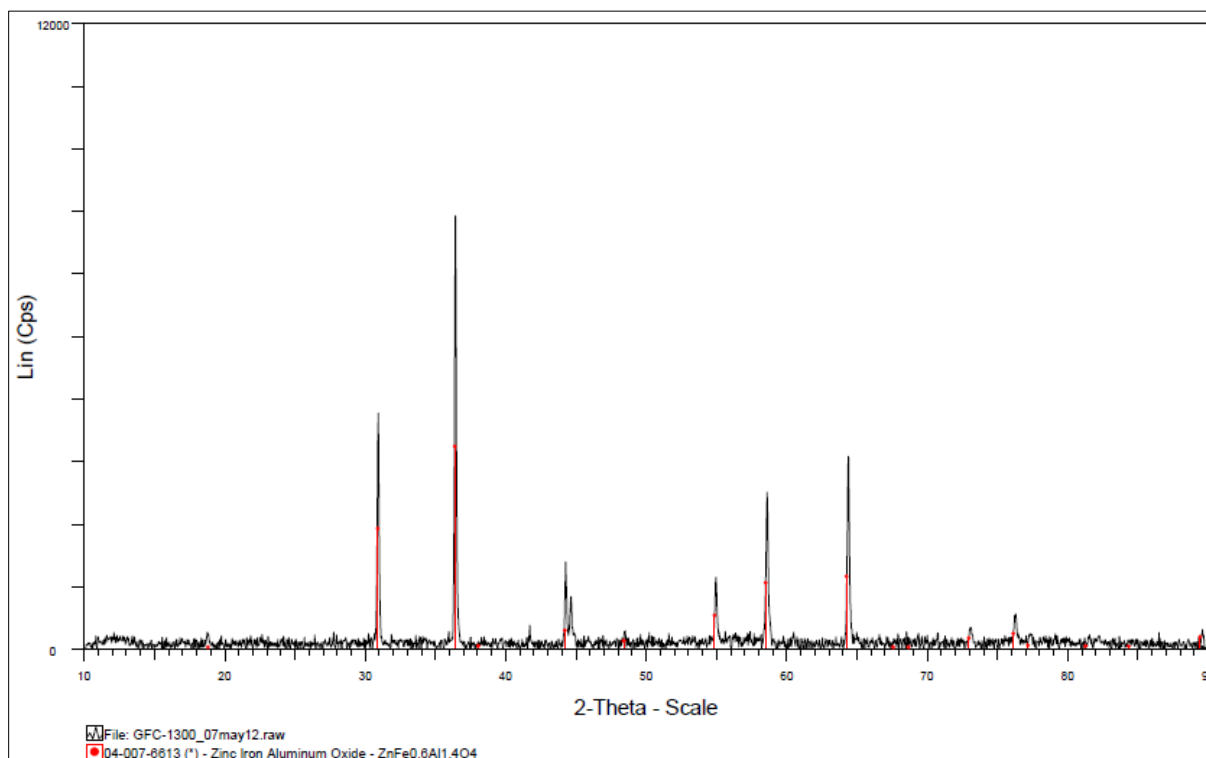


Figure 6.47 XRD pattern of the residue for the test G + F + C at 1300 °C.



XRF analysis of the residue confirms that a full reduction took place during this experiment.  $\text{Al}_2\text{O}_3$  from the original gahnite amounts 33.065 %,  $\text{Fe}_2\text{O}_3$  from the original ferrite amounts 61.756 %, whereas the total ZnO found is only a marginal 0.249 %.

	Compound	Conc.	Absolute
	Name	wt(%)	Error (%)
1	$\text{Al}_2\text{O}_3$	33.065	0.2
2	$\text{CaO}$	0.367	0.03
3	$\text{Fe}_2\text{O}_3$	61.756	0.5
4	$\text{MgO}$	0.6	0.02
5	$\text{MnO}$	0.234	0.03
6	$\text{Na}_2\text{O}$	2.645	0.07
7	$\text{SO}_3$	0.825	0.03
8	$\text{TiO}_2$	0.259	0.03
9	$\text{ZnO}$	0.249	0.01

Figure 6.48 XRF results of the residue for the test G + F + C at 1300 °C.

From calculations, this 0.249 % of ZnO detected corresponds to only 0.01 g of ZnO left in the residue versus the 4.07 g of ZnO in the original mix of gahnite and ferrite, or 0.01 g of Zn versus 3.27 g of Zn respectively. This represents a 99.65 % Zn extraction performance, a full reduction of the mixture.

The following pictures show the state of the G + F + C powder mix before and after heat treatment. The residue has changed to a more solid configuration, colour is now black, and shape somehow is the same as the original (taken the crucible's outline) but diminished in size.



Figure 6.49 Photographs taken before (L) and after the experiment of G + F + C at 1300 °C.

The temperature of 1300 °C was chosen for this particular experiment because it was found in the carbothermic reduction of gahnite that a full reduction could only be achieved at this level (please see Section 6.1), not lower, and already knowing that zinc ferrite is reduced in the range 1100-1200 °C (please see Chapter 2).

## 6.4 Reduction test for gahnite and ferrite and ZnO combined

This test was also conducted in the very final phase of the research. Again, the idea was to examine the reduction result for the mixture of gahnite  $\text{ZnO} \cdot \text{Al}_2\text{O}_3$  and ferrite  $\text{ZnO} \cdot \text{Fe}_2\text{O}_3$  and zincite  $\text{ZnO}$ , a combination of zinc compounds found in industrial environments as well.

This test is referred to as G + F + ZnO + C.

A thorough mix for 30 min at full stirring rate in the Retsch machine was executed of 3.69 g of pure gahnite powder, 4.84 g of pure ferrite powder, 1.64 g of ZnO, and 0.92 g of pure carbon powder (graphite), for a 1:1:1:1 stoichiometric ratio and a total mass of 11.09 g in crucible. Furnace temperature was set for this particular test to 1300 °C too, at a heating rate of 10 °C/min for a dwell of 1.0 h. Argon gas injection was set fixed to 3.0 L/min flowrate. Temperature measured with an independent, external thermocouple from the one set in the furnace controller was 1296 °C.

The mix was put in the crucible as a powder.

After heat treatment, mass of the residue amounted 4.46 g, meaning a 6.63 g loss or 59.8 %.

From the following XRD pattern, it can be observed that the only compounds present in the residue are again a transition phase of iron aluminium oxide (identified as hercynite, a member of the spinel group) and iron. Neither gahnite, ferrite nor zincite are found, suggesting a complete reduction of the mix.

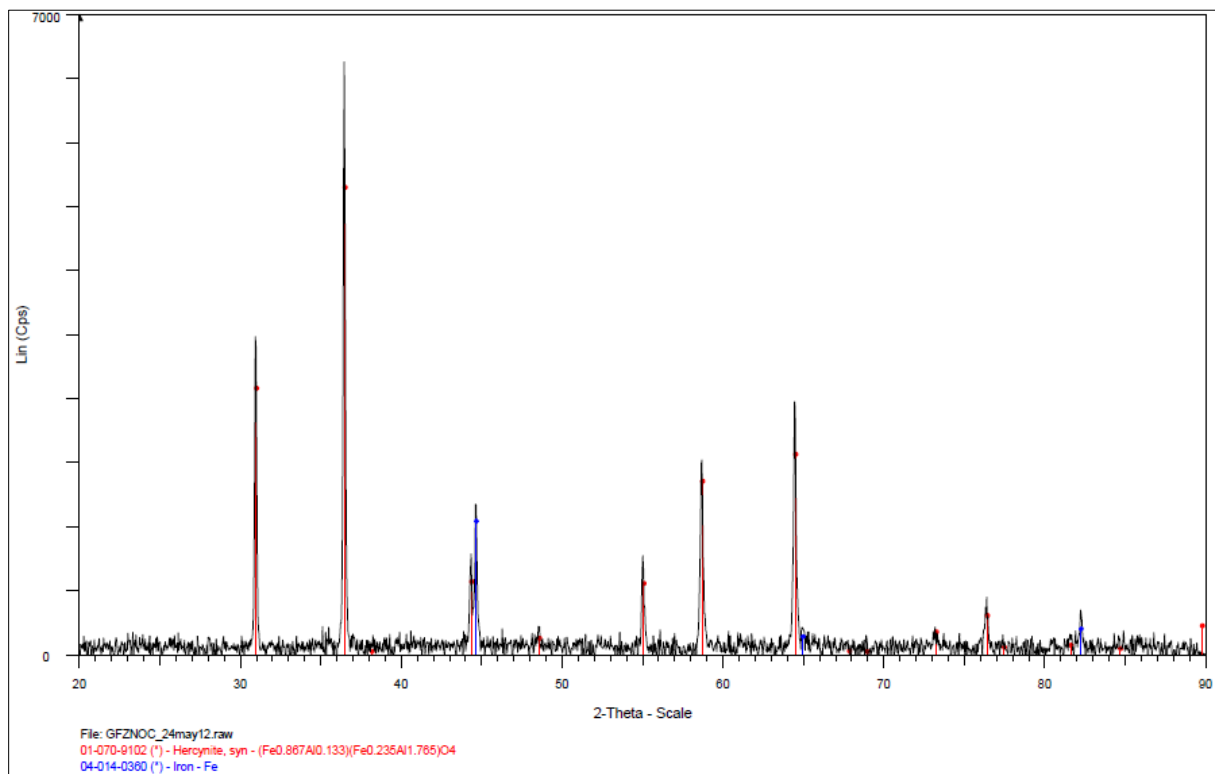


Figure 6.50 XRD pattern of the residue for the test G + F + ZnO + C at 1300 °C.



XRF analysis of the residue confirms that a total reduction of the mix took place during this experiment.  $\text{Al}_2\text{O}_3$  left from gahnite amounts 38.566 % while  $\text{Fe}_2\text{O}_3$  left from ferrite is 59.052 %. No zinc compound is found whatsoever.

	Compound	Conc.	Absolute
	Name	wt(%)	Error (%)
1	$\text{Al}_2\text{O}_3$	38.566	0.2
2	$\text{CaO}$	0.413	0.03
3	$\text{Cl}$	0.009	0.003
4	$\text{CuO}$	0.03	0.01
5	$\text{Fe}_2\text{O}_3$	59.052	0.4
6	$\text{HgO}$	0.011	0.004
7	$\text{MgO}$	0.705	0.03
8	$\text{MnO}$	0.214	0.02
9	$\text{Na}_2\text{O}$	0.177	0.02
10	$\text{SO}_3$	0.534	0.02
11	$\text{SiO}_2$	0.056	0.009
12	$\text{TiO}_2$	0.234	0.02

Figure 6.51 XRF results of the residue for the test  $\text{G} + \text{F} + \text{ZnO} + \text{C}$  at 1300 °C.

This result represents a 100 % extraction performance.

Finally, from the following images, it is observed that the residue assumed a black colour, keeping the shape of the crucible's outline but diminished in size, and was left in a more solid state than the original loose powder.



Figure 6.52 Photographs taken before (L) and after the experiment of  $\text{G} + \text{F} + \text{ZnO} + \text{C}$  at 1300 °C.

## 6.5 Exploratory reduction tests with addition of $\text{SiO}_2$

Two tests were conducted to study the reduction of gahnite with the additional presence of silica, both with carbon (referred to as G + C +  $\text{SiO}_2$ ) and aluminium (referred to as G + Al +  $\text{SiO}_2$ ) as reducing agents, being based on Sections 3.3.1 and 3.3.2 respectively.

### 6.5.1 G + C + $\text{SiO}_2$

A thorough mix for 30 min at full stirring rate in the Retsch machine was executed of 9.165 g of pure gahnite powder, 0.60 g of pure carbon powder (graphite), and 3.00 g of pure silica powder, for a 1:1:1 stoichiometric ratio and a total mass of 12.77 g in crucible. Furnace temperature was set for this particular test to 1200 °C, at a heating rate of 10 °C/min for a dwell of 1.0 h. Argon gas injection was set fixed to 3.0 L/min flowrate. Temperature measured with an independent, external thermocouple from the one set in the furnace controller was 1195 °C.

The mixture was put in the crucible as one single perfect tablet after a simple pressing procedure. After heat treatment, mass of the residue amounted 12.11 g, meaning only a 0.65 g loss or 5.1 %.

From the following XRD pattern, it can be observed that the compounds present in the residue are  $\text{Al}_2\text{O}_3$ , as expected, but also clearly gahnite and silica, suggesting an incomplete reduction of the spinel.

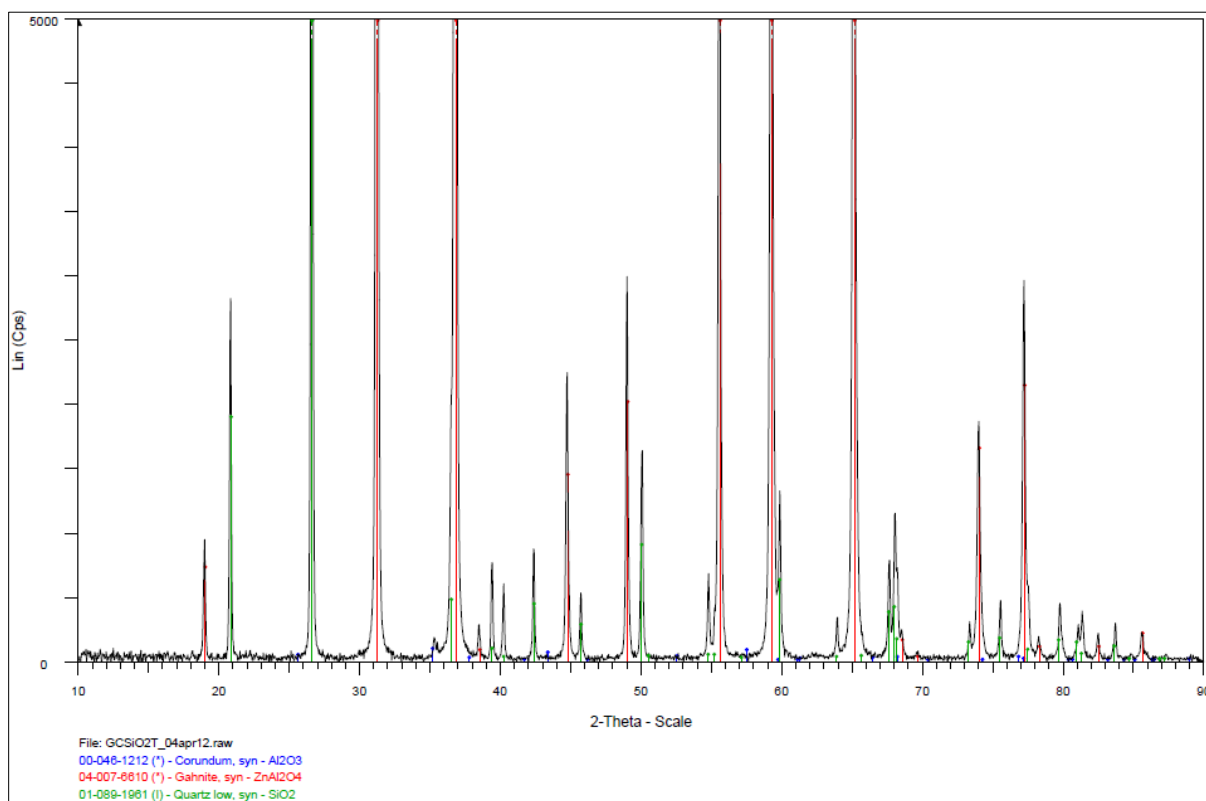


Figure 6.53 XRD pattern of the residue for the test G + C +  $\text{SiO}_2$  + C at 1200 °C.

This situation is confirmed by the XRF result, which shows a 34.2 % of  $\text{Al}_2\text{O}_3$  and an important 25.8 % of  $\text{ZnO}$  in the residue.

	Compound	Conc.	Absolute
	Name	wt(%)	Error (%)
1	$\text{Al}_2\text{O}_3$	34.2	0.1
2	$\text{CaO}$	0.00941	0.003
3	$\text{Fe}_2\text{O}_3$	0.0727	0.008
4	$\text{K}_2\text{O}$	0.149	0.01
5	$\text{MgO}$	10.8	0.3
6	$\text{SiO}_2$	28.9	0.1
7	$\text{TiO}_2$	0.0166	0.004
8	$\text{ZnO}$	25.8	0.1
9	$\text{ZrO}_2$	0.00274	0.002

Figure 6.54 XRF results of the residue for the test  $\text{G} + \text{C} + \text{SiO}_2$  at 1200 °C.

From calculations, this 25.8 % of  $\text{ZnO}$  detected corresponds to 3.124 g of  $\text{ZnO}$  left in the residue versus the 4.07 g of  $\text{ZnO}$  in the original gahnite, or 2.512 g of Zn versus 3.27 g of Zn respectively. This represents a 23.14 % Zn extraction performance, a low reduction.

From the following images, it is observed that the residue assumed a very whitish colour, but the original shape of the tablet did not vary.



Figure 6.55 Photographs taken before (L) and after the experiment  $\text{G} + \text{C} + \text{SiO}_2$  at 1200 °C.

Considering the low results of zinc extraction, this carbothermic route with addition of silica was not continued.

### 6.5.2 G + Al + SiO<sub>2</sub>

A thorough mix for 30 min at full stirring rate in the Retsch machine was executed of 9.165 g of pure gahnite powder, 1.35 g of pure carbon powder (graphite), and 3.00 g of pure silica powder, for a 1:1:1 stoichiometric ratio and a total mass of 13.52 g in crucible. Furnace temperature was set for this particular test to 1200 °C, at a heating rate of 10 °C/min for a dwell of 1.0 h. Argon gas injection was set fixed to 3.0 L/min flowrate. Temperature measured with an independent, external thermocouple from the one set in the furnace controller was 1192 °C.

The mixture was put in the crucible as one single perfect tablet after a simple pressing procedure.

After heat treatment, mass of the residue amounted 12.62 g, meaning only a 0.90 g loss or 6.6 %.

From the following XRD pattern, it can be observed that the compounds present in the residue are Al<sub>2</sub>O<sub>3</sub>, as expected, but, as in the test G + C + SiO<sub>2</sub>, also clearly gahnite and silica, suggesting an incomplete reduction of the spinel.

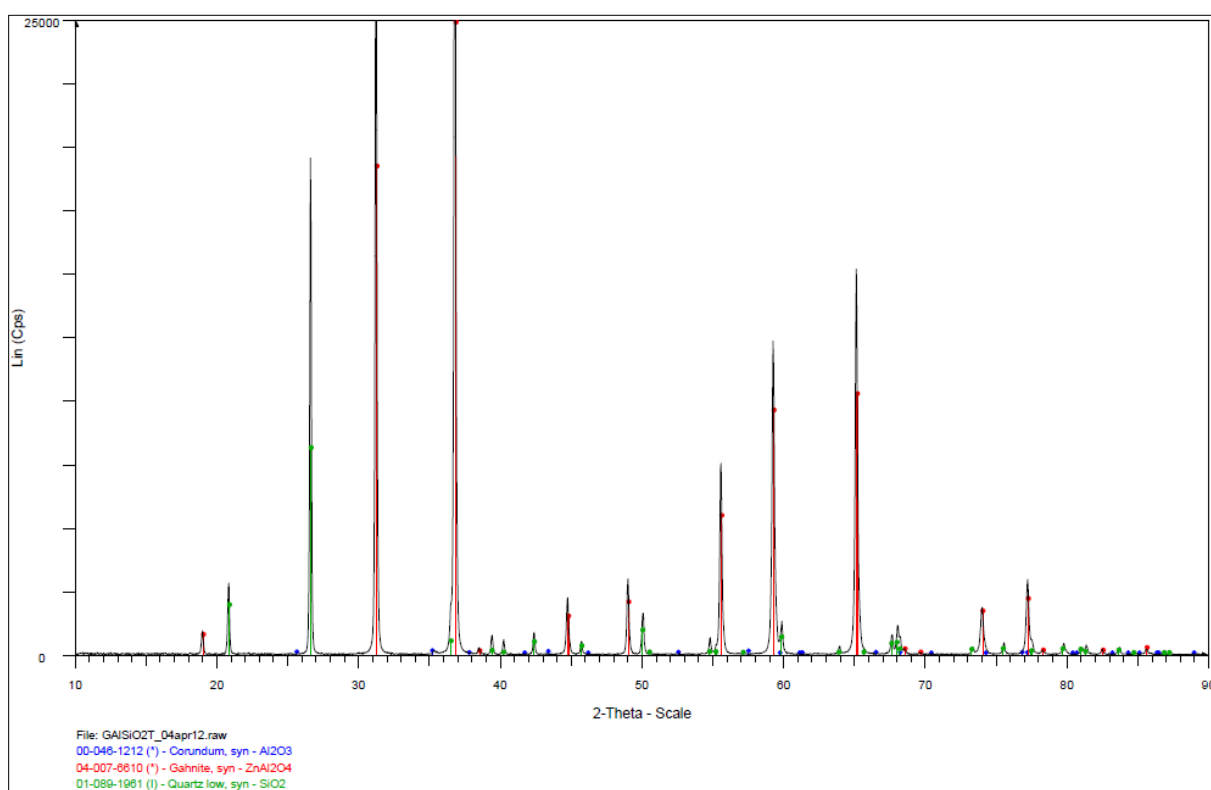


Figure 6.56 XRD pattern of the residue for the test G + Al + SiO<sub>2</sub> + C at 1200 °C.

This situation is confirmed by the XRF result, which shows a 46.5 % of Al<sub>2</sub>O<sub>3</sub> and an important 30.7 % of ZnO in the residue.

	Compound	Conc.	Absolute
	Name	wt(%)	Error (%)
1	Al <sub>2</sub> O <sub>3</sub>	46.5	0.1
2	CaO	0.0282	0.005
3	Cr <sub>2</sub> O <sub>3</sub>	0.0117	0.003
4	CuO	0.0101	0.003
5	Fe <sub>2</sub> O <sub>3</sub>	0.132	0.01
6	Ga <sub>2</sub> O <sub>3</sub>	0.018	0.004
7	K <sub>2</sub> O	0.309	0.02
8	MgO	0.134	0.01
9	NiO	0.00565	0.002
10	P <sub>2</sub> O <sub>5</sub>	0.012	0.003
11	SO <sub>3</sub>	0.047	0.007
12	SiO <sub>2</sub>	22.1	0.1
13	ZnO	30.7	0.1

Figure 6.57 XRF results of the residue for the test G + Al + SiO<sub>2</sub> at 1200 °C.

From calculations, this 30.7 % of ZnO detected corresponds to 3.87 g of ZnO left in the residue versus the 4.07 g of ZnO in the original gahnite, or 3.11 g of Zn versus 3.27 g of Zn respectively. This represents a 4.69 % Zn extraction performance, a low reduction.

From the following images, it is observed that the residue assumed, again, a very whitish colour, but the original shape of the tablet did not vary.



Figure 6.58 Photographs taken before (L) and after the experiment G + Al + SiO<sub>2</sub> at 1200 °C.

Considering the low results of zinc extraction, this aluminothermic route with addition of silica was not continued further.

## 6.6 Exploratory reduction tests with addition of $\text{SiO}_2$ and $\text{CaO}$

Two more tests were conducted directly after the ones with addition of silica, now plus lime. Once again, one with carbon and another with aluminium.

### 6.6.1 G + C + $\text{SiO}_2$ + $\text{CaO}$

A thorough mix for 30 min at full stirring rate in the Retsch machine was executed of 4.60 g of pure gahnite powder, 0.31 g of pure carbon powder (graphite), 5.12 g of pure silica powder, and 5.12 g of pure lime, for a 20 % (1:1) : 10 % : 40 % : 40 % stoichiometric ratio and a total mass of 15.15 g in crucible. Furnace temperature was set for this particular test to 1400 °C, at a heating rate of 10 °C/min for a dwell of 1.0 h. Argon gas injection was set fixed to 3.0 L/min flowrate. Temperature measured with an independent, external thermocouple from the one set in the furnace controller was 1399 °C.

The mixture was put in the crucible as one single perfect tablet after a simple pressing procedure.

After heat treatment, mass of the residue amounted 12.46 g, meaning a 2.69 g loss or 17.8 %.

This loss of mass is probably due to the reduction that took place. However, the thermal treatment resulted in a sort of glass residue in the crucible, completely adhered to the crucible itself, as can be observed in the following photograph, and no XRD/XRF analysis could be performed to the residue.



Figure 6.59 Photographs taken before (L) and after the experiment G + C +  $\text{SiO}_2$  +  $\text{CaO}$  at 1400 °C.

The black powder that is found on top of the glass residue was somehow loose, and then taken for XRF analysis, resulting to be carbon only.

No calculations could be done for an estimation of zinc extraction. No other tests for this route of  $\text{SiO}_2$  +  $\text{CaO}$  addition were performed.



### 6.6.2 G + Al + SiO<sub>2</sub> + CaO

A thorough mix for 30 min at full stirring rate in the Retsch machine was executed of 4.58 g of pure gahnite powder, 0.675 g of pure aluminium powder, 5.10 g of pure silica powder, and 5.10 g of pure lime, for a 20 % (1:1) : 10 % : 40 % : 40 % stoichiometric ratio and a total mass of 15.455 g in crucible. Furnace temperature was set, as in the previous carbon test, to 1400 °C, at a heating rate of 10 °C/min for a dwell of 1.0 h. Argon gas injection was set fixed to 3.0 L/min flowrate. Temperature measured with an independent, external thermocouple from the one set in the furnace controller was 1384 °C.

The mixture was put in the crucible as one single perfect tablet after a simple pressing procedure.

After heat treatment, mass of the residue amounted 13.31 g, meaning a 2.15 g loss or 13.9 %.

This loss of mass is, as before, probably due to the reduction that took place. However, the thermal treatment resulted in a sort of slag residue in the crucible, black in colour and very hard in texture, completely adhered to the crucible itself, as can be observed in the following photograph, and no XRD/XRF analysis could be performed to the residue.



Figure 6.60 Photographs taken before (L) and after the experiment G + Al + SiO<sub>2</sub> + CaO at 1400 °C.

No calculations could be done for an estimation of zinc extraction. No other tests for this route of SiO<sub>2</sub> + CaO addition were performed.

## 7 DISCUSSION

### 7.1 Hydrometallurgical treatment

#### 7.1.1 Atmospheric leaching

Results from ALX of gahnite were a non-detected dissolution and no relevant mass change with respect to the leaching conditions applied. Adequate leaching conditions were utilized for this route (high concentration of acids, temperature, L/S ratio and time), yet no zinc was leached out from the spinel. This was readily settled after doing a mass balance between initial gahnite and product. A further indication was obtained through both XRD pattern of the residue, which showed the presence of gahnite only, and XRF analysis of the same residue, which resulted in a quite similar composition to pure gahnite. Samples for each test were taken every 15 min, however it was considered unnecessary to have then analyzed by ICP, and therefore no extraction/time curves could be established. The following table summarizes the findings for this initial route.

Table 7.1 Results from atmospheric leaching of gahnite.

RESULTS OF ATMOSPHERIC LEACHING OF GAHNITE								
LX agent	Concentration [M]	Gahnite [g]		Pressure [bar]	Temperature [°C]	L/S	Time [min]	Zinc extraction [%]
		Before	After					
H <sub>2</sub> SO <sub>4</sub>	4.0	11.70	11.66	1.01	95	10	120	non-detected
HCl	4.0	10.13	10.10	1.01	95	10	120	non-detected
HNO <sub>3</sub>	4.0	9.93	9.91	1.01	95	10	120	non-detected

#### 7.1.2 Pressure leaching

Results from PLX of gahnite were better than ALX but still low or moderate. Harsher leaching conditions were applied, in relation to temperature, pressure and L/S ratio. Leaching agents utilized for this route were H<sub>2</sub>SO<sub>4</sub> and HNO<sub>3</sub>; HCl was discarded due to corrosion constraints<sup>[12] [13]</sup>. In comparison, nitric acid gave better results than sulphuric acid. Zinc extraction results (in %) come from ICP analyses of samples taken every 15 min per test. The following table reviews the best results per test (achieved at 90 min leaching time).

Table 7.2 Results from pressure leaching of gahnite.

RESULTS OF PRESSURE LEACHING OF GAHNITE						
LX agent	Concentration [M]	Pressure [bar]	Temperature [°C]	L/S	Time [min]	Zinc extraction [%]
H <sub>2</sub> SO <sub>4</sub>	0.50	30.6	235	40	90	2.55
	0.75	3.6	140			2.93
HNO <sub>3</sub>	0.50	36.5	245	40	90	20.69
	4.00	39.7	250			22.20



The following graph combines the results for the tests with sulphuric acid. It can be observed that the increment on the acid concentration gives a slightly better result, while both trials show the same tendency in time.

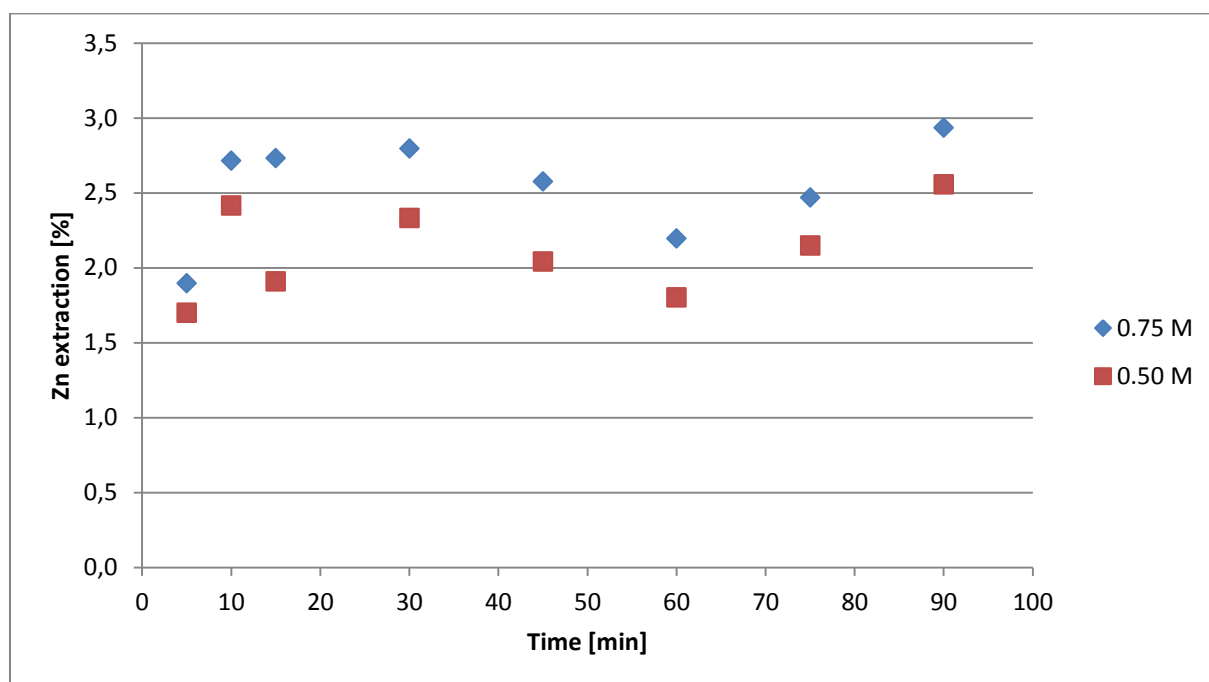


Figure 7.1 Results of PLX of gahnite with  $\text{H}_2\text{SO}_4$ .

On the other hand, Figure 7.2 combines the results with nitric acid. As in the previous case, the increment on acid concentration produces better extraction results of zinc, while showing the same tendency in time.

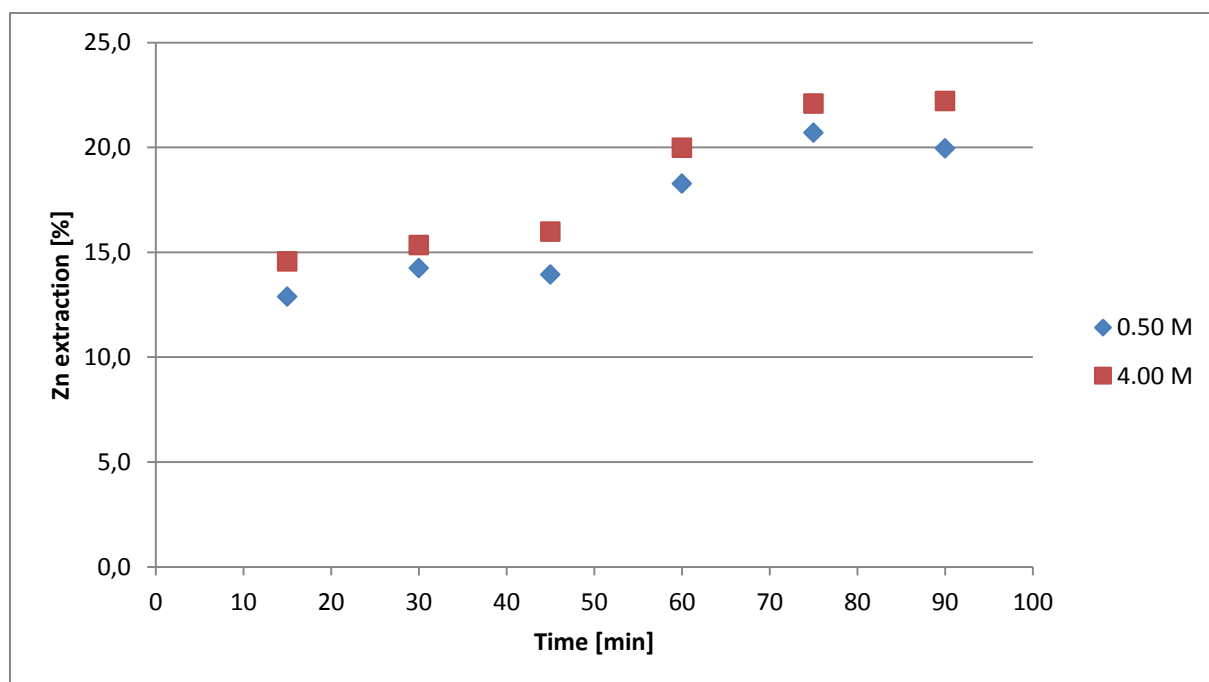


Figure 7.2 Results of PLX of gahnite with  $\text{HNO}_3$ .

## 7.2 Pyrometallurgical treatment

### 7.2.1 Carbothermic reduction

This route proved to be very effective for processing gahnite and extracting zinc out, achieving a full reduction at 1300 °C. General working conditions were a powder mix of 1:1.25 stoichiometric ratio between pure gahnite and carbon (graphite), 10.0 °C/min heating rate of the furnace, and argon gas injected at a ~ 3.0 L/min constant flowrate. The following table summarizes tests and results (4<sup>th</sup> row corresponds to a tablet mix).

Table 7.3 Main results from carbothermic reduction of gahnite.

Temperature [°C]	Dwell [h]	AFTER HEAT TREATMENT			
		Mass loss [%]	Al <sub>2</sub> O <sub>3</sub> [wt %]	ZnO [wt %]	Zn extraction [%]
1300	2.0	45.56	99.7	0.0719	99.90
1250	1.0	25.83	66.8	32.9	40.43
1200	1.0	11.67	52.6	47.2	0.00
1300	2.0	45.77	98.7	0.97	98.72

With this data, the following graph can be established. It is observed that, as temperature is increased, zinc extraction is increased accordingly, from 0.00 % at 1200 °C to 99.90 % at 1300 °C, a condition of full reduction of the spinel. Also, ZnO wt% in the residue is diminished while Al<sub>2</sub>O<sub>3</sub> wt% consequently is augmented. Clearly, as zinc is extracted from the compound, there is a larger mass loss when increasing temperature.

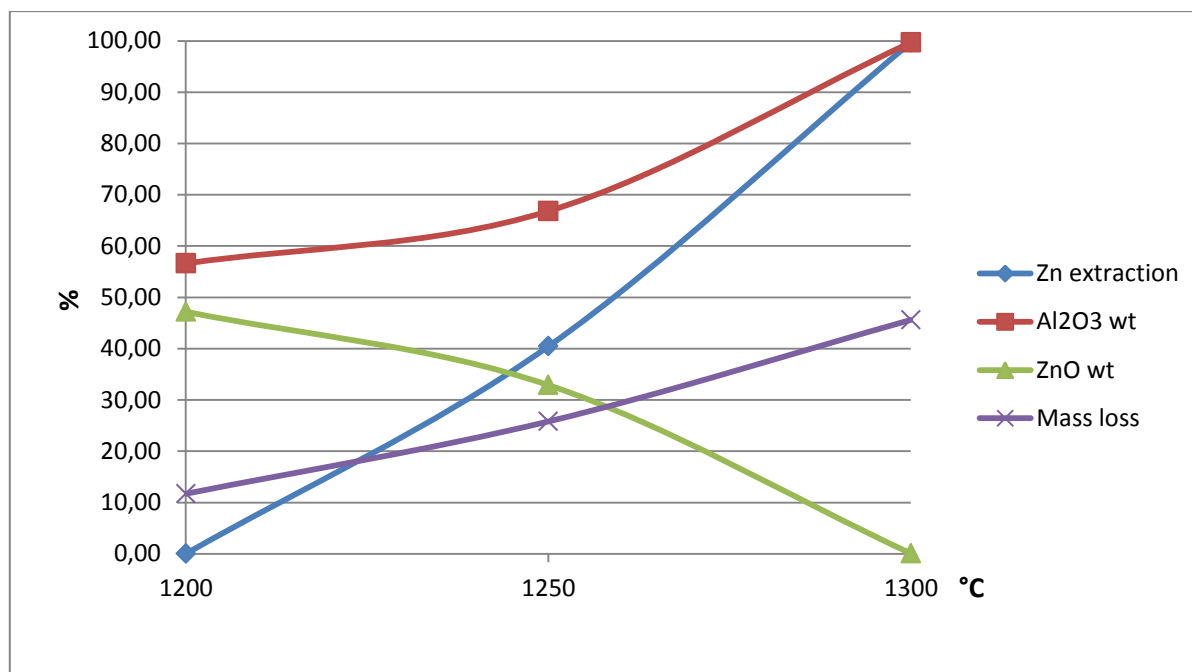


Figure 7.3 Zinc extraction from gahnite through carbothermic treatment in the range 1200 – 1300 °C.

With the previous extraction data, it is possible to update the HSC Chemistry result and establish the following graph (wide blue line to the right):

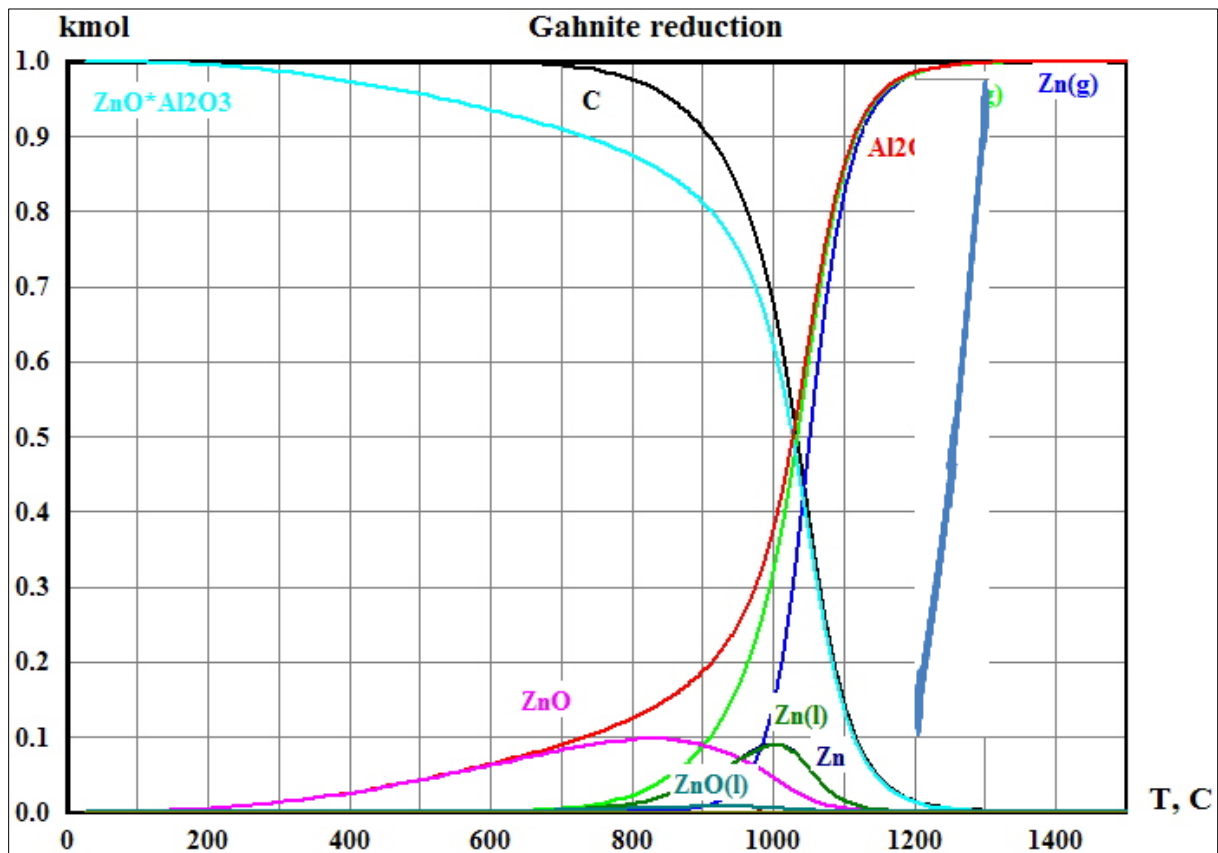


Figure 7.4 Original HSC Chemistry thermodynamic graph combined with real zinc extraction.

It can be observed that reduction of gahnite starts to increase rapidly not at around 1000 °C but higher than 1200 °C, and that a full reduction of gahnite is not achieved at around 1400 °C but at a lower temperature, 1300 °C.

### 7.2.2 Aluminothermic reduction

This novel route proved to be very effective for processing gahnite and extracting zinc out, achieving a full reduction at 1200 °C. General working conditions were a powder mix of 1.5:2 stoichiometric ratio between pure gahnite and pure aluminium, 10.0 °C/min heating rate of the furnace, a dwell of 1.0 h, and argon gas injected at a ~ 3.0 L/min constant flowrate. The following table summarizes tests and results.

Table 7.4 Main results from carbothermic reduction of gahnite.

Temperature [°C]	AFTER HEAT TREATMENT			
	Mass loss [%]	Al <sub>2</sub> O <sub>3</sub> [wt %]	ZnO [wt %]	Zn extraction [%]
1200	29.87	99.60	0.169	99.68
1150	27.27	95.00	3.00	94.11
1100	27.91	94.70	4.20	91.82
1000	25.83	92.60	6.48	87.03
950	20.95	89.11	9.37	81.23
900	19.15	86.85	12.36	73.03

With these results, the following chart has been established. It summarizes graphically the zinc extraction from gahnite as temperature is being increased from 900 °C to 1200 °C.

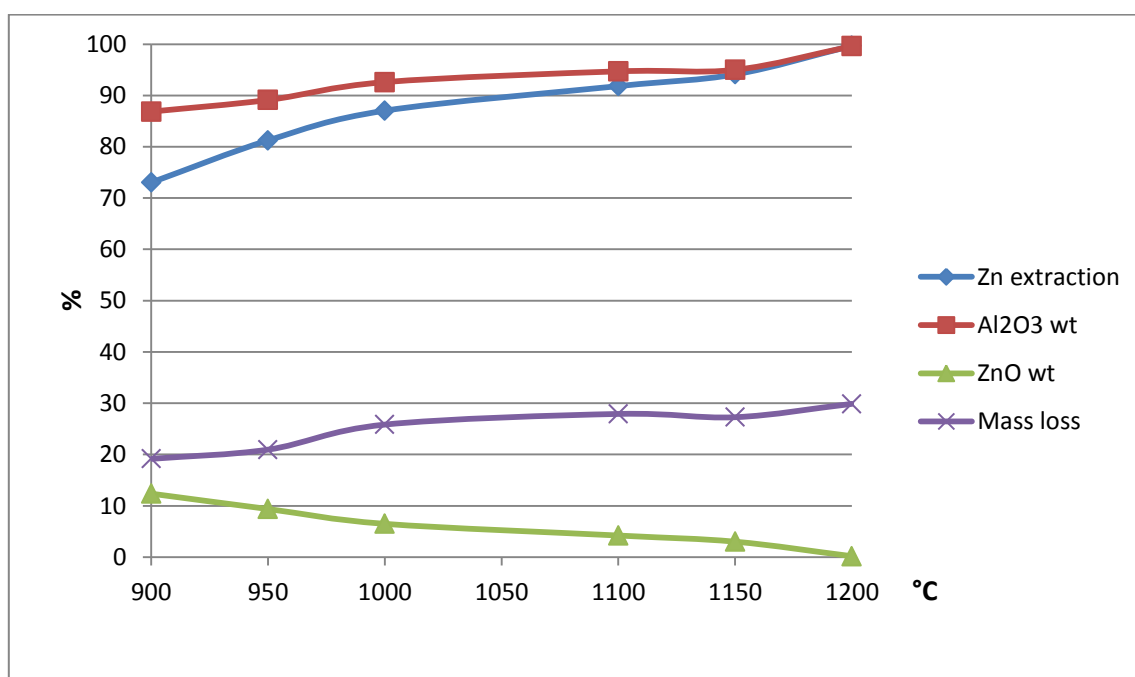


Figure 7.5 Zinc extraction from gahnite through carbothermic treatment in the range 1200 – 1300 °C.

It is observed that, as temperature of the heat treatment is augmented gradually in the furnace, metal extraction is increased accordingly, from an interesting 73.03 % at 900 °C to a full extraction of zinc from gahnite at 1200 °C.

This result is in concordance with earlier thermodynamic calculations performed with HSC Chemistry, which state that reduction of gahnite with aluminium should start occurring in the 900 °C range and achieve a complete conversion as the reaction approximates to the 1200 °C level. Furthermore, as it turns out to be, what is left in the residue should have a higher wt% of  $\text{Al}_2\text{O}_3$  and a lower wt% of ZnO as the reaction temperature is increased. This is consistent with the same thermodynamic calculations. This result is also included in the chart, for the same temperature range.

Also, as zinc is extracted from the compound, there is a larger mass loss when increasing temperature.

Finally, in the following graph, both original thermodynamic calculations and real zinc extraction have been combined, for the given temperature range.

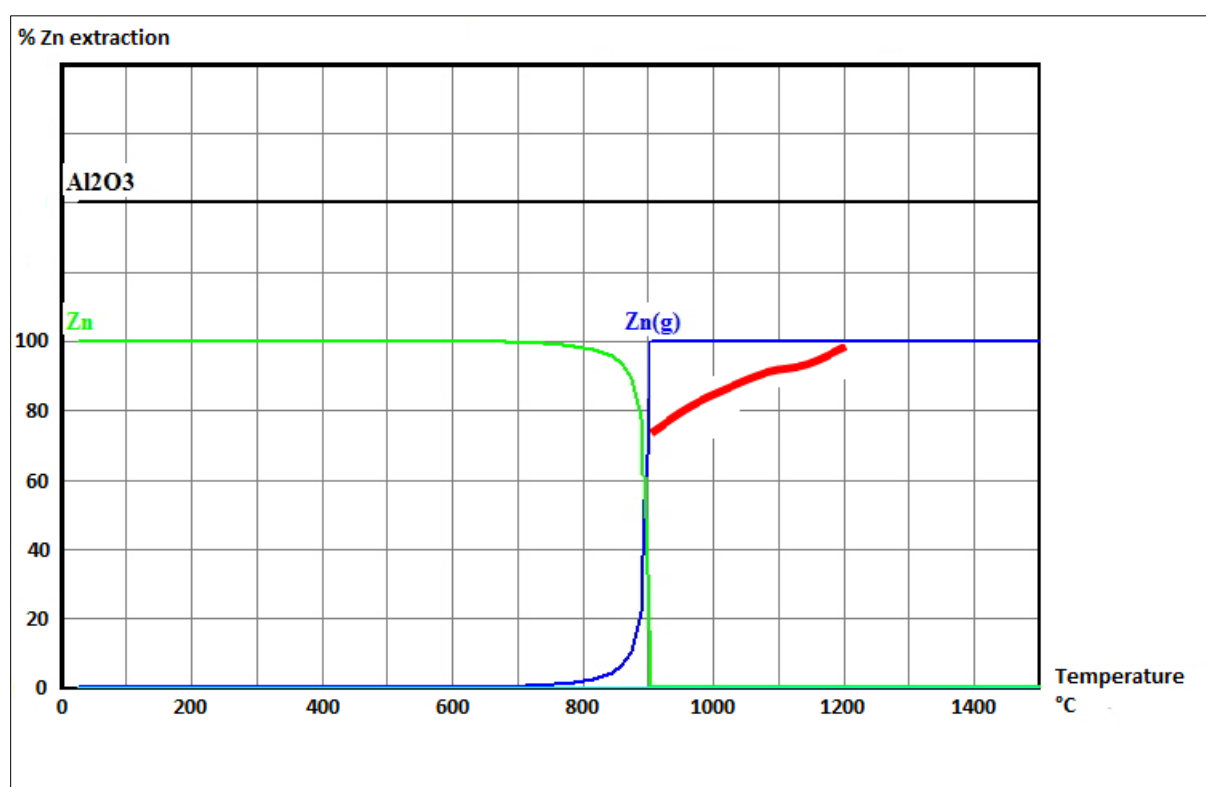


Figure 7.6 Original thermodynamic calculation combined with real zinc extraction.

As explained earlier, the green line represents zinc in the solid phase and the blue line zinc in the gas phase as the temperature of the reaction is being increased. Around 800 °C, reduction of gahnite with aluminium starts to take place, being complete right after the 900 °C range. This calculation only gives a probability of the process. Now with the real extraction results in the range 900 – 1200 °C, exhibited in the red line to the right of the graph, it is observed that actually the conversion takes places at a lower rate in that temperature range, achieving the full reduction status only at 1200 °C and not before, yet the tendency is correct.

Other results for this route (balls, tablet) are summarized in the following table:

Table 7.5 Other results from aluminothermic reduction of gahnite.

Mix	Ratio	Temperature [°C]	Dwell [min]	AFTER HEAT TREATMENT			
				Mass loss [%]	Al <sub>2</sub> O <sub>3</sub> [wt %]	ZnO [wt %]	Zn extraction [%]
tablet	1.5:2	1200	60	30.5	99.6	0.0109	99.98
powder	1.5:2	1100	5 – 6	34.9	96.2	2.64	95.35
powder	1.5:2	950	66	26.7	95.307	3.899	92.27
balls	1.5:1	1000	60	7.3	56.0	44.0	0.00
balls	1.5:2	1000	60	1.3	53.0	47.0	0.00
balls	1.5:2	1200	60	6.0	56.0	44.0	0.00

General working conditions were a 10.0 °C/min heating rate and argon gas injection at a constant flowrate of ~ 3.0 L/min.

From the tablet tests, it is observed that not much difference exists between loose powder and pressed tablet, in terms of zinc extraction.

The 5 – 6 min test was a test which failed due to over-injection of argon gas, resulting in the sudden uncover of one of the extreme corks of the furnace tube, after that amount of time. However, it was still interesting since, even though heat treatment only lasted for a few minutes at 1100 °C, it was enough for an almost full reduction of gahnite.

The three tests with aluminium balls were performed in the earlier study stage of this processing route, and resulted in a null extraction of zinc from the spinel. Although the same amount of aluminium is added as powder to the mix with gahnite, there is a lower surface interaction with balls than with powder, resulting in a much better reaction with the latter.

### 7.2.3 Other pyrometallurgical tests

The following table summarizes the results from the tests described in Sections 6.3 to 6.6.

Table 7.6 Results from additional pyrometallurgical tests with gahnite.

Test	Mix	Ratio	Temperature [°C]	AFTER HEAT TREATMENT			
				Mass loss [%]	Al <sub>2</sub> O <sub>3</sub> [wt %]	ZnO [wt %]	Zn extraction [%]
G + C + SiO <sub>2</sub>	tablet	1:1:1	1200	5.13	34.2	25.8	23.14
G + Al + SiO <sub>2</sub>	tablet	1:1:1	1200	6.62	46.5	30.7	4.69
G + F + C	powder	1:1:1	1300	49.56	33.065	0.249	99.65
G + F + ZnO + C	powder	1:1:1:1	1300	59.78	38.566	0.000	100.00

General working conditions were dwell time of 1.0 h, heating rate of 10.0 °C/min, and argon gas injection at a constant flowrate of ~ 3.0 L/min.

The addition of  $\text{SiO}_2$  to the mix was meant to explore the reduction of gahnite at a lower temperature, however that was not the case and, at 1200 °C, ZnO content in the residue was quite high (25.8 % and 30.7 % for the mix with carbon and aluminium respectively), resulting in moderate and low extraction (correspondingly) of zinc from the spinel.

The purpose of adding  $\text{SiO}_2$  and  $\text{CaO}$  combined to the mix was the same, though at 1400 °C a glass was formed from the mix G + C, and a solid slag was formed from the mix G + Al. A loss of mass was observed after heat treatment (17.76 % and 13.91 % respectively), but no zinc extraction could be calculated from the products.

Finally, the processing of the mix of gahnite and zinc ferrite was excellent, resulting in a full reduction at 1300 °C (a temperature level established earlier for gahnite conversion with carbon) for a 99.65 % extraction of zinc from the spinel. Likewise, a full reduction of the mix of gahnite and zinc ferrite and zinc oxide was achieved at the same temperature, resulting in a 100.0 % extraction of the metal from the spinel.

## 8 CONCLUSIONS

### 8.1 Hydrometallurgical treatment

Atmospheric hot leaching (ALX) of gahnite  $\text{ZnO} \cdot \text{Al}_2\text{O}_3$  was performed at 95 °C with sulphuric acid  $\text{H}_2\text{SO}_4$ , hydrochloric acid  $\text{HCl}$ , and nitric acid  $\text{HNO}_3$ , in all cases at a concentration of 4.0 M, with a L/S of 10 and continuous stirring of the mix during two hours. Sampling was executed every 15 min, so that zinc extraction curves could afterwards be established with data from ICP analyses. However, mass balances in all three cases showed that no relevant difference. There was no dissolution detected of the zinc spinel during leaching at the given conditions of temperature and acid concentration. A further indication was given by the XRD pattern analysis of the residue, which turned out to be quite similar to pure gahnite, and also by XRF analysis of the residue, which correspondingly indicated a similar composition to pure gahnite.

A series of pressure leaching (PLX) tests was carried out with an autoclave so that gahnite was put under more aggressive conditions of temperature and pressure. Corrosion restrictions of the titanium-based container limited though the concentration of acids and precluded the use of  $\text{HCl}$ . Therefore, lab tests were run with  $\text{H}_2\text{SO}_4$  and  $\text{HNO}_3$  as leaching agents, in both cases with a very high L/S of 40, and sampling every 15 min. After 90 min, PLX with  $\text{H}_2\text{SO}_4$  0.50 M and 0.75 M resulted in only 2.5 % (235 °C, 30.6 bar) and 2.9 % (140 °C, 3.6 bar) of zinc extraction respectively, whereas with  $\text{HNO}_3$  0.50 M it was 20.7 % (245 °C, 36.5 bar). The best result was achieved with nitric acid (4.00 M) for a 22.2 % extraction of the metal (250 °C, 39.7 bar) from the spinel in question.

The following table summarizes the overall findings for the hydrometallurgical route.

Table 8.1 Overall results of hydrometallurgical treatment of gahnite.

OVERALL RESULTS OF HYDROMETALLURGICAL TREATMENT OF GAHNITE							
Route	LX agent	Concentration [M]	Pressure [bar]	Temperature [°C]	L/S	Time [min]	Zinc extraction [%]
ALX	$\text{H}_2\text{SO}_4$	4.0	1.01	95	10	120	non-detected
	$\text{HCl}$						non-detected
	$\text{HNO}_3$						non-detected
PLX	$\text{H}_2\text{SO}_4$	0.50	30.6	235	40	90	2.55
		0.75	3.6	140			2.93
	$\text{HNO}_3$	0.50	36.5	245			20.69
		4.00	39.7	250			22.20

This data can be visualized by means of the next graph, which combines both ALX and PLX results. Best zinc extraction outcomes are obtained when increasing acid concentration and leaching for longer time.



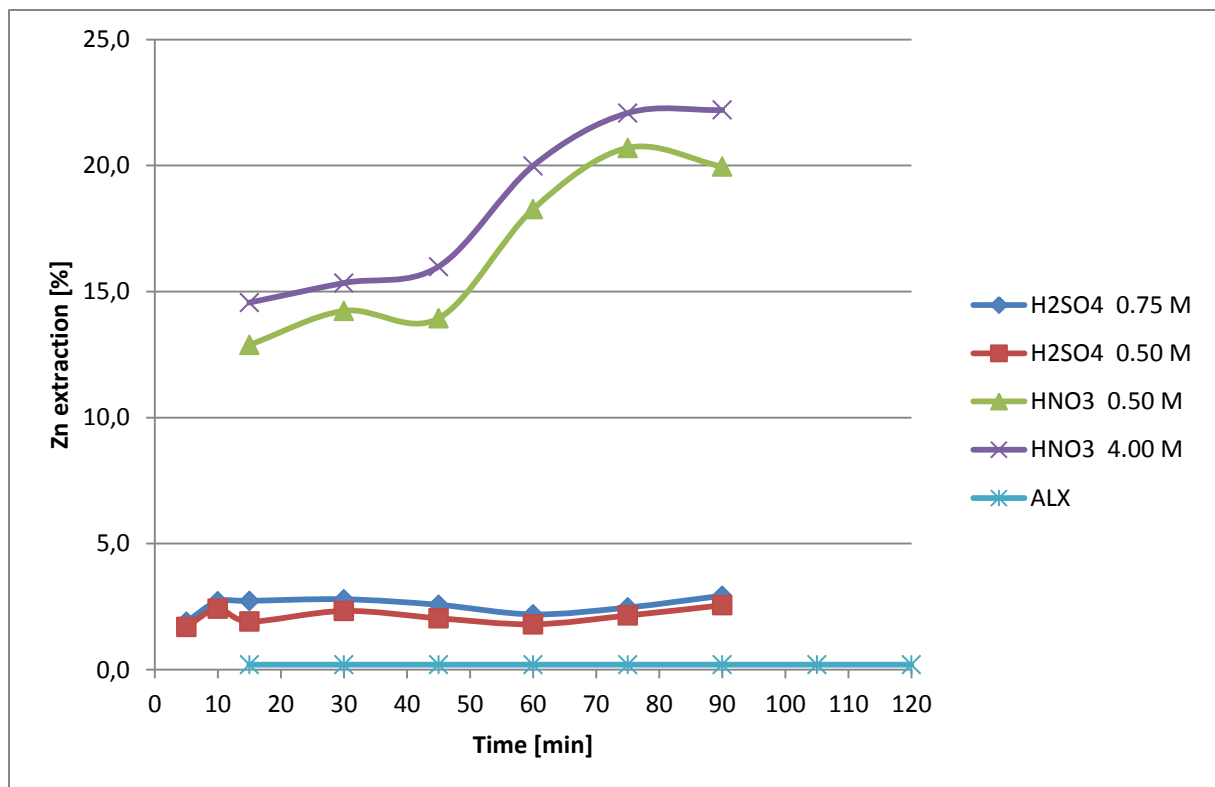


Figure 8.1 Overall results of hydrometallurgical treatment of gahnite.

## 8.2 Pyrometallurgical treatment

Carbothermic reduction tests of gahnite were performed with a 1:1.25 stoichiometric ratio between gahnite and graphite, as a powder mix thoroughly mixed for 30 min, in a horizontal tube furnace. Conditions for this heat treatment were 1.0 h dwell time, 10 °C/min heating rate, and 3.0 L/min constant flowrate of argon gas injection, resulting in a full reduction of the spinel at 1300 °C (99.90 % extraction of zinc), 1250 °C (40.43 %), and 1200 °C (0.00 %). Also, one extra test was done under the same conditions but the mix pressed as a tablet, at 1300 °C, resulting in a 98.72 % extraction of zinc, suggesting that not much difference exists between arranging the mix as loose powder and pressing it as a tablet.

Aluminothermic reduction tests of gahnite were performed first with aluminium balls (10 °C/min heating rate, 1.0 h dwell time, 3.0 L/min flowrate of argon injection), resulting in a 0.00 % metal extraction, due to the low reaction surface between the balls and the gahnite powder. Afterwards, a new series of tests was carried out with aluminium powder with a 1.5:2 stoichiometric ratio, under the same operational conditions, resulting in a 99.98 % extraction of zinc at 1200 °C, 94.11 % at 1150 °C, 91.82 % at 1100 °C, 87.03 % at 1000 °C, 81.23 % at 950 °C, and 73.03 % at 900 °C. Tests with pressed tablets did not indicate relevant differences.

Additionally, one test for the mix of gahnite and ferrite with carbon (1:1:1 stoichiometric ratio, 1300 °C, 1.0 h dwell time, 10.0 °C/min heating rate, 3.0 L/min flowrate of argon injection) resulted in a 99.65 % extraction of zinc, a full reduction of the mix. Also, one more test for the mix this time of gahnite and ferrite and ZnO with carbon (1:1:1:1 stoichiometric ratio, 1300 °C, 1.0 h dwell time, 10.0 °C/min heating rate, 3.0 L/min flowrate of argon injection) resulted in a 100.0 % metal extraction, a full reduction of this mix.

Finally, two more pyrometallurgical routes were explored for processing gahnite, consisting in the addition of SiO<sub>2</sub>, achieving a moderate 23.14 % extraction of zinc for the mix of gahnite and carbon and silica, and a low 4.69 % extraction of zinc for the mix of gahnite and aluminium and silica (in both cases 1:1:1 stoichiometric ratio, 30 min of thorough mixing, 1200 °C, 1.0 h dwell time, 10.0 °C/min heating rate, 3.0 L/min flowrate of argon injection).

General working conditions were 10.0 °C/min heating rate of the furnace and argon gas injection at a ~ 3.0 L/min constant flowrate.

The following table summarizes the overall findings for the pyrometallurgical route.

Table 8.2 Overall results of pyrometallurgical treatment of gahnite.

OVERALL RESULTS OF PYROMETALLURGICAL TREATMENT OF GAHNITE					
Route	Mix	Ratio	Temperature [°C]	Dwell [min]	Zn extraction [%]
Carbothermic	Powder	1:1.25	1300	120	99.90
			1250	60	40.43
			1200		0.00
	Tablet	1:1.25	1300	120	98.72
Aluminothermic	Powder	1.5:2	1200	60	99.68
			1150		94.11
			1100		91.82
			1000		87.03
			950		81.23
			900		73.03

The following graph combines the results from these two routes.

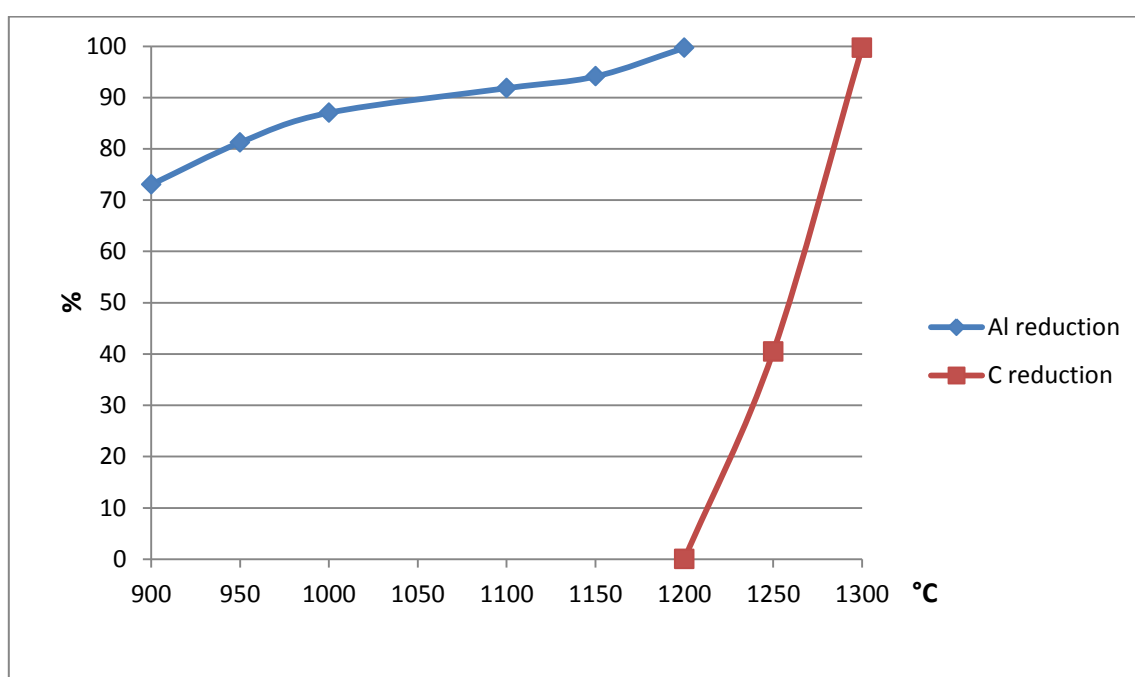


Figure 8.2 Overall results of pyrometallurgical treatment of gahnite.

Finally, the following table gives the main results of a set of additional tests that were performed to explore the reduction possibilities of several mixtures with gahnite.

Again, general working conditions were a heating rate of 10.0 °C/min, and argon gas injection at a constant flowrate of ~ 3.0 L/min.

Table 8.3 Additional results of pyrometallurgical treatment of gahnite.

OVERALL RESULTS OF PYROMETALLURGICAL TREATMENT OF GAHNITE					
Route	Mix	Ratio	Temperature [°C]	Dwell [min]	Zn extraction [%]
G + C + SiO <sub>2</sub>	tablet	1:1:1	1200	60	23.14
G + Al + SiO <sub>2</sub>					4.69
G + F + C	powder	1:1:1	1300	60	99.65
G + F + ZnO + C	powder	1:1:1:1	1300	60	100.00

These additional findings are represented graphically in the following chart, in terms of zinc extraction.

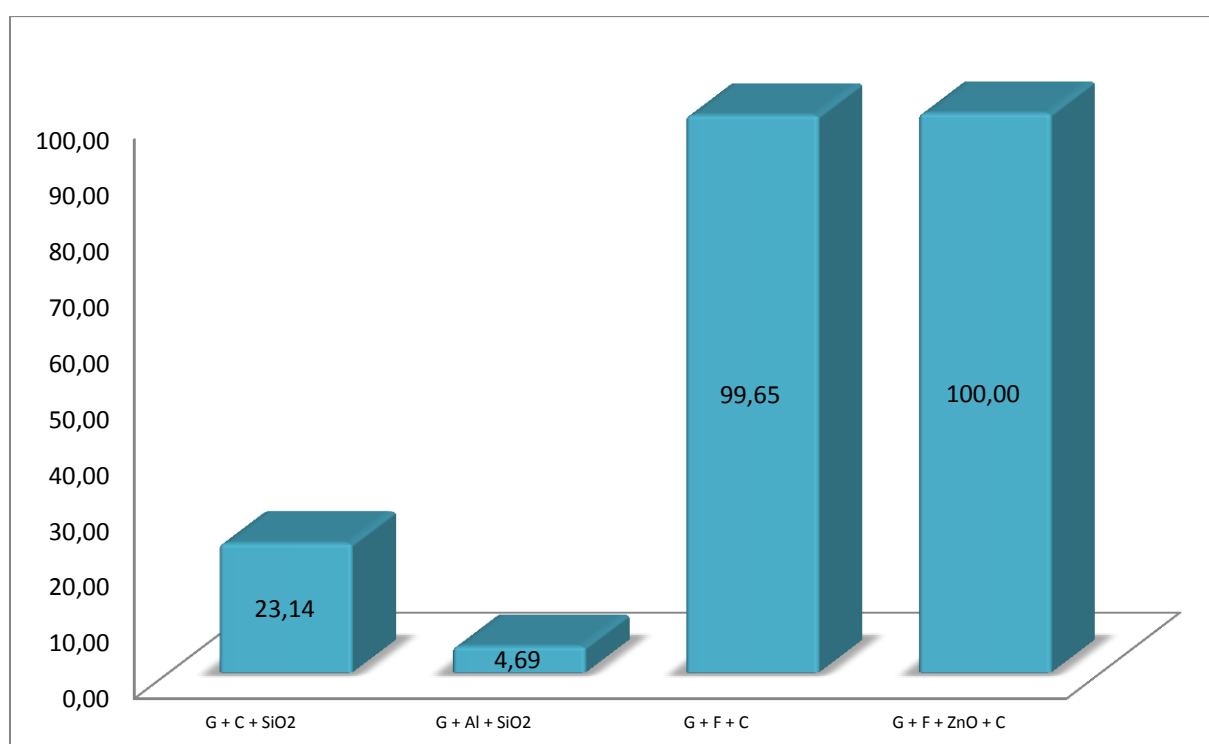


Figure 8.3 Additional results of pyrometallurgical treatment of gahnite.

### 8.3 Overall treatment of gahnite

Combining the data from Sections 8.1 and 8.2, it is possible, as a final point, to establish the following graph of metal extraction of zinc from gahnite  $\text{ZnO} \cdot \text{Al}_2\text{O}_3$ .

It is concluded then that this zinc spinel is actually treatable, both hydro (low and moderate extraction of zinc) and pyrometallurgically (full extraction of zinc). The most interesting results are patently the heat treatment by means of a carbothermic reduction process at 1300 °C and aluminothermic reduction process at 1200 °C in order to achieve a complete conversion of gahnite, producing zinc metal in the gas phase and leaving a solid, stable residue of  $\text{Al}_2\text{O}_3$ .

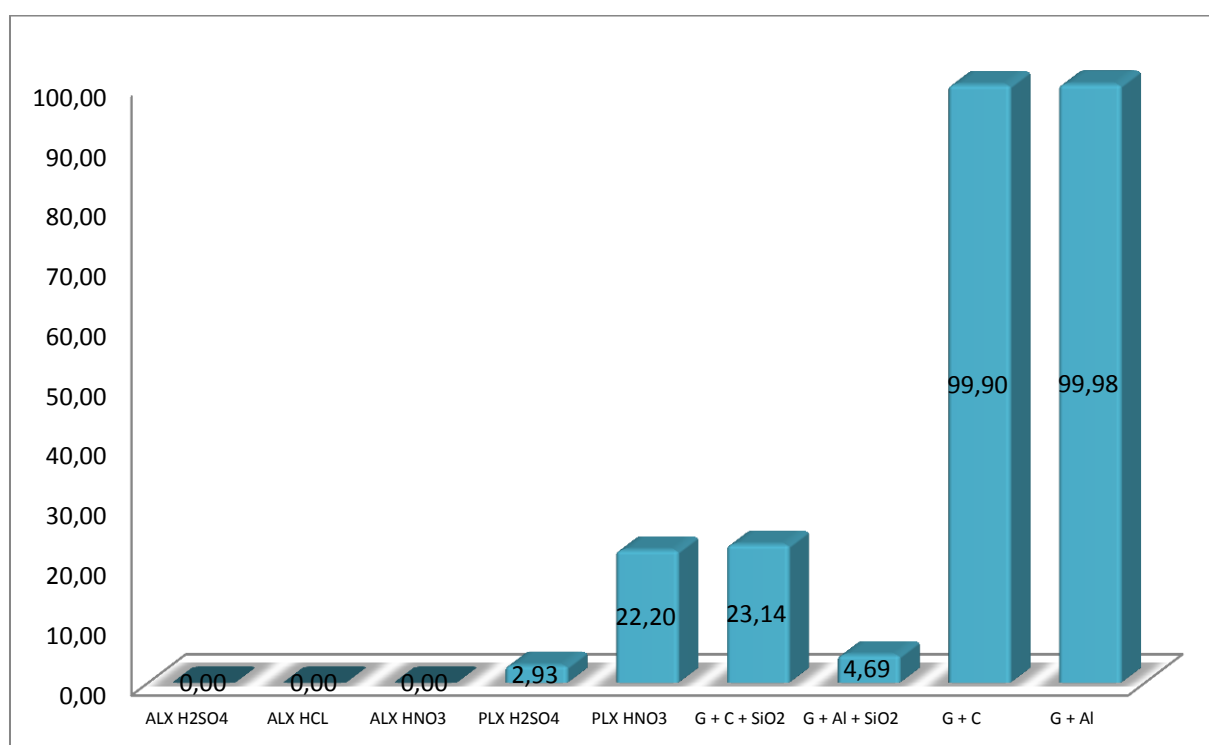


Figure 8.4 Zinc extraction of gahnite.

## 9 RECOMMENDATIONS

### 9.1 Hydrometallurgical treatment

Since non-detected dissolution results were obtained with atmospheric acid leaching of gahnite (95 °C, 1.01 bar, 2 h), utilizing H<sub>2</sub>SO<sub>4</sub>, HCl and HNO<sub>3</sub> as leaching agents, experiments at higher concentrations or longer periods of time are not suggested. Instead, more attention should be given to pressure leaching.

Given the corrosion limitations of the Parr autoclave currently available at the LMP facilities, it is not advisable to run more tests with neither H<sub>2</sub>SO<sub>4</sub> nor HCl, even at low concentrations (below 0.75 M). However, working with HNO<sub>3</sub> proved to be not so aggressive and the following test plan is suggested to be carried out, in order to find more information on the leaching characteristics of gahnite at high temperature/pressure.

Table 9.1 Plan recommended for pressure leaching of gahnite with HNO<sub>3</sub>.

PLX of ZnO·Al <sub>2</sub> O <sub>3</sub> with HNO <sub>3</sub>					
Temperature [°C]	Pressure [bar]	Concentration [M]	L/S	Sampling [min]	Stirring rate
100 150 200 250 300	Dependant on the working temperature	0.5 1.0 1.5 2.0 2.5 3.0 3.5 4.0	40 (decreasing later if interesting results are found)	every 15	Maximum and constant

If a container different from the Ti-based one, with better corrosion resistance to acids at high working temperatures, becomes at hand for the experimental set-up, then it turns interesting to plan a set of trials for studying the leaching behaviour of gahnite with H<sub>2</sub>SO<sub>4</sub> or HCl, for instance. In that case, the following plan is recommended.

Table 9.2 Plan recommended for pressure leaching of gahnite with H<sub>2</sub>SO<sub>4</sub> or HCl.

PLX of ZnO·Al <sub>2</sub> O <sub>3</sub> with H <sub>2</sub> SO <sub>4</sub> or HCl					
Temperature [°C]	Pressure [bar]	Concentration [M]	L/S	Sampling [min]	Stirring rate
From 100 up to almost the limit capabilities of the new container	Dependant on the working temperature	From 0.5 up to almost the limit capabilities of the new container	40 (decreasing later if interesting results are found)	every 15	Maximum and constant

According to corrosion references <sup>[12]</sup> <sup>[13]</sup>, materials which could stand HCl 35 % are: borosilicate glass, up to ~ 120 °C; fluorocarbons, up to ~ 230 °C; fluoro elastomers, up to ~ 175 °C; and nardel, up to ~ 140 °C.

The same is applied for H<sub>2</sub>SO<sub>4</sub> 95 %, with the exception of nardel, which only is advisable for H<sub>2</sub>SO<sub>4</sub> 50 % downwards.

## 9.2 Pyrometallurgical treatment

Regarding the carbothermic route, temperature range was well defined in terms of reduction performance (1300 °C full, 1200 °C null), so there are no suggestions for that parameter. Also, almost no carbon was found left in the residues (please refer to Section 6), meaning that the amount of graphite added to the mix was adequate for a successful reduction process of gahnite, and then no variations for that parameter are proposed either.

One factor that may be interesting to study further is the heating rate. All the pyrometallurgical tests performed in this research were performed at 10 °C/min; therefore the following plan is suggested.

Table 9.3 Plan recommended for carbothermic reduction of gahnite changing the heating rate.

<b>Carbothermic Reduction of ZnO·Al<sub>2</sub>O<sub>3</sub></b>						
Temperature [°C]	Heating rate [°C/min]	Dwell time [h]		Temperature [°C]	Heating rate [°C/min]	Dwell time [h]
1300	5.0	1.0		1300	15.0	1.0
1250				1250		
1200				1200		

Regarding the aluminothermic reduction of gahnite, even though the temperature range was well studied in terms of reduction performance (1200 °C full, 900 °C good), it may be still interesting to go lower, and run five more tests, from 650 °C upwards, since the HSC Chemistry calculations give only a probability of the conversion and it was concluded that the reaction actually takes place at a slightly lower temperature range than expected, therefore these four tests could give a more complete picture of the reaction in that lower zone.

650 °C may appear too low, but according to the calculation, this reduction process is supposed to commence slowly around 700 °C, and can be an interesting starting point. So the subsequent plan is recommended to be carried out.

Table 9.4 Extended plan recommended for aluminothermic reduction of gahnite.

<b>Aluminothermic Reduction of ZnO·Al<sub>2</sub>O<sub>3</sub></b>		
Temperature [°C]	Heating rate [°C/min]	Dwell time [h]
850	10.0	1.0
800	10.0	1.0
850	10.0	1.0
700	10.0	1.0
650	10.0	1.0



As in the carbothermic route, almost no aluminium was found in the residue after heat treatment, meaning that the amount of this reductant added to the mix was adequate for a successful reduction process of gahnite, so no variations in this respect are advised. However, it may be interesting, again, to study the reaction at a different heating rate, since all the experiments were done at a fixed 10 °C/min. The following plan is proposed.

Table 9.5 Plan recommended for aluminothermic reduction of gahnite changing the heating rate.

<b>Aluminothermic Reduction of ZnO·Al<sub>2</sub>O<sub>3</sub></b>						
Temperature [°C]	Heating rate [°C/min]	Dwell time [h]		Temperature [°C]	Heating rate [°C/min]	Dwell time [h]
1200	5.0	1.0		1200	15.0	1.0
1150				1150		
1100				1100		
1050				1050		
1000				1000		
950				950		
900				900		

If interesting results in terms of zinc extraction are found after this plan, it could be extended to the lower range of temperature suggested in Table 9.4.

Finally, no others tests are suggested for the addition of SiO<sub>2</sub> or CaO route.

Nonetheless, one last interesting suggestion is to install a device for collecting zinc in the gas phase, at one of the extremes of the furnace.

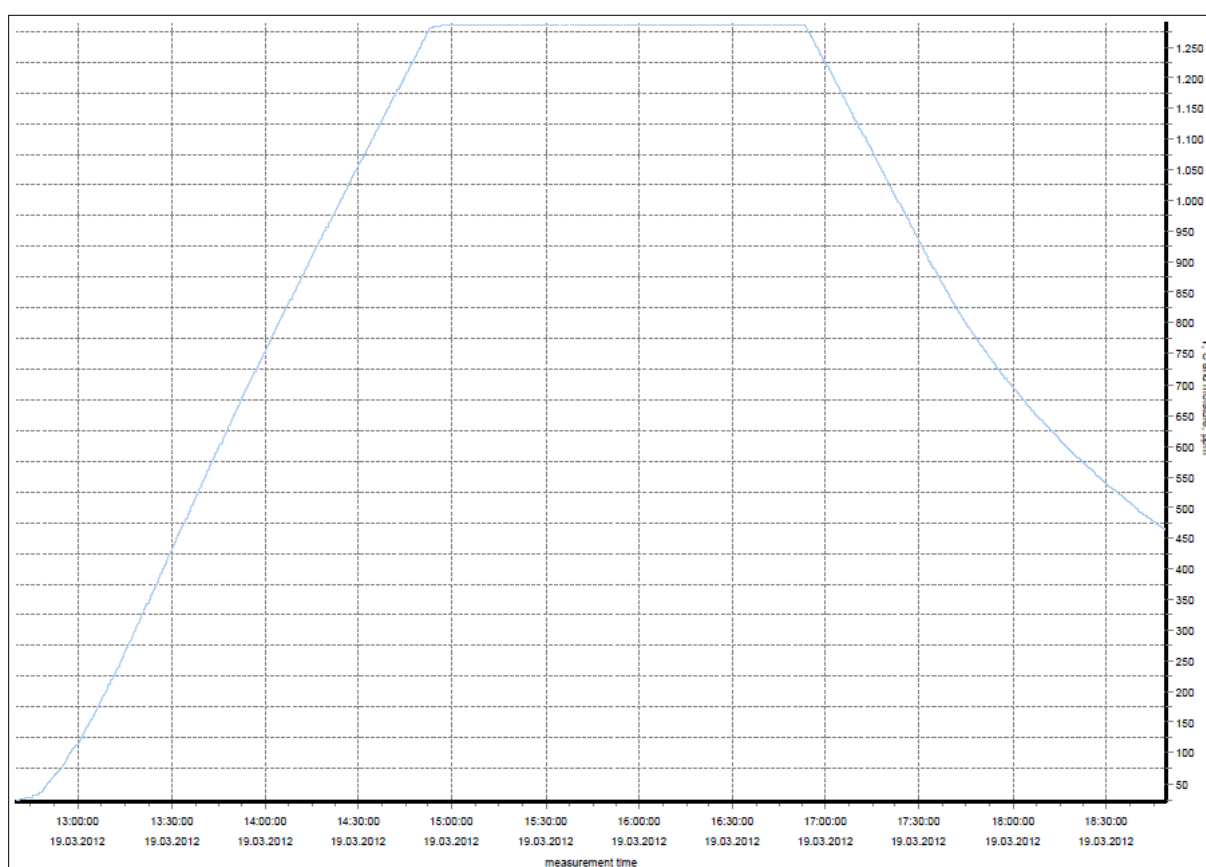
## 10 REFERENCES

- [1] Brouwer, D. Smart Processing of Brass Smelter Residues. M.Sc. thesis, October 2010, TU Delft.
- [2] Kemperman, D. Metallurgical processing of zinc-bearing residues. M.Sc. thesis, June 2010, TU Delft.
- [3] Sampath, S.K., Kahnere, D.G., Pandey, R. Electronic structure of spinel oxides: zinc aluminate and zinc gallate. *J. Phys.: Condensed Matter* 11 (1999) 3635–3644.
- [4] [www.mindat.org](http://www.mindat.org) (referenced in August 2012).
- [5] Aguilar, J.A., González, M., Gómez, I. Microwaves as an energy source for producing magnesia-alumina spinel. *J. of Microwave Power and Electromagnet Energy* 32 (1997) 74–79.
- [6] Sinclair, R.J. The Extractive Metallurgy of Zinc. *The Australasian Institute of Mining and Metallurgy, Spectrum Series* 13 (2005) 287.
- [7] Assis, G. Emerging pyrometallurgical processes for zinc and lead recovery from zinc bearing waste materials. *Proceedings Zinc and Lead Processing* (1998) 243–263.
- [8] Arregui, V., Gordon, A.R., Steintviet, G. The jarosite process, past, present and future. *Proceedings Lead-Zinc-Tin* 80 (1980) 97–123.
- [9] Rao, S.R. Resource recovery and recycling from metallurgical wastes. *Waste Management Series* 7 (2006) 209–215.
- [10] Havlík, T., Friedrich, B., Stopić, S. Pressure leaching of EAF dust with sulphuric acid. *World of Metallurgy – Erzmetall* 57 (2004) 113–120.
- [11] Ye, G., Burstrom, E., Maccagni, M., Bianco, L., Stripply, H. Elimination of zinc ferrite for hydrometallurgical recovery of zinc from EAF dust. *Advanced processing of metals and materials* 6 (2006) 397–411.
- [12] Hamner, N.E. Corrosion Data Survey. Metals Section. 5<sup>th</sup> Edition, National Association of Corrosion Engineers, USA (n.d.)
- [13] Schweitzer, P.A. Corrosion Resistance Tables. Metals, Plastics, Nonmetallics, and rubbers. 2<sup>nd</sup> Edition, Marcel Dekker Inc., USA. (n.d.)

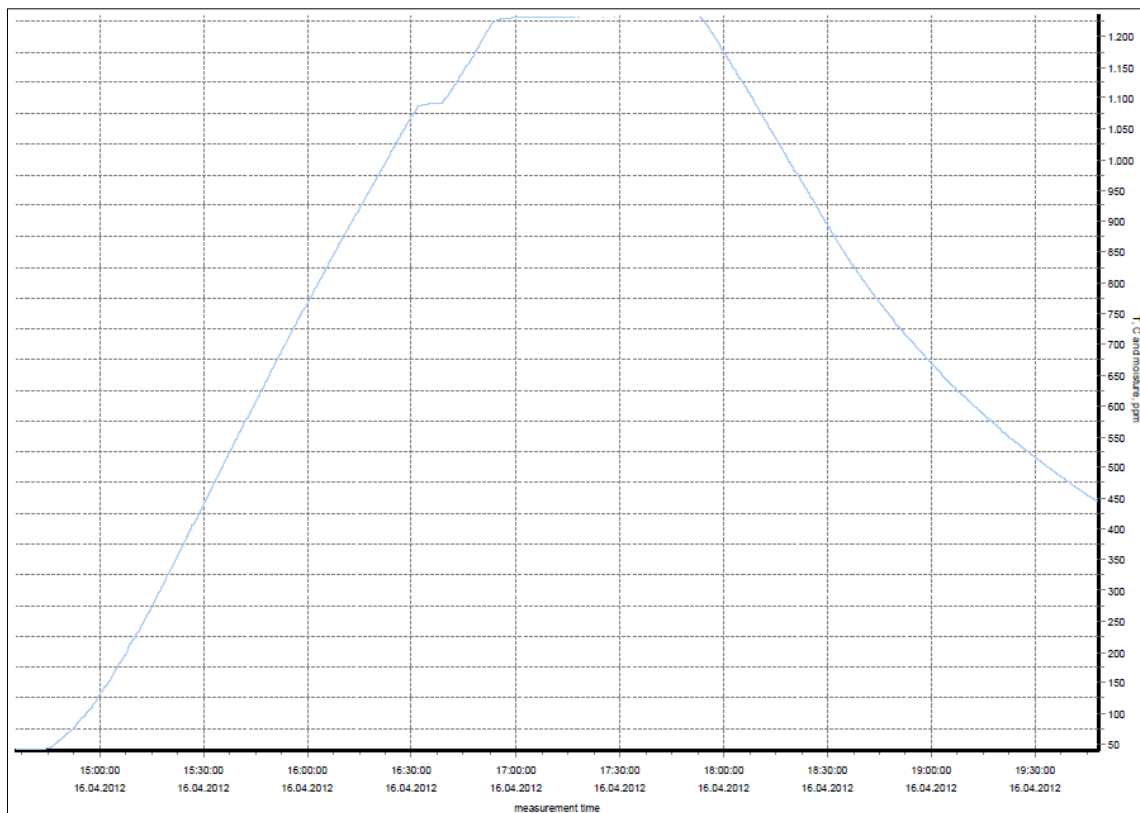
## APPENDIX: Additional dwell graphs

These graphs were obtained by measuring the temperature of the experiment in course with a thermocouple whose extreme was situated in the center of the furnace tube, almost touching the crucible, a gap of no more than 1 cm. These measurements were thus independent from the temperature established in the furnace controller, and were registered through the gas analyzer system adjacent to the furnace set-up. Almost every pyrometallurgical test was recorded.

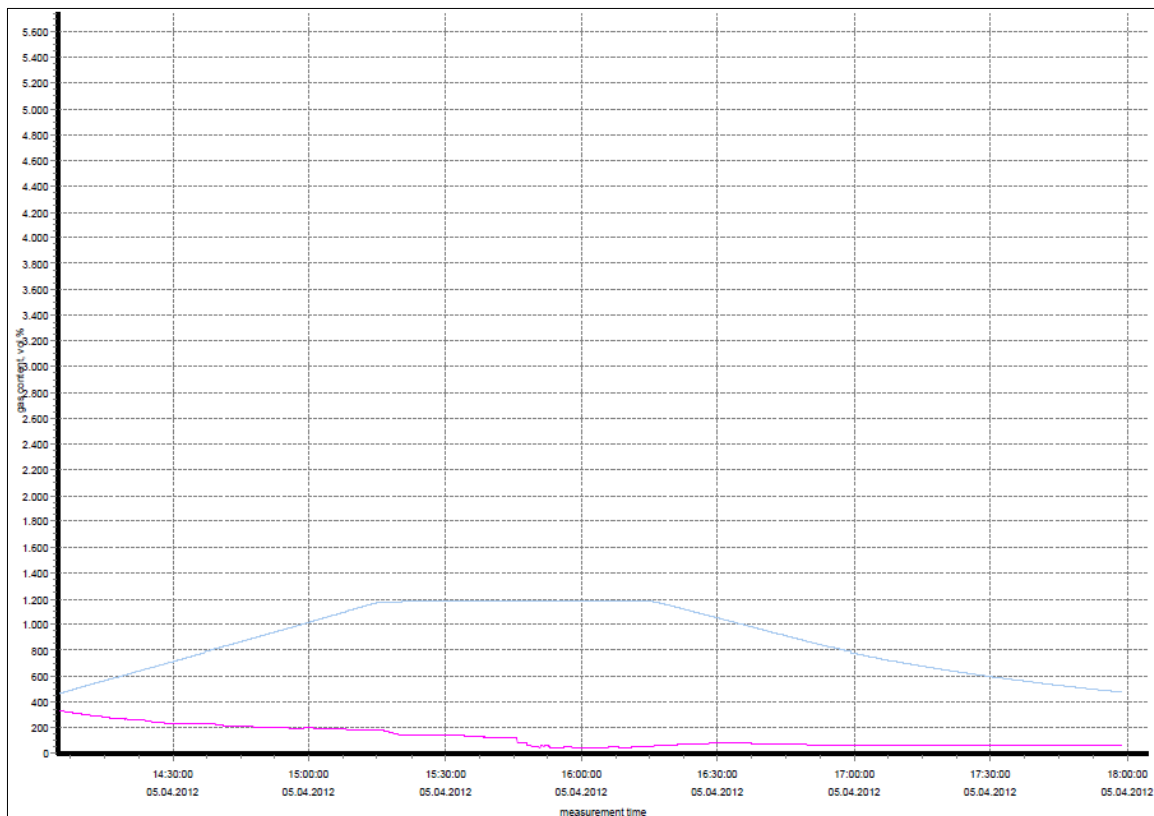
### A.1.1 Dwell graph for test G + C at 1300 °C for 2 h



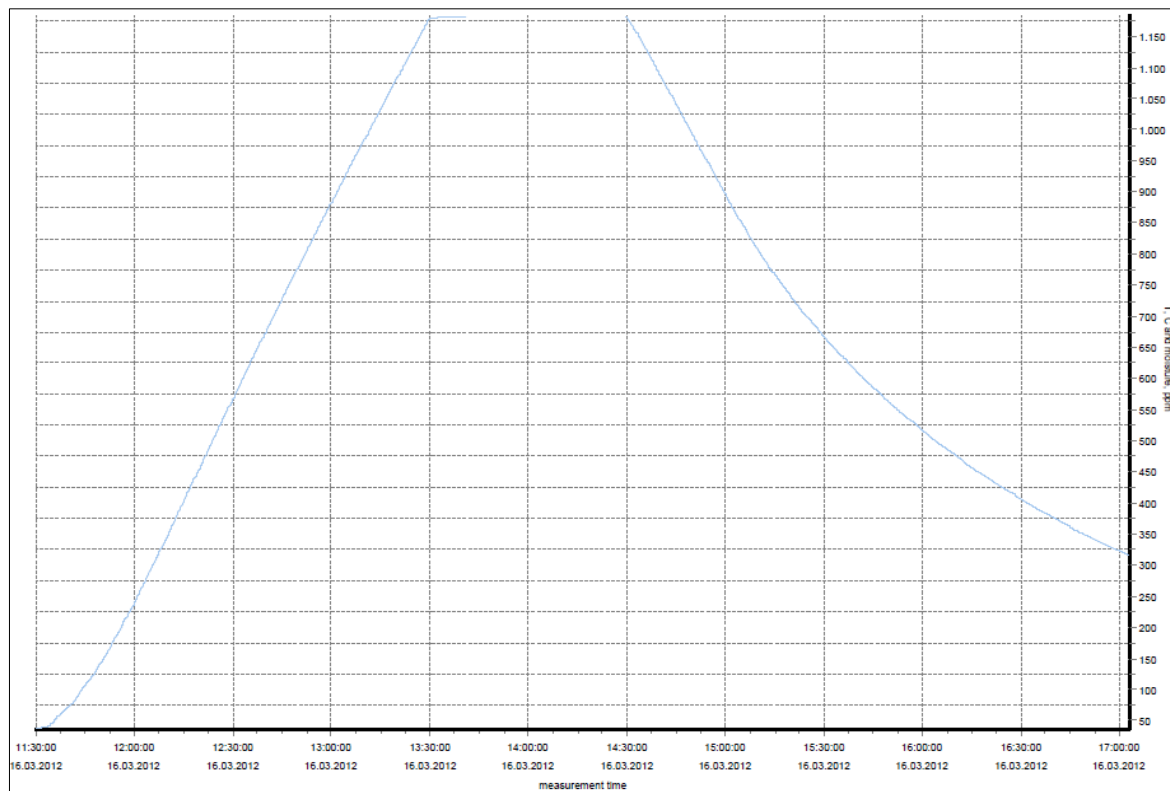
### A.1.2 Dwell graph for test G + C at 1250 °C for 1 h



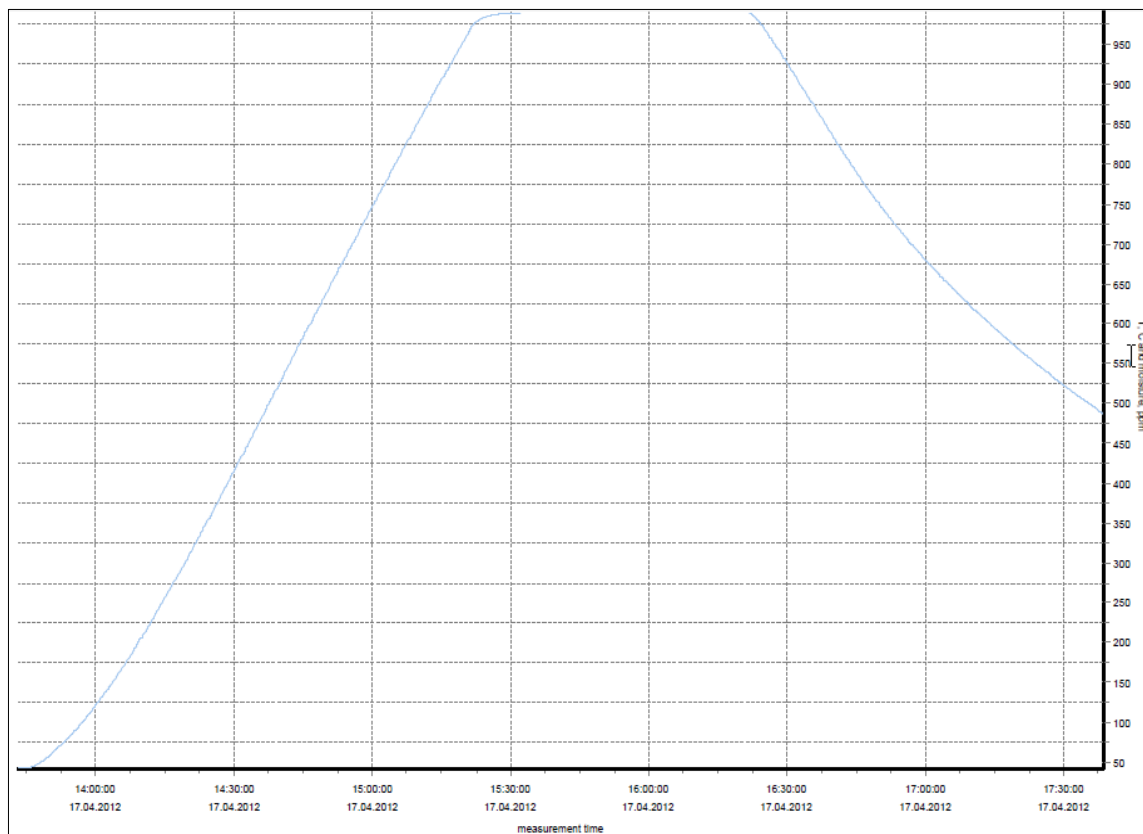
### A.1.3 Dwell graph for test G + C at 1200 °C for 1 h



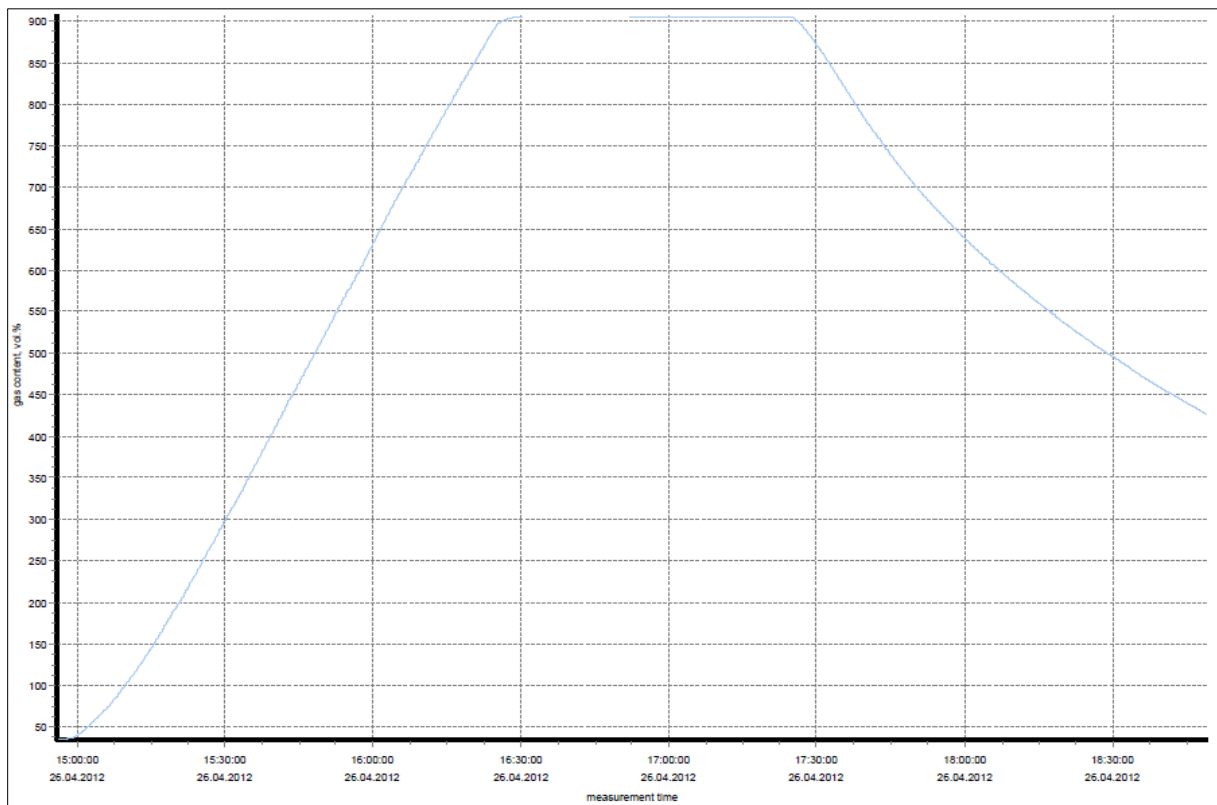
### A.2.1 Dwell graph for test G + Al at 1200 °C for 1 h



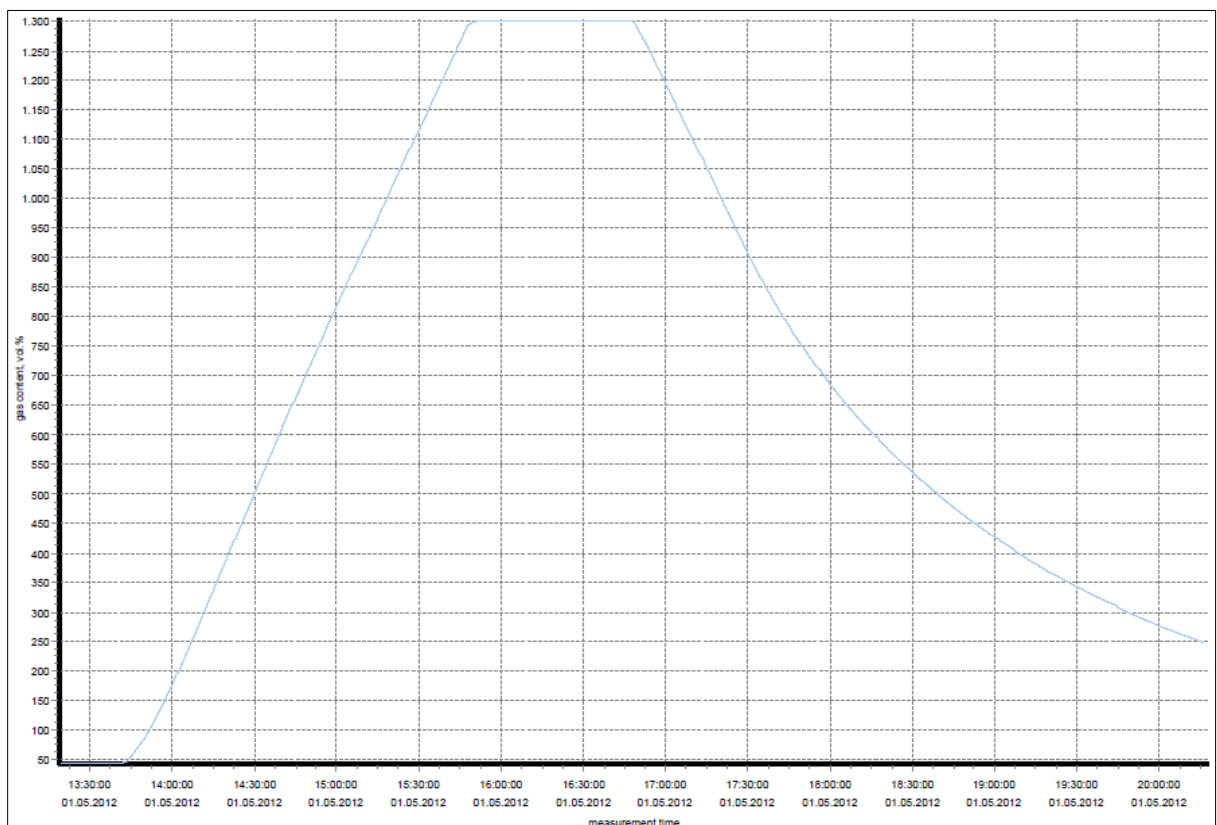
### A.2.2 Dwell graph for test G + Al at 1000 °C for 1 h



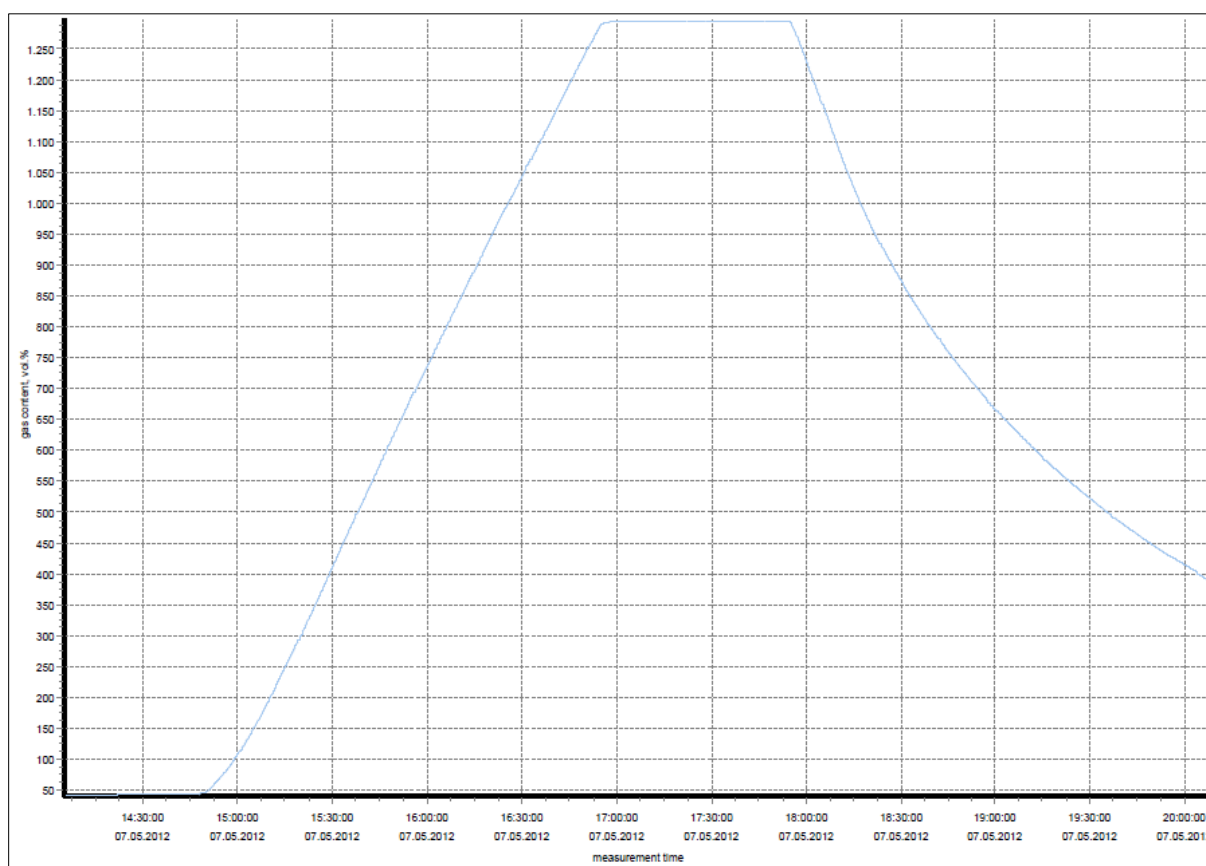
### A.2.3 Dwell graph for test G + Al at 900 °C for 1 h



### A.3 Dwell graph for test G + F + C at 1300 °C for 1 h



#### A.4 Dwell graph for test G + F + ZnO + C at 1300 °C for 1 h







Een huishouden van Jan Steen...

